PB85-138535

Thermal Degradation Products from Dielectric Fluids

Midwest Research Inst., Kansas City, MO

Prepared for

Environmental Protection Agency, Washington, DC

19 Nov 84

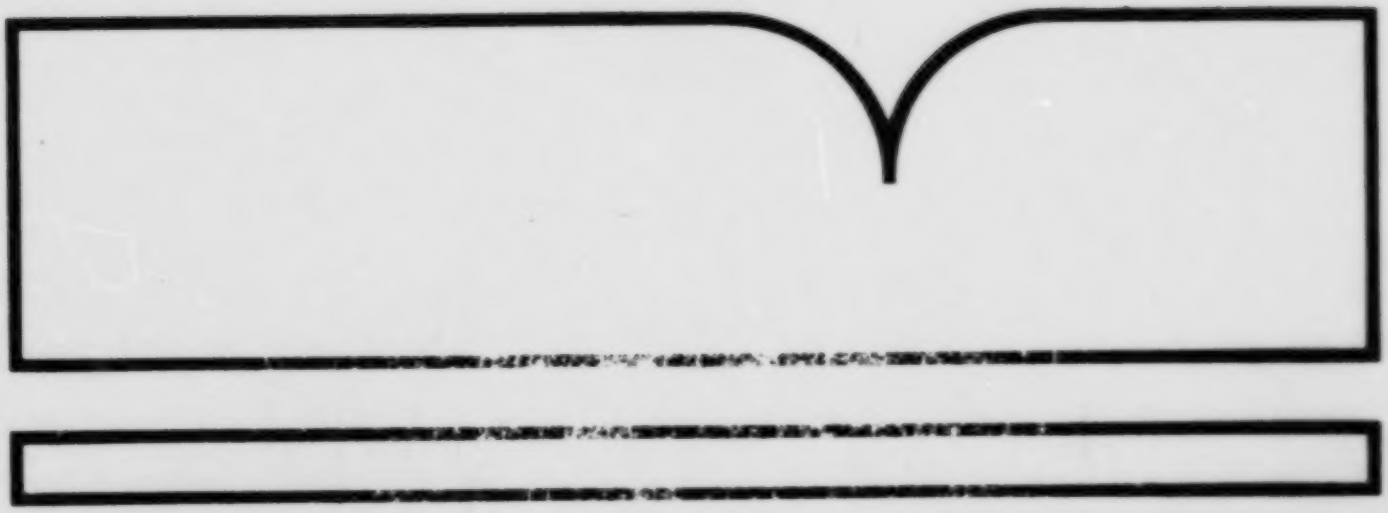

U.S. Department of Commerce
National Technical Information Service
NTIS

United States
Environmental Protection
Agency

Office of
Toxic Substances
Washington DC 20460

EPA-560/5-84-009
December, 1984

PB85-138535

Toxic Substances

EPA

Thermal Degradation Products from Dielectric Fluids

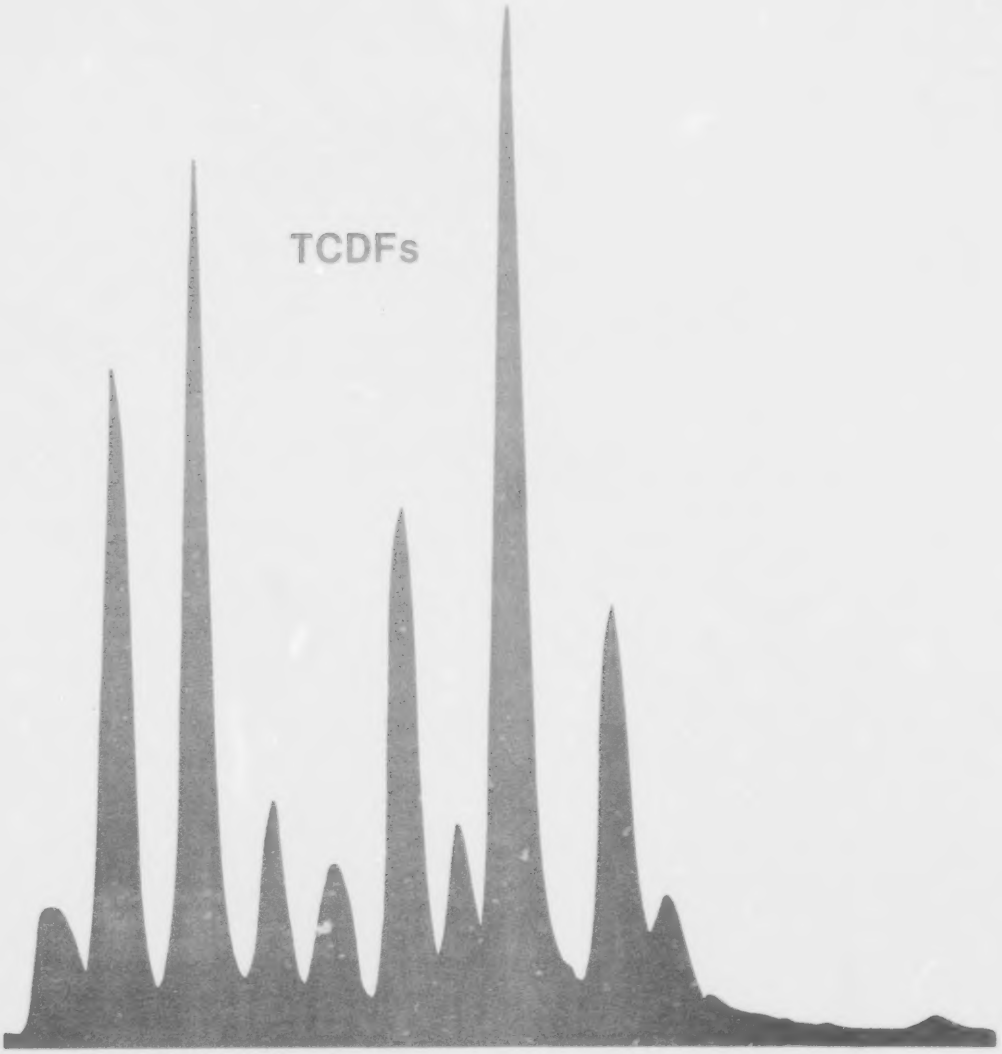

REPRODUCED BY
NATIONAL TECHNICAL
INFORMATION SERVICE
U.S. DEPARTMENT OF COMMERCE
SPRINGFIELD, VA. 22161

TECHNICAL REPORT DATA
(Please read Instructions on the reverse before completing)

1. REPORT NO. EPA 560/5-84-009	2.	3. RECIPIENT'S ACCESSION NO. PB85 138535
4. TITLE AND SUBTITLE Thermal Degradation Products from Dielectric Fluids		5. REPORT DATE December 1984 6. PERFORMING ORGANIZATION CODE 8201-A(23)
7. AUTHOR(S) Mitchell D. Erickson, Christopher J. Cole, Jairus D. Flora Jr., Paul G. Gorman, Clarence L. Haile, Gary D. Hinshaw, Fred C. Hopkins, Stephen E. Swanson		8. PERFORMING ORGANIZATION REPORT NO. Interim Report No. 1
9. PERFORMING ORGANIZATION NAME AND ADDRESS Midwest Research Institute 425 Volker Boulevard Kansas City, Missouri 64110		10. PROGRAM ELEMENT NO. Work Assignment 23 11. CONTRACT/GRANT NO. EPA Contract No. 68-02-3938
12. SPONSORING AGENCY NAME AND ADDRESS U.S. Environmental Protection Agency Office of Toxic Substances Field Studies Branch, TS 798 401 M Street, S.W., Washington, DC 20460		13. TYPE OF REPORT AND PERIOD COVERED Interim (May-November 1984) 14. SPONSORING AGENCY CODE

15. SUPPLEMENTARY NOTES
The EPA Work Assignment Manager is Daniel T. Heggem, (202) 382-3990.
The EPA Project Officer is Frederick W. Kutz, (202) 382-3569.

16. ABSTRACT

Electrical transformer fires can cause extensive smoke damage, especially when polychlorinated biphenyls (PCBs) are involved since they can form polychlorinated dibenzofurans (PCDFs) and other toxic by-products. To characterize the potential for by-product formation, this study was undertaken to optimize conditions for PCDF formation from PCBs and to study the potential for formation of PCDFs and polychlorinated dibenzodioxins (PCDDs) from combustion of selected dielectric fluids, including those contaminated with PCBs. A bench-scale thermal destruction system was used to combust the samples. The dielectric fluid was fed continuously using a syringe pump. The concentrations of CO, CO_2, and O_2 in the effluent were monitored continuously. The entire effluent from the thermal destruction system was passed through an XAD-2 trap to collect PCDFs and other semivolatile organics. The XAD-2 trap and a rinse of connective tubing were Soxhlet extracted. Extracts were cleaned using column chromatography to isolate the PCDFs and PCDDs. All samples were analyzed for PCDFs using HRGC/EIMS in the selected ion monitoring mode. The results of this work indicate that the optimum conditions for PCDF formation from PCBs are near 675°C for 0.8 s or longer, with 8% excess oxygen. Under these conditions, percent levels of PCDFs are formed from mineral oil or silicone oil contaminated with PCBs at 5 ppm or greater. PCDFs and PCDDs are also formed from a trichlorobenzene dielectric fluid which contained no detectable PCBs.

17. KEY WORDS AND DOCUMENT ANALYSIS

a. DESCRIPTORS		b. IDENTIFIERS/OPEN ENDED TERMS	c. COSATI Field/Group
PCBs	Polychlorinated biphenyl		
PCDF	Polychlorinated dibenzofuran		
PCDD	Polychlorinated dibenzo-p-dioxin		
TCDD	Tetrachloro dibenzo-p-dioxin		
TCDF	Tetrachloro dibenzofuran		
Combustion	Transformer		
Pyrolysis	PCB fires		

18. DISTRIBUTION STATEMENT UNLIMITED	19. SECURITY CLASS *(This Report)* UNCLASSIFIED	21. NO. OF PAGES 100
	20. SECURITY CLASS *(This page)* UNCLASSIFIED	22. PRICE

EPA Form 2220-1 (Rev. 4-77) PREVIOUS EDITION IS OBSOLETE

THERMAL DEGRADATION PRODUCTS FROM DIELECTRIC FLUIDS

by

Mitchell D. Erickson, Christopher J. Cole, Jairus D. Flora, Jr.,
Paul G. Gorman, Clarence L. Haile, Gary D. Hinshaw,
Fred C. Hopkins, and Stephen E. Swanson

WORK ASSIGNMENT NO. 23

INTERIM REPORT NO. 1

EPA Contract No. 68-02-3938
MRI Project No. 8201-A(23)

November 19, 1984

For

U.S. Environmental Protection Agency
Office of Toxic Substances
Field Studies Branch, TS 798
401 M Street, S.W.
Washington, DC 20460

Attn: Frederick W. Kutz, Project Officer
Daniel T. Heggem, Work Assignment Manager

DISCLAIMER

This document has been reviewed and approved for publication by the Office of Toxic Substances, Office of Pesticides and Toxic Substances, U.S. Environmental Protection Agency. The use of trade names or commercial products does not constitute Agency endorsement or recommendation for use.

PREFACE

This report presents the results of Work Assignment No. 23 on U.S. Environmental Protection Agency Contract No. 68-02-3938, "Incineration Testing of PCBs." The work was done at Midwest Research Institute (MRI) during the period May 22, 1984 to November 19, 1984. Mitchell D. Erickson was the MRI Work Assignment Leader. This report was prepared by Dr. Erickson, Jairus D. Flora, Jr., Clarence L. Haile, Gary D. Hinshaw, and Stephen E. Swanson. The thermal destruction system was operated by Mr. Hinshaw, Christopher J. Cole, Paul G. Gorman, and Fred C. Hopkins. Laboratory work was done by Mr. Swanson, with assistance from Alice Cheng, Michael McGrath, and Edward Olsen. The GC/MS data were acquired by John Gamble, Jon Onstot, Gil Radolovich, and Margaret Wickham. Mass spectral data were interpreted by Dr. Erickson, Mr. Swanson, and Leslie Moody. Additional support was provided by Audrey Sanford.

The EPA Work Assignment Manager, Daniel T. Heggem of Field Studies Branch, provided helpful guidance and advice.

MIDWEST RESEARCH INSTITUTE

Clarence L. Haile
Deputy Program Manager

John E. Going
Program Manager

Approved:

James L. Spigarelli, Director
Chemical and Biological Sciences
Department

TABLE OF CONTENTS

		Page
I.	Introduction	1
II.	Summary	1
III.	Recommendations	2
IV.	Background	3
	A. PCDF Occurrence in PCB Fires	3
	B. Reaction Mechanisms	3
	C. Relationship of Conditions of PCDF Formation	5
V.	Experimental Plan	8
	A. Thermal Destruction System	8
	B. Phase 1 - System Refitting and Preliminary Plans	8
	C. Phase 2 - Experimental Optimization	9
	D. Phase 3 - Aroclor 1254 Test Runs	12
VI.	Experimental Methods	13
	A. Reagents and Supplies	13
	B. Destruction Facility Operation	15
	C. Chemical Analysis	22
	D. Statistical Analysis	30
VII.	Results and Discussion	33
	A. Phase 1	33
	B. Phase 2	33
	C. Phase 3	50
VIII.	References	90

Preceding page blank

LIST OF TABLES

Table		Page
1	Thermochemical Conversion of PCBs to PCDFs	6
2	Concentrations of PCB Congeners in Mineral Oil for Phase 2	13
3	Concentrations of Aroclor 1254 in Feed Samples Used in Phase 3.	14
4	Phase 3 Surrogate Spiking Solution	24
5	Types of Analyses Used for Samples from Phase 3.	27
6	Operating Parameters for Gas Chromatography/Mass Spectrometers Used to Analyze Phase 3 Samples.	28
7	Scan Ranges and Selected Ions Monitored for Individual Analytes	29
8	PCDD/PCDF Standard Used in Phase 3	31
9	Type of Quantitation Used During Phase 3 HRGC/EIMS Analysis.	32
10	Phase 1 Non-PCB Combustion Test Conditions	34
11	Operating Conditions for Phase 2 Tests	36
12	Nominal and Actual Values for Operating Conditions During Phase 2 Tests.	37
13	Weights of PCBs Used During Phase 2 Tests.	42
14	Weights of PCDFs in Combined XAD-2/Rinse Samples from Phase 2 Tests.	44
15	Conversion Efficiencies (PCBs to PCDFs) for Phase 2 Tests.	45
16	Full Model Analysis of Variance.	49
17	Reduced Analysis of Variance Model Using Only Temperature and Oxygen	51
18	Means for Total PCDF Conversion Efficiency (%) Grouped by Variable.	52
19	Analysis of Variance for TetraCDF.	53
20	Means for TetraCDF Conversion Efficiency (%) Grouped by Variable	54

LIST OF TABLES (continued)

Table		Page
21	Operating Conditions for Phase 3 Tests	56
22	PCB Feed Characteristics in Phase 3.	57
23	Amounts of PCDFs Formed in Phase 3	60
24	PCDF Formation in Phase 3.	61
25	Conversion Efficiencies (PCBs to PCDFs) for Phase 3.	62
26	Amounts of PCDDs Formed in Phase 3	63
27	PCDD Formation in Phase 3.	64
28	Conversion Efficiencies (PCBs to PCDDs) for Phase 3.	65
29	Results of Analysis of PCBs in Phase 3 Samples	83
30	PCB Destruction Efficiencies in Phase 3 Runs	84
31	Means of PCDF Formed in Phase 3, Grouped by Matrix and Concentration.	86

LIST OF FIGURES

Figure		Page
1	Laboratory-scale combustion system.	16
2	Temperature profiles in combustion furnace.	18
3	Sample analysis scheme.	23
4	Two-part cleanup column	25
5	Continuos gas monitoring results for Run 6-20-13-MMH.	39
6	Continuous gas monitoring results for Run 6-19-11-MHM	40
7	Combustion efficiency versus temperature.	41
8	Total PCDFs formed as a function of oxygen.	47
9	Tetra CDFs formed as a function of oxygen concentration . . .	48
10	Mono and di CDFs and CDDs in sample 8-22-52-S500.	66
11	Tri and tetra CDFs and CDDs in sample 8-22-52-S500.	67
12	Penta and hexa CDFs and CDDs in sample 8-22-52-S500	68
13	Hepta and octa CDFs and CDDs in sample 8-22-52-S500	69
14	Mono and di CDFs and CDDs in sample 8-30-62-ASKL.	70
15	Tri and tetra CDFs and CDDs in sample 8-30-62-ASKL.	71
16	Penta and hexa CDDFs and CDDs in sample 8-30-62-ASKL.	72
17	Hepta and octa CDFs and CDDs in sample 8-30-62-ASKL	73
18	Tri and tetra CDFs and CDDs in sample 8-15-43-M5.	74
19	Tri and tetra CDFs and CDDs in sample 8-17-47-S5.	75
20	Tri and tetra CDFs and CDDs in sample 8-28-57-CLBZ.	76
21	Average PCDF formation versus PCB concentration for Phase 3 .	78
22	PCDF formation in PCB-spiked mineral oil by homolog	79
23	PCDF formation in PCB-spiked silicone oil by homolog.	80
24	PCDF formation from PCB askarel fluid	81
25	PCDF and PCDD formation from trichlorobenzene transformer fluid	82
26	Comparison of PCDFs formed with PCB feed composition (mineral oil)	87
27	Comparison of PCDFs formed with PCB feed composition (silicone oil).	88
28	Comparison of PCDFs formed with PCB feed composition (askarel)	89

I. INTRODUCTION

The Environmental Protection Agency (EPA) issued a final rule on August 25, 1982, authorizing indefinite use of certain electrical transformers containing polychlorinated biphenyls (PCBs). This rule is known as the PCB Electrical Use Rule. At that time, information available to the EPA indicated that fires involving electrical transformers were rare, isolated incidents. However, several recent transformer fires in buildings have brought into question EPA's earlier assumption. The Agency has therefore issued an Advance Notice of Proposed Rulemaking (ANPR) (USEPA 1984a) and proposed rule (USEPA 1984b) to gather data on the specific risks posed by fires involving electrical transformers that contain PCBs and also on mechanisms for mitigating or eliminating these risks. Depending upon the results of EPA's analysis of these data, the Agency may propose further control measures on the use of this equipment.

This report describes the methods and results of a study, conducted in support of EPA's data gathering activities under the ANPR, of the potential for formation of polychlorinated dibenzofurans (PCDFs) and polychlorinated dibenzo-p-dioxins (PCDDs) from uncontrolled fires involving PCB-containing dielectric fluids. The following two sections present a summary of the study and recommendations for further study, respectively. Section IV provides a brief literature review of PCDF and PCDD formation from PCBs. Sections V and VI describe the experimental plan and methods. The results of the study are presented and discussed in Section VII.

II. SUMMARY

At high temperatures, such as those in transformer fires, polychlorinated biphenyls (PCBs) react to form polychlorinated dibenzofurans (PCDFs) and other toxic by-products. The purpose of this study was to optimize conditions for PCDF formation in order to examine the potential for formation of PCDFs and polychlorinated dibenzodioxins (PCDDs) from combustion of selected PCB-containing dielectric fluids.

The study was conducted in three phases. In Phase 1, a bench-scale thermal destruction system, developed by MRI, was refitted with specific components installed to accommodate this study. Then, a few test runs were made under preliminary temperature and oxygen conditions to ensure an acceptable system blank. The concentrations of CO, CO_2, and O_2 in the effluent were monitored continuously. The entire effluent from the thermal destruction system was passed through an XAD-2 trap to collect PCDFs and other semivolatile organics. The XAD-2 trap and a rinse of connective tubing were Soxhlet-extracted and cleaned using column chromatography to isolate the PCDFs and PCDDs. All samples were analyzed for PCDFs (and PCDDs in Phase 3), using high resolution (capillary) gas chromatography/electron impact mass spectrometry (HRGC/EIMS) in the selected ion monitoring (SIM) mode. No PCBs or PCDFs were detected in the Phase 1 samples.

The Phase 2 experiments were conducted to determine the optimum temperature, oxygen, and residence time conditions for PCDF formation. The feed

into the system was mineral oil spiked with three individual PCB congeners which form PCDFs by the four known reaction mechanisms. A statistical analysis of the results for 33 runs indicates that both temperature and oxygen have significant effects on the PCDF yield and that the interaction between temperature and oxygen is synergistic. The results indicate that the optimum values are a temperature of 675°C and an excess oxygen concentration of 8%. The residence time did not significantly affect the yield in the range of 0.3 to 1.5 s, although lower times appeared to yield less PCDFs. Since residence time does not appear to significantly affect the PCDF formation, 0.8 s was chosen as convenient for the Phase 3 runs.

In Phase 3, duplicate test runs were conducted with mineral oil and silicone oil dielectric fluids containing PCBs (Aroclor 1254) at concentrations of 0, 5, 50 and 500 ppm. A PCB askarel containing 70% Aroclor 1260 and a non-PCB askarel, containing mostly trichlorobenzene with some tetrachlorobenzene, were also tested in duplicate. PCDFs were found in all samples, except blanks. PCDDs were found in the samples from the trichlorobenzene runs and occasionally at low levels in some of the other samples. Up to 5,700 ng total PCDFs/mL of spiked feed oil or 4% conversion efficiency (PCBs to PCDFs) was observed for the mineral oil and silicone oil runs. The PCB destruction efficiencies calculated for the 5, 50, and 500 ppm runs ranged from 79 to > 99%. Up to 19,000,000 ng total PCDFs/mL feed oil (19 mg/mL) or 3% conversion efficiency was observed for the askarel fluid. Statistical analysis showed a linear relationship for PCDFs formed versus the amount of PCBs. Although not statistically different, about twice the quantity of PCDFs was formed from PCBs in silicone oil than from the corresponding mineral oil samples. All eight PCDF homologs were detected in the askarel runs with a maximum at the pentaCDF. With a few exceptions, only tri- through hexaCDFs were observed in the lower level runs, with a maximum generally at the triCDF homolog.

PCDFs and, to a lesser extent, PCDDs are formed from the trichlorobenzene dielectric fluid under the optimum PCB-to-PCDF conversion conditions. Up to > 110,000 ng total PCDFs/mL feed oil (> 0.004% yield) and 1,900 ng total PCDD/mL feed oil (0.0001% yield) were observed for the trichlorobenzene runs. The homolog distribution of PCDFs is similar to that found from feeding PCBs. The amount of PCDFs formed is one to two orders of magnitude lower than for the askarel, but substantially higher than that for dielectric fluid containing 500 ppm or less PCBs.

The results of this work indicate that the optimum conditions for PCDF formation from PCBs are near 675°C for 0.8 s or longer, with 8% excess oxygen. Under these conditions, PCDFs are formed from mineral oil or silicone oil contaminated with PCBs at 5 ppm or greater. PCDFs are also formed from a trichlorobenzene dielectric fluid which contained no detectable PCBs.

III. RECOMMENDATIONS

Further work on the Phase 3 sample extracts can yield important additional information. These samples should be analyzed by full scan HRGC/EIMS to (a) identify any other products of the thermal destruction, (b) confirm the identity and amount of the PCDFs and PCDDs detectable by this technique, and (c) attempt to identify and quantitate the polychlorinated biphenylenes (PCBPs).

Additional statistical treatment of the data may be useful, especially if the full scan HRGC/EIMS analysis yields additional quantitative information.

Additional runs of the thermal destruction system should (a) replicate some of the runs reported here for QC purposes, (b) examine the PCDF formation from other PCB mixtures, specifically Aroclors 1242 and 1260, and (c) examine the formation of toxic products from other dielectric fluids, such as tetrachloroethylene and HTH. Since the formation of PCDFs, PCDDs, and other toxic products from the non-PCB fluids likely occurs via different reaction mechanisms, the optimum conditions established for PCBs in Phase 2 may not be appropriate for these fluids. Additional optimization runs should be conducted for these fluids. This optimization should also be conducted on the chlorobenzene fluid for which there are preliminary results in this report.

If additional information becomes available on the actual conditions in transformer fires, the thermal destruction system could be operated at these conditions to mimic the formation of toxic products during transformer fires.

IV. BACKGROUND

A. PCDF Occurrence in PCB Fires

A number of fires involving electrical equipment containing PCBs have been reported in Europe and the United States. Following a capacitor fire in Sweden in 1978, Jansson and Sundstrom (1982) determined that the amount of PCDF in the PCB oil had increased from about 1 µg/g before the fire to an average concentration of 81 µg/g after the fire. Jansson and Sundstrom also reported their analysis of the soot from a transformer fire in Toronto (Canada) in 1979. The soot from this fire contained PCDF at 5 µg/g soot. As an aftermath of an electrical fire in Binghamton (New York) in 1981, soot was spread throughout an office building. Soot samples were analyzed by two groups of researchers (Smith et al. 1982) and 2,3,7,8-TCDF was determined in the samples in the range of 3.7 to 2,160 ppm. Rappe et al. (1983) discuss the results of analyses of PCDFs from various combustion sources. They reported the results of the analysis of wipes from a metal treatment factory in Skövde (Sweden) taken after an electrical fire in which 12 capacitors were damaged. The results showed total tetrachlorodibenzofurans at 1 to 600 ng/m^2 and pentachlorodibenzofuran at < 1 to 100 ng/m^2. No other PCDFs were detected above 100 ng/m^2. Previously unpublished data from a number of other electrical fires were presented in a state-of-the-art review by Vuceta et al. (1983). The PCDF concentrations detected in transformer oils and in soot from electrical fires indicate that chlorinated dibenzofurans are formed in electrical fires and may pose a significant threat of exposure (USEPA 1984).

B. Reaction Mechanisms

The formation of polychlorinated dibenzofurans by air oxidation of PCBs has been studied by only a few researchers. Morita (1977) reported that heating Aroclor 1248 to 300°C in a sealed glass ampule for 2 weeks produced approximately a four-fold increase in the amount of PCDF in the Aroclor.

Morita again reported on the formation of PCDFs in Aroclor 1248 in 1978 (Morita et al. 1978). In the presence of oxygen, PCDF formation began when samples were heated for 1 week above 270°C, reaching a maximum of approximately 0.2% conversion at 300°C. Dichloro- and trichlorodibenzofurans were also formed from the tetrachlorobiphenyls in Aroclor 1248. Reaction mechanisms involving the loss of Cl_2 or HCl were postulated from the observations.

Buser et al. (1978) reported the formation of PCDFs from three individual PCB isomers. In these experiments, the PCB isomers were heated from room temperature to 550 or 850°C in about 55 s and held at these temperatures for 5 s. In these experiments, more than half of each of the chlorinated biphenyl congeners (2,6,2',6'-tetrachloro-, 2,4,5,2',4',5'-hexachloro-, and 2,4,6,2',4',6'-hexachloro-) had decomposed at 550°C. Decomposition was essentially complete above 650°C. The hexachlorobiphenyls formed tetrachloro- and pentachlorodibenzofurans at 550-650°C at yields of 0.1% to 1.6%. The tetrachlorobiphenyl formed dichloro- and trichlorodibenzofurans at 550° at yields of 1.6 to 2.5%, depending on the temperature. At temperatures above 700°C, apparent complete destruction of the PCDFs was observed. It was proposed from this work that a third reaction mechanism involving rearrangement was responsible for formation of some isomers.

In the work of Buser and Rappe (1979), 18 individual PCB isomers were pyrolyzed in the presence of air at 600°C in sealed ampules. The individual PCDF isomers formed were identified. From this study four thermochemical reaction mechanisms were proposed for formation of PCDFs from PCBs. The four reaction mechanisms and the observed reactions are shown below.

1. Mechanism 1: Loss of Ortho-Cl_2

Example:

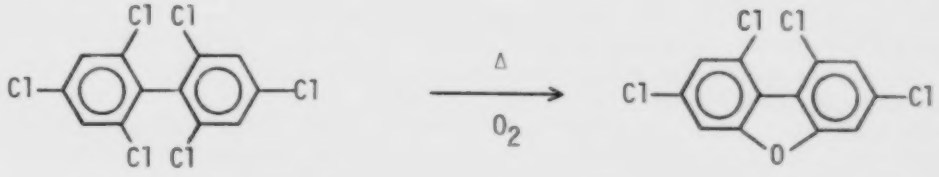

2,4,6,2',4',6'-Hexachlorobiphenyl 1,3,7,9-Tetrachlorodibenzofuran

2. Mechanism 2: Loss of HCl Involving 2,3-Chlorine Shift at the Benzene Nucleus

Example:

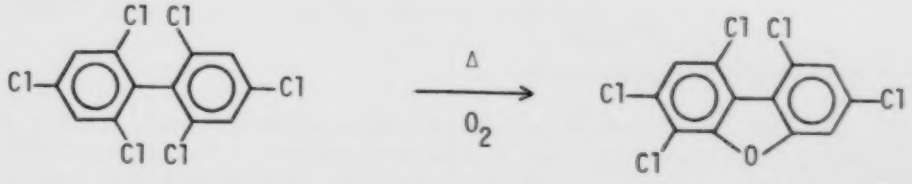

2,4,6,2',4',6'-Hexachlorobiphenyl 1,3,4,7,9-Pentachlorodibenzofuran

3. Mechanism 3: Loss of Ortho-HCl

Example:

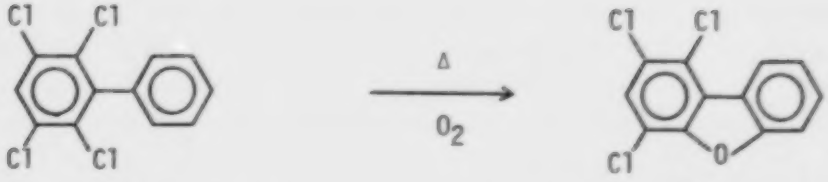

2,3,5,6-Tetrachlorobiphenyl 1,2,4-Trichlorodibenzofuran

4. Mechanism 4: Loss of Ortho-H_2

Example:

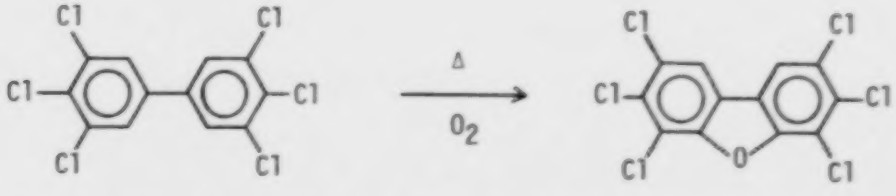

3,4,5,3',4',5'-Hexachlorobiphenyl 2,3,4,6,7,8-Hexachlorodibenzofuran

The results observed by Buser and Rappe are summarized in Table 1, which lists each chlorinated biphenyl isomer, its chlorinated dibenzofuran reaction products, and the associated thermochemical reaction mechanism.

The studies of PCDF formation from PCBs are continuing. In his review of PCDD and PCDF analyses, Rappe (1984) cites recent results giving further support to thermochemical generation of PCDFs from PCBs. Rappe's review also discusses the work of Buser (1979) in which PCDF and PCDD formation was observed during the sealed ampul pyrolysis of chlorobenzenes. Buser reported a complex mixture of PCDD and PCDF isomers with a thermochemical conversion of approximately 1%.

C. Relationship of Conditions to PCDF Formation

Morita et al. (1978) and Buser et al. (1978) each reported on the conditions which produced maximum formation of chlorinated furans and the conditions at which these furans were subsequently destroyed. Morita studied PCDF formation from PCBs heated to 250 to 330°C for 3 to 28 days in air, oxygen, and nitrogen atmospheres. The optimum furan formation conditions were found by heating Aroclor 1248 in an oxygen atmosphere for 1 week at 300°C. Under these conditions, a conversion rate of 0.2% was achieved. However, the yield was quite temperature-dependent. At 270 and 330° the furan yields were 100 times less than at the 300° optimum. When the Aroclor 1248 was heated to 300° in an air atmosphere, the optimum furan formation was not achieved until after 14 days of heating. Only 0.04% of the PCBs were converted to PCDFs.

Table 1. Thermochemical Conversion of PCBs to PCDFs
(From Buser and Rappe, 1979)

Reaction mechanism	PCB congener studied	PCDF reaction products
4	2,3,4,5-	1,2,3,4-[a]
3		2,3,4-[a,b]
3	2,3,5,6-	1,2,4-[a]
2	2,6,2',6'-	1,4,9-[a,b]
1		1,9[a]
3	2,3,4,5,6-	1,2,3,4-[a]
1	2,4,5,2',5'-	2,3,8-[b]
2	2,4,5,2',5'-	2,3,6,8- and 2,3,4,8[a]
3	2,4,5,2',5'-	2,3,6,9-[a] and 1,3,4,8-[a]
4	2,4,5,2',5'-	1,3,4,6,9[a]
3	2,4,5,3',4'-	2,3,7,8-[b] and 2,3,6,7-[a]
4	2,4,5,3',4'-	1,3,4,7,8- and 1,3,4,6,7-[a]
1	2,4,6,2',4'-	1,3,7-[b]
2	2,4,6,2',4'-	1,3,6,7- and 1,3,4,7-[a]
3	2,4,6,2',4'-	1,3,7,9-
1	2,3,6,2',5'-	1,4,8-[a,b] and 1,2,8-[a,b]
2		1,4,6,8-[a,b], 1,2,6,8-[a], and 1,2,4,8-[a]
3		1,2,6,9-[a] and 1,4,6,9-[a]
1	2,3,6,2',4',6'-	1,4,6,9-[a], 1,2,6,9-[a], and 1,2,8,9-[a]
2		1,2,4,8,9[b] and 1,2,4,6,9-[a,b]
4	3,4,5,3',4',5'-	2,3,4,6,7,8-
1	2,4,5,2',4',5'-	2,3,7,8-[b]
2		2,3,4,7,8-
3		1,3,4,7,8-
1	2,4,6,2',4',6'-	1,3,7,9-
2		1,3,4,7,9-

Table 1 (continued)

Reaction mechanism	PCB congener studied	PCDF reaction products
1	2,4,5,2',4',6'-	1,3,7,8-[a,b]
2		2,3,4,7,9-[a] and 1,3,4,7,8-
3		1,3,4,7,9-
1	2,3,4,2',3',4'-	3,4,6,7-
3		1,2,3,6,7-
1	2,3,5,2',3',5-	2,4,6,8-
3		1,2,4,6,8-
1	2,3,4,5,2',3',4'-	2,3,4,6,7-
3		1,2,3,4,6,7-[a], and 1,2,3,6,7,8[b]
4		1,2,3,4,7,8,9-[a]
?		1,2,3,4,6,7,8-[a] and 1,2,3,4,6,7,9-[a]
1	2,3,4,5,2',4',5'-	2,3,4,7,8-[b]
2		2,3,4,6,7,8-
3		1,2,3,4,7,8- and 1,3,4,6,7,8-[a,b]
4		1,2,3,4,6,7,9-[a]
1	2,3,4,5,2',3',4',5'-	2,3,4,6,7,8- and (other hexa)
3		1,2,3,4,6,7,8-[b]
4		Octachlorodibenzofuran

[a]Tentative isomer identification.
[b]Major isomer among reaction products.

The results reported by Buser et al. (1978) indicate that the optimum conditions for furan formation may be different for each reaction mechanism. When the reaction temperature was raised from 550 to 650°, the amount of chlorinated furan formed by loss of ortho-Cl_2 (Mechanism No. 1) decreased. However, the amount of furan formed by loss of ortho-HCl (Mechanism No. 3) increased. At a reaction temperature of 650 to 700°, no chlorinated furans were detected. The reaction time for all of Buser's experiments was stated to be 5 s. However, a 55-s heating period and an undefined cooling period may imply that the PCBs were hot enough for some PCBF formation for periods longer than 5 s (i.e., a minute or more).

The incidence of transformer fires, their effects, and the formation of PCDFs from PCBs under fire conditions were recently reviewed by USEPA (1984a) in the ANPR on use of PCBs in electrical transformers.

V. EXPERIMENTAL PLAN

A. Thermal Destruction System

MRI has developed a bench-scale thermal destruction test system which can be used to examine various combustion processes. It has also been used to provide data on the incinerability (i.e., destruction efficiency) of hazardous compounds in solid or liquid waste material, and to provide data on products of incomplete combustion that may be formed. This system can provide destruction data on gram-quantity samples of materials in either solid or liquid form or even semisolid materials, such as tars. In contrast, other related systems often can handle only very small quantities of pure compounds.

The system is described in detail in Section VI. Briefly, the system consists of a volatilizing/pyrolysis heater for the sample, an air preheater furnace, and the main combustion furnace (all electrically heated). Separate volatilization/pyrolysis furnaces are used for solid/semisolid feed and for liquid feed. Gas flow through the combustion furnace is laminar and can be varied to provide different gaseous residence times. The combustion temperature can also be varied, up to a maximum of 1200°C (2192°F).

Primary operating conditions that can be varied and controlled in this system are temperature, oxygen concentration, and residence time. Byproducts that can be determined include O_2, CO_2, CO, and total hydrocarbons (by continuous monitoring) and volatile or semivolatile organic compounds (by adsorption and concentration in a sampling trap, followed by extraction or desorption and analysis). The system has been operated using continuous injection (for liquid feed) and by batch feeding (for solid feed). For this program, continuous liquid injection of feed was used.

B. Phase 1 - System Refitting and Preliminary Runs

Prior to testing with PCBs, the system had to be refitted to accommodate the special needs of this project and then tested without feeding PCBs to ensure proper operation of the system and to assess the system blank for interfering compounds and background levels of PCBs, PCDFs, and other analytes of interest.

C. Phase 2 - Experimental Optimization

1. Operational Conditions

Experiments in this phase were to investigate the influence of combustion conditions on PCDF formation. The conditions which were to be varied were oxygen concentration, incineration temperature, and residence time. The other factors, the PCB concentration and matrix effects, were to be investigated in Phase 3. Each parameter was initially evaluated at three levels, high, medium, and low.

2. Values of Evaluation Parameters

The incineration temperature was to be evaluated at three levels.

High - 750°C
Medium - 600°C
Low - 450°C

These selected values were based on the PCDF formation conditions reported in the literature.

The excess oxygen content, as measured after the combustion furnace, was to be evaluated at three levels.

High - as large an excess as is feasible (e.g., 16%)
Medium - about 3%
Low - essentially 0%

These levels span the range of possible conditions in a fire, from oxygen-rich to oxygen-starved.

The residence time was to be evaluated at three values.

High - 1.5 s
Medium - 0.8 s
Low - 0.3 s

These times span the operating range of the bench-scale reaction system. These values will either identify an optimum residence time, or as a minimum, show a trend line. It is not known how closely they approximate the residence time of a PCB in a specific temperature region of a fire.

3. Experimental Design and Analysis of Results

The primary goal is to determine the values of temperature, oxygen concentration, and residence time that will produce a maximum PCDF yield. Under the assumption that the runs can be made sequentially and that the GC/MS results can be obtained in time to plan the subsequent runs, a sequential approach to the experimental design is the most efficient means of identifying the optimum conditions.

The range of each factor was initially divided into three levels with L, M, and H denoting the low, medium, and high levels of a given factor. A complete factorial design of the three factors at three levels would entail $3^3 = 27$ experiments. The levels selected represent points on a continuum. The optimum is probably not precisely at one of the three values selected, so an efficient method for converging on the optimum parameters was sought. If only two levels (say L and M for purposes of demonstration) are selected, the trend of the PCDF formation can be assessed with a complete 2^3 factorial design (8 runs). Even more efficiently, a half-fractional design (4 runs) can still show the trends. An example half-fractional design is:

Run	Temperature	Oxygen	Residence Time
1	L	L	L
2	L	M	M
3	M	L	M
4	M	M	L

Although this example used L and M values for all three parameters, other combinations could be used (e.g., L, M; M, H; L, H).

The results from the four runs listed above can yield one of four conclusions:

(1) The response (PCDF yield) increases as the level increases for all three factors;

(2) The response increases as the level increases for two of the three factors, and decreases with increasing level of the third factor;

(3) The response increases as the level increases for one factor and decreases with increasing level of the other two factors; or

(4) The response decreases as the level increases for all three factors.

If situation (1) arises, the data imply that the optimum for all three parameters is between M and H. Therefore, the logical choice of a level for the next iteration is the midpoint between M and H: (M + H)/2. The second set of four runs would then be:

Run	Temperature	Oxygen	Residence Time
5	(M + H)/2	(M + H)/2	(M + H)/2
6	(M + H)/2	M	M
7	M	(M + H)/2	M
8	M	M	(M + H)/2

The results of runs 5 through 8 will again yield one of the four situations above. This process of iteration and narrowing the interval of the values should result in a rapid convergence to the optimum values.

If situation (2) arises, the second iteration of the half-fraction of the 2^3 design would entail changing the low level of the two factors showing increasing response with increasing levels to (M + H)/2, and changing the low level of the third factor to (M + L)/2.

If situation (3) arises, one can proceed as in (2) with one substitution of L to (M + H)/2 and two of L to (M + L)/2.

If situation (4) arises, the second iteration would be designed by substituting all L levels with (M + L)/2.

This procedure can theoretically be iterated until the optimum combination of levels of the three factors which yields the highest response is found. After the first set of four runs, the maximum is likely to be within R/2 for each factor, where R denotes the range for a given factor. After a second set of four runs, it is likely to be within R/4. After a fourth set of runs, it is likely to be within R/16 on each variable. Thus, the best a priori knowledge about the ranges of the different factors will accelerate the convergence process to locate the solution.

The procedure described above can allow for readjusting the upper or lower limit of the factor ranges, if necessary. This might be necessary if the ranges were chosen without sufficient data. For example, if the optimum residence time is higher than 1.5 s, then one could raise the upper limit in subsequent iterations, subject to limitations imposed by the reaction system.

In the absence of problems, two runs can be made per day, and the results from the GC/MS can be obtained about 3 days later. This would then require a week for the results from four runs and thus require at least a 3-day shut-down of the thermal destruction facility between each set of runs. In view of the project deadlines, these delays would have been intolerable. Therefore, after the first set of four runs, a second set was to be conducted immediately thereafter. This second set of four runs would begin with the other half-fraction of the 2^3 factorial design, using the medium-high combination if the first sequence used low-medium. As the experiments progress, the results of both sequences were to be considered and the levels of the factors adjusted appropriately. Since at each stage the next set of runs was to be determined on only that part of the data that was available from the GC/MS analysis, convergence may not have been as efficient, but was more rapid.

4. Selection of Compounds for Evaluation

The Phase 2 incineration tests were performed using individual PCB congeners rather than an Aroclor mixture. This approach simplified the chemical analysis and data evaluation associated with selecting the optimum conditions for use in Phase 3. The use of specific congeners also allowed assessment of the PCDF formation via all four proposed reaction mechanisms (Buser and Rappe 1979). Optimization using a commercial mixture such as Aroclor 1254 would likely have generated a confusing array of products.

Three PCB congeners were selected for the Phase 2 experiments:

(a) 2,3,5,6-tetrachlorobiphenyl,
(b) 3,4,,5,3',,4',5'-hexachlorobiphenyl, and
(c) 2,4,6,2',4',6'-hexachlorobiphenyl.

The first compound, 2,3,5,6-tetrachlorobiphenyl (Ballschmiter No. 65), forms 1,2,4-trichlorodibenzofuran by loss of ortho-HCl (Mechanism No. 3). The compound 3,3',4,4',5,5'-hexachlorobiphenyl (No. 169) forms 2,3,4,6,7,8-hexachlorodibenzofuran by loss of ortho-H_2 (Mechanism No. 4). The final compound, 2,2',4,4',6,6'-hexachlorobiphenyl (No. 155), forms two PCDF reaction products in nearly equal amounts (Buser et al., 1978). The reaction product 1,3,7,9-tetrachlorodibenzofuran is formed by loss of ortho-Cl_2 (Mechanism No. 1) and 1,3,4,7,9-pentachlorodibenzofuran is formed by loss of HCl with a 2,3-chlorine shift at the benzene nucleus (Mechanism No. 2).

Using these three PCB congeners, only four chlorinated dibenzofurans should be formed and each thermochemical reaction mechanism could be studied. The identification of thermochemical reaction products was also simplified since only one each of the tri-, tetra-, penta-, and hexachlorodibenzofurans are produced. In the one reaction mechanism where two products are formed (2,2',4,4',6,6'-hexachlorobiphenyl to 1,3,7,9-tetrachlorodibenzofuran and 1,3,4,7,9-pentachlorodibenozfuran), these two products are produced in nearly equal amounts (Buser and Rappe 1979). Although the PCB congeners chosen for Phase 2 are not found in Aroclors at significant levels, these compounds are commercially available and produce a single isomer of each PCDF homolog as reaction products using all four reaction mechanisms. Hence, they were appropriate for the proposed range-finding experiments.

D. Phase 3 - Aroclor 1254 Test Runs

During Phase 3, PCBs in dielectric fluids were to be subjected to the conditions determined to be optimal for PCDF formation in Phase 2. The PCB mixture chosen was Aroclor 1254, a commercial mixture commonly used in transformer askarels. The concentrations were to range from 5 ppm to about 70% PCB. The samples used were:

(a) 50 ppm PCB in mineral oil,
(b) 50 ppm PCB in silicone oil,
(c) 500 ppm PCB in mineral oil,
(d) 500 ppm PCB in silicone oil,
(e) Chlorobenzene dielectric fluid,
(f) 5 ppm PCB in mineral oil,
(g) 5 ppm PCB in silicone oil, and
(h) Used askarel-type dielectric fluid (e.g., 70% Aroclor 1254/30% trichlorobenzene, Type D).

VI. EXPERIMENTAL METHODS

A. Reagents and Supplies

1. PCBs

In Phase 2, three PCB isomers--2,3,5,6-tetrachlorobiphenyl, 3,3',4,4',5,5'-hexachlorobiphenyl, and 2,2',4,4',6,6'-hexachlorobiphenyl--were added to the mineral oil (Exxon HPLX 355077) feed. These compounds were purchased from Ultra Scientific. The concentrations of the feed solutions are presented in Table 2.

Table 2. Concentrations of PCB Congeners in Mineral Oil for Phase 2

Run no.	Concentrations (mg/mL) 2,3,5,6-Tetrachlorobiphenyl	3,3',4,4',5,5'-Hexachlorobiphenyl	2,2',4,4',6,6'-Hexachlorobiphenyl
5-7	0.54	0.37	1.08
8-14	0.51	0.48	1.2
15-27	0.50	0.46	1.0
28-38	0.59	0.59	1.2

Four types of dielectric fluids were fed during Phase 3: mineral oil, silicone oil, a chlorobenzene fluid, and an askarel. The mineral oil (Exxon type HPLX 355077) and silicone oil (Union Carbide type L-305) were spiked with Aroclor 1254 at 5 to 500 ppm. The actual concentrations spiked are shown in Table 3. The chlorobenzene fluid (mostly trichlorobenzene isomers with some tetrachlorobenzene, Electro-Chem FR-15, Standard Chlorine Chemical Company, Kearney, New Jersey) and askarel (PPM, Inc., Kansas City, Missouri) were run without modification. The askarel was obtained from a transformer draining operation and was characterized (by MRI) as containing 70% Aroclor 1260 and the balance trichlorobenzenes.

Table 3. Concentrations of Aroclor 1254 in Feed Samples Used in Phase 3

Run type	Run no.	Concentration of Aroclor 1254 in feed (μg/g)
5 ppm Mineral oil	43, 44	5
5 ppm Silicone oil	47, 48	5
50 ppm Mineral oil	45, 46	50
50 ppm Silicone oil	49, 50	50
500 ppm Mineral oil	39, 40, 41	500
500 ppm Silicone oil	51, 52	500

2. Calibration Gases

A Scott Specialty Gases Acublend mixture of 15.05% O_2, 12.34% CO_2, and 2,069 ppm CO was used during Phase 2 and part of Phase 3. A second Acublend mixture with 15.11% O_2, a lower CO_2 concentration of 4.10%, and a higher CO concentration of 3,987 ppm was used for the remaining Phase 3 runs.

3. Surrogates, Standards, Reagents, and Adsorbents

Surrogate spiking compounds, ($^{13}C_{12}$)-2,3,7,8-tetrachlorodibenzofuran and ($^{13}C_{12}$)-2,3,7,8-tetrachlorodibenzo-p-dioxin, were purchased from Cambridge Isotopes. During Phase 3 a column recovery surrogate solution was also used. This column recovery mixture was purchased from KOR Isotopes and contained a mixture of ^{37}Cl-labeled tetrachlorodibenzofurans and pentachlorodibenzofurans.

Tetrachlorodibenzofurans were quantitated against a standard purchased from Cambridge Isotopes containing unlabeled 2,3,7,8-tetrachlorodibenzofuran. Tetrachlorodibenzodioxins were quantitated against a 2,3,7,8-tetrachlorodibenzodioxin standard reference solution (Lot No. 20603-01/83) supplied by the EPA Quality Assurance Materials Bank, EMSL-LV.

All solvents used for extraction, probe rinses, and sample cleanup were Burdick and Jackson "Distilled-in-Glass" grade. The 100-200 mesh acid alumina used for sample cleanup was Part No. AG-4 purchased from Bio-Rad Laboratories. The silica gel used for sample cleanup was Kieselgel 60 (70-230 mesh) purchased from L. M. Reagents.

Each 200-g batch of XAD-2 (Supelco) resin was precleaned by successive washing in a continuous extraction column with:

- One liter distilled water
- One liter 0.1 N sodium hydroxide
- One liter distilled water
- One liter 0.1 N hydrochloric acid
- One liter distilled water
- One liter methanol (2 times)

The resin was then Soxhlet-extracted 24 h with methanol, followed by 24-h Soxhlet extractions with acetonitrile, and methylene chloride. It was then placed into a container with a screw-cap top and dried in a vacuum oven at 110°C for several hours. The container was capped immediately upon removal from the oven. The resin was stored under methanol in a tightly capped jar until it was loaded into the sampling cartridges.

B. Destruction Facility Operation

1. System Refitting

A schematic diagram of the MRI laboratory-scale system is shown in Figure 1. The system was previously used in a batch fed mode of operation. For the current program, the system was first refitted to the continuous liquid injection mode. This operation involved disassembly at the tee located near the incineration furnace inlet, removal of the vaporization/ pyrolysis furnace chamber (tube section) used for batch fed operation, replacement of the vaporization/pyrolysis furnace chamber (tube section) used for continuous liquid injection, installation of the pumping system (syringe pump, polytetrafluoroethylene lines, and flowmeter), and replacement of all heating tape and insulation. While disassembled, all tubes and chambers were cleaned with solvent and allowed to dry. All connections and fittings were carefully inspected and replaced if defective. The system was then reassembled and leak checked.

Modifications were also performed at the outlet side of the incineration furnace. The condensation tube was modified so that it was heated to ~ 300°C above a compression nut fitting. A short length (6-12 in.) of 3/4 in. stainless steel tubing was attached at the compression nut fitting. The other end of the tube was connected to a ball joint fitting that attaches to the XAD-2 trap. This section allows cooling of the heated gases prior to entry of the XAD-2 trap and forms part of an interchangeable sampling train assembly. Thus any PCDFs that condense in the cool-down tube are recovered during the rinse of the train.

After reassembly of the system, the furnaces were operated at high temperature for several hours, with air, to bake out any organic residues.

2. Feed Oil

The composition and nature of the various dielectric fluids that were subjected to thermal decomposition during this program are discussed in Section V.

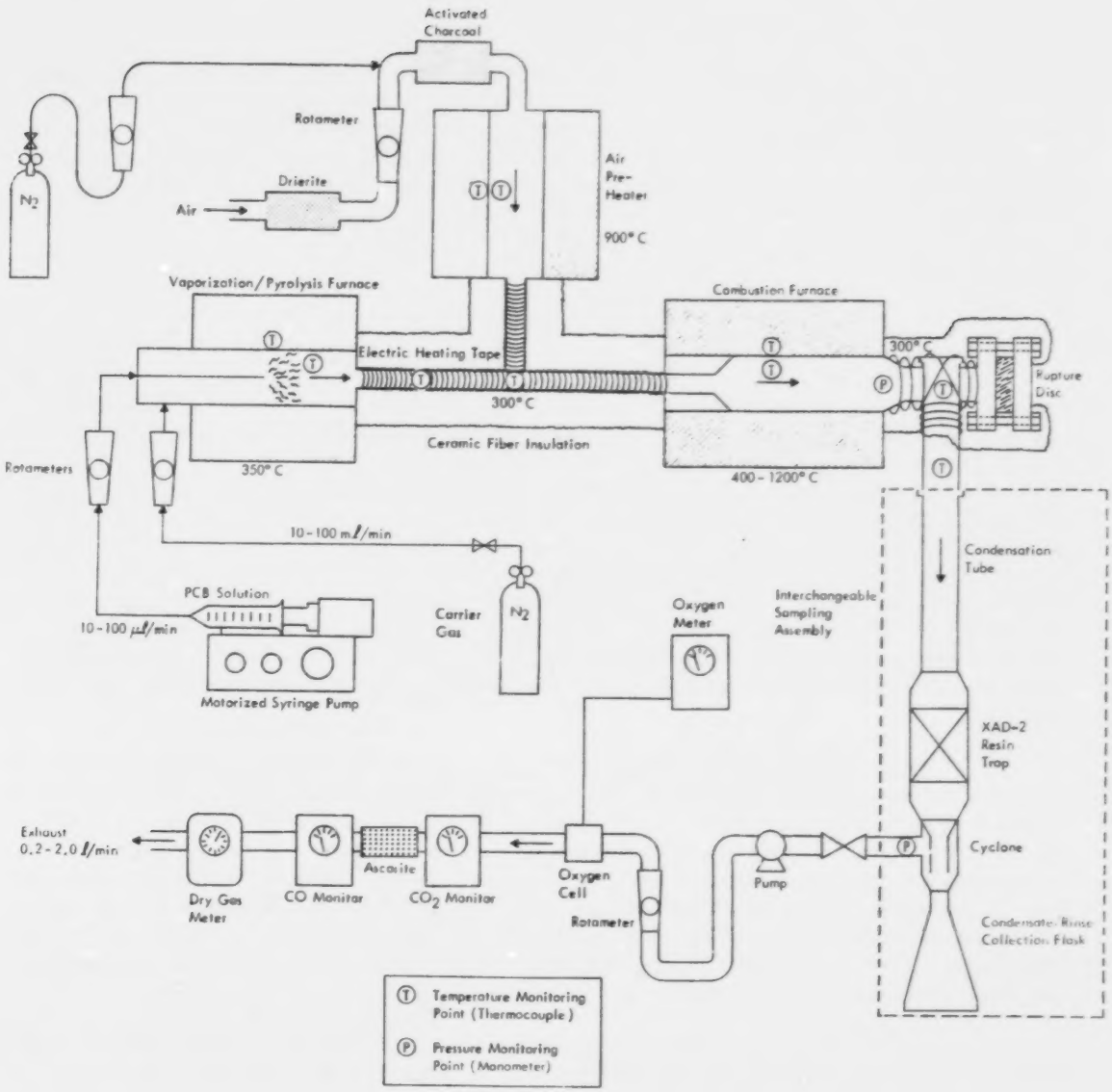

Figure 1. Laboratory-scale combustion system.

The fluid feed rate was maintained at a constant 13.5 μL/min for all of the runs. The constant displacement pumping system consisted of a syringe pump (Sage Instrument Model 355) and 30-mL glass syringe with a PTFE-tipped plunger (Manostat P5178-30-L Varipet). Narrow-bore PTFE tubing (1/16 in. ID) connected the pumping system to the thermal destruction system, passing the feed through a flow meter (Manostat 36-541-03) that verified constant flow. The pump/syringe combination was calibrated by pumping a liquid of known density (mineral oil) through the system into a vial which was placed on a top-loading analytical balance. The weight of the pumped liquid was periodically recorded to verify both the amount of oil pumped and the consistency of the flow rate.

3. Thermal Destruction System

a. System Description

As discussed above, the system was operated in a continuous injection mode, using a motorized syringe pump to slowly feed a liquid into a vaporization/pyrolysis furnace (see Figure 1). The vaporization/pyrolysis furnace consisted of a section of 3/4-in. stainless steel pipe heated by an electric tube furnace to a nominal operating temperature of 300°C. The feed oil solution entered the heated pipe section in the center of the furnace via a 1/16-in. diameter section of stainless steel tubing connected to the pipe with appropriate reducers. A small flow of inert carrier gas (prepurified nitrogen) entered the vaporization/pyrolysis furnace as shown and continuously purged the chamber of vaporized waste. The flow rate used for this carrier gas was a constant 0.05 L/min. These gases exited the vaporization/pyrolysis furnace through a 1/4-in. diameter Inconel® tube.

A mixture of prepurified nitrogen and room air was first passed through a charcoal trap and then preheated (nominally to 900°C) before mixing with the waste vapors at a tee (maintained at 300°C). The resulting mixture was passed through a short section of 1/4-in. diameter Inconel® tubing into the combustion furnace where exposure of the waste/air mixture occurred at a constant elevated temperature for a predetermined residence time. The combustion furnace consisted of a section of 3/4-in. Inconel® pipe, heated by a larger electric tube furnace. The effective volume of the incineration furnace was $\sim$ 50 cm^3. A rupture disk was provided at a point just outside the combustion furnace as a safety measure, should any explosive condition arise in the furnace.

The temperature profiles of both the pyrolysis furnace and the combustion furnace were determined by measuring gas temperatures at incremental distances using a thermocouple probe. This characterization of the furnaces was performed prior to running any destruction tests. The permanent locations for thermocouples inside these furnaces was selected from the results of those studies. Also, the effective volume of the incineration furnace was determined by multiplying the cross-sectional area enclosed by the Inconel® pipe by the axial distance through the electric tube furnace in which at least ± 25°C of the desired temperature was maintained. The mean gaseous residence time was determined by dividing this effective volume by the temperature-corrected total gas flow rate through the furnace. Figure 2

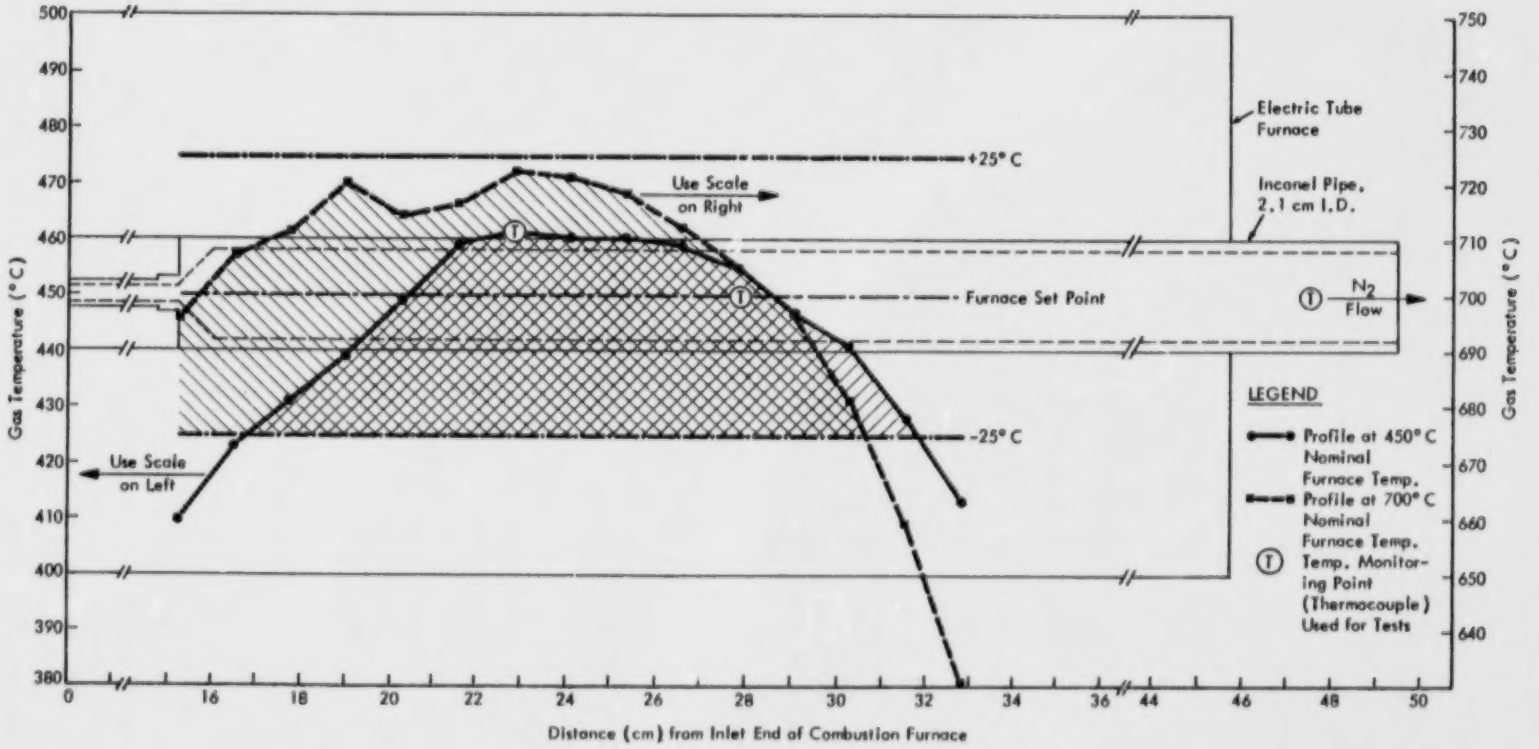
Gas Temperature (°C)
Gas Temperature (°C)
Distance (cm) from Inlet End of Combustion Furnace
+25° C
-25° C
Use Scale on Right
Use Scale on Left
Furnace Set Point
Electric Tube Furnace
Inconel Pipe, 2.1 cm I.D.
N2 Flow
LEGEND
Profile at 450° C Nominal Furnace Temp.
Profile at 700° C Nominal Furnace Temp.
Temp. Monitoring Point (Thermocouple) Used for Tests

Figure 2. Temperature profiles in combustion furnace.

shows the profiles of the combustion for two furnace temperature set points, using a typical gas flow rate. The method of obtaining the effective distance (length) of the retention volume is illustrated by the shaded regions. A length of 15 cm was used to calculate the effective furnace volume for all runs in Phases 1, 2, and 3.

After exiting the combustion furnace, the effluent gases passed through a vertical section of 3/4-in. stainless steel pipe where cooling of the hot gases occurred. After cooling in this condensation tube, the gas stream entered an XAD-2 adsorbent resin sampling trap that collected semivolatile organic compounds. The sampling system is described in detail below. A vacuum pump pulled the gases through the sampling train.

The gases then passed sequentially through continuous gas monitors for oxygen (O_2), carbon dioxide (CO_2), and carbon monoxide (CO) determination. The operation of these instruments is described below. The gases were pumped through a dry gas meter (Singer Model 817) before venting into a Class A laboratory fume hood.

Water manometers were used to monitor the pressure of the combustion furnace relative to atmospheric pressure and also the pressure drop across the XAD-2 sampling trap (to indicate plugging of the trap). Locations of pressure sensing points are shown in Figure 1 above.

Thermocouples were used to monitor both refractory and internal gas temperatures in the vaporization/pyrolysis furnace, the makeup air heater, and the combustion furnace. Gas temperatures were also monitored in the vaporization/pyrolysis furnace outlet, the tee (combustion furnace inlet), and the combustion furnace outlet, and the condensation tube inlet. Electrically powered heating tape maintained the gas temperature on either side of the incineration furnace near 300°C. Locations of all thermocouples in the system are also shown in Figure 1.

b. System Operation

The generalized operating procedures for the destruction system are as follows. At the beginning of each working day, the entire system was first leak-checked. All furnaces and heaters were then turned on at desired settings and allowed to warm up.

The nitrogen carrier gas, used to purge the vaporization/pyrolysis furnace, was started and the flow rate checked for stability. The pump was turned on and the total flow rate adjusted to pull air through the system for the desired temperature-corrected residence time in the combustion furnace.

The combustion system was fitted with a special assembly similar to the XAD-2 sampling train assembly, which contained activated charcoal and XAD-2 resin as adsorbents for organic compounds. This served as a safety measure for operating periods when a test was not actually being conducted. This provided for capture of any toxic compounds in the effluent gases while the facility was in operation, and no test was in progress. The activated charcoal was replaced routinely and disposed of as hazardous waste.

The continuous gas monitors were calibrated with standards and zeroed as necessary. The ratio of air and nitrogen in the makeup gas heater was then adjusted so that the effluent O_2 concentration was near the desired operating value. Final adjustment for effluent O_2 occurred after flow of the feed oil was started and the continuous monitors had stabilized. A detailed discussion of the continuous gas monitor operation is provided below.

The syringe pump was loaded with the desired sample and the pump was started when the proper operating conditions were achieved. When all operating conditions were stabilized after adding feed oil flow, a sampling train assembly (described below) was installed, replacing the assembly containing activated charcoal. This step marked the beginning of a test run. Once the sampling train was installed, the test start time and initial gas meter volume were recorded in a laboratory notebook. Operating data were recorded every 10-15 min, including feed oil flow rate, total gas flow rate, nitrogen carrier gas flow rate, makeup airflow and nitrogen rates, continuous gas monitor readings, and appropriate pressures and temperatures.

After sampling for the desired time (typically 60 min), the test was concluded by removing the sampling train assembly and replacing it with the activated charcoal assembly. The ending time and final gas meter volume were then recorded. Appropriate changes in operating conditions were made and the system allowed to stabilize before another run was initiated.

Quality control measures were integrated into the preparation of the system for this program and also into daily operations. During the refitting activities, temperature profiles were checked, flow meters and dry gas meters calibrated, and the system checked for leaks to ensure proper performance. During each test run, the operation was checked by monitoring the pressure and temperature sensors. Temperature and flow rate were monitored and recorded at least every 15 min. All of the continuous monitors were calibrated and checked according to either manufacturer's instructions or in-house standard operating procedures (SOPs). In addition, some of the test runs were blank (no feed) runs to check carryover of analytes in the system.

Before any organic samples were collected, the combustion system was operated under a variety of conditions during preliminary testing. Only after the system was demonstrated to be capable of performing under most of the operating conditions desired for this program did testing commence.

4. Sample Collection

An interchangeable sampling system was designed, and several units were fabricated and tested before use. This sampling system consists of a stainless steel condensation tube, XAD-2 trap, cyclone, condensate collection flask, and appropriate fittings and transitions. The sample collection system for the thermal destruction tests is outlined by dashed lines in Figure 1, showing its relationship to the rest of the thermal destruction system. All effluent gases were drawn through this sampling train.

The sampling system was designed to collect all organic constituents of interest. Condensation of these organic compounds prior to entering the sampling system was prevented by maintaining the incinerator exit above 300°C. A thermocouple was used to monitor the gas temperature immediately ahead of the sampling assembly. The condensation tube provided a temperature gradient from > 300° to ambient, before the effluent gases entered the sorbent trap.

Each effluent sample consisted of two parts: the XAD-2 resin cartridge and a solvent rinse of the sample collection apparatus. Following each experimental run, the XAD-2 trap was removed from the sampling assembly, the ends capped with precleaned aluminum foil, and the trap labeled. The condensation tube was then clamped to the sampling cyclone, and the entire assembly rinsed with acetone and cyclohexane. The solvent rinse was collected in a precleaned labeled bottle. Both the XAD-2 trap and rinse sample were stored at 4°C until the samples were prepared for analysis.

5. Continuous Monitoring of O_2, CO_2, and CO

The O_2, CO_2, and CO concentrations in the effluent gases were continuously monitored during each run. The O_2 concentration is an evaluation parameter selected for Phase II experiments. The CO_2 and CO concentrations were measured in the effluent gas so that the combustion efficiency could be calculated. These monitors and their operation are described below.

Oxygen was measured using a Beckman 7003 polarographic analyzer. In this type of analyzer, oxygen diffuses across a membrane to a cathode where it is electrochemically reduced. This results in a current flow proportional to the partial pressure of oxygen in the sample. The instrument can operate in four ranges, 0-1%, 0-5%, 0-10%, and 0-25% O_2. Calibration was performed by spanning with a specific calibration gas and zeroing with nitrogen gas. Instrument precision of 0.3% absolute concentration or ± 6% of a measured concentration, whichever is greater, at 95% confidence intervals, can be obtained, according to the manufacturer's specifications.

The Horiba Model PIR-2000S carbon dioxide analyzer uses a nondispersive infrared (NDIR) method of detection. The instrument can operate in three ranges, 0-5%, 0-15%, and 0-25% CO_2. Concentrations can be read directly on a meter and also displayed on a recorder. Calibration is performed by spanning with a calibration gas at the desired concentration and zeroing with nitrogen gas. Instrument precision of < 0.1% absolute concentration or ± 0.6% of a measured concentration, whichever is greater, at 95% confidence intervals, can be obtained, according to the manufacturer's specifications.

A Horiba PIR-2000L carbon monoxide analyzer also uses an NDIR detector. A silica gel/Ascarite cartridge was used to remove interferences such as CO_2 and water.

Multicomponent standard gas mixtures were used to concurrently calibrate all three instruments. Two tees in the sample line allowed the sample stream from the reaction system to be vented and the calibration gas to be directed to the monitors. This allowed a calibration of the instruments to be done immediately before and after each run.

A data-logging system, consisting of an Epson HX-20 portable computer with a Wintec MCS data interface, was used to collect and reduce the data for each run. Concurrently, a strip chart recorder for each monitor gave a real-time, visual indication of the state of the run. An advantage of the data-logging system was that it printed out a minute-to-minute quantitation of the three gases, automatically correcting for instrument nonlinearity and for CO_2 removal in the CO analyzer. In addition, the computer was able to estimate a corrected CO value up to 2-1/2 times the calibration span. Three records of the monitoring data are retained: the strip chart recording, the minute-to-minute run data from the computer, and the reduced data from the computer.

C. Chemical Analysis

Each effluent sample consisted of two parts, the XAD-2 resin cartridge and a solvent rinse of the sample collection apparatus. As shown in the analysis scheme in Figure 3, the XAD-2 samples were Soxhlet-extracted. This extract combined with the associated solvent rinse to make a combined effluent extract. The combined extract was evaporatively concentrated to 2 mL and one-half of each extract was cleaned by chromatography on acidified silica and acidified alumina. These cleaned extracts were analyzed for chlorinated biphenylenes, chlorinated dibenzodioxins, and chlorinated dibenzofurans. The fraction of each extract which had not been cleaned up was analyzed for PCBs. Some of these extracts were screened for other chlorinated organics. The specific analysis procedures are given below.

1. Sample Extraction and Concentration

The contents of the XAD-2 resin trap were transferred from the sampling cartridge to a Soxhlet extractor. The resin was then spiked with surrogate compounds. During Phase 2, each XAD-2 resin was only spiked with 25 ng of ($^{13}C_{12}$)-2,3,7,8-tetrachlorodibenzofuran in isooctane. For Phase 3, each XAD-2 was spiked with the surrogate solution listed in Table 4. The resin samples were then extracted for approximately 16 h with benzene. This extract was combined with the rinse of the sampling apparatus and concentrated to < 5 mL using a Kuderna-Danish concentrator. Each extract was further concentrated to 2 mL under a gentle stream of dry nitrogen.

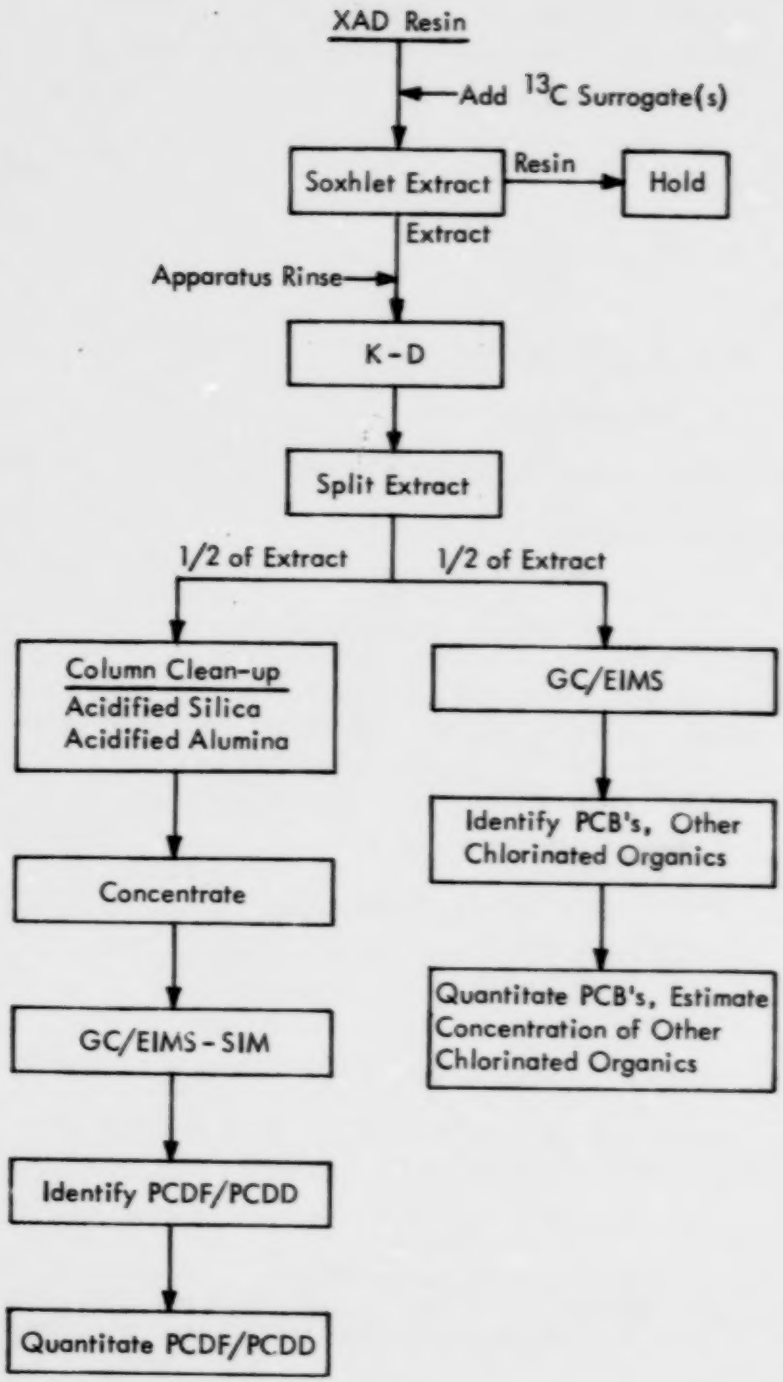

Figure 3. Sample analysis scheme.

Table 4. Phase 3 Surrogate Spiking Solution

Surrogate compound	Spiking level, ng
($^{13}C_{12}$)-2,3,7,8-TCDF	250
($^{13}C_{12}$)-2,3,7,8-TCDD	250
($^{13}C_{12}$)-OCDD	250
(1',2',3',4',5',6'-$^{13}C_6$)-4-Chlorobiphenyl	104
($^{13}C_{12}$)-3,3',4,4'-Tetrachlorobiphenyl	257
($^{13}C_{12}$)-2,2',3,3',5,5',6,6'-Octachlorobiphenyl	407
($^{13}C_{12}$)-Decachlorobiphenyl	502

2. Cleanup

One-half of each concentrated extract was cleaned by elution from a multi-phase column, shown in Figure 4, using the following elution procedure:

a. Add sample extract to top of column.

b. Elute with 45 mL of hexane.

c. Remove top (silica) column.

d. Elute lower column with 20 mL of hexane.

e. Archive eluate.

f. Elute with 20 mL of 50% dichloromethane in hexane.

g. Collect eluant, concentrate just to dryness, under a gentle stream of dry nitrogen. Redissolve residue in 0.5 mL isooctane.

h. Elute with 20 mL of $MeCl_2$ and archive eluate.

This cleanup procedure was monitored by observing the recovery of the two surrogate compounds ($^{13}C_{12}$)-2,3,7,8-TCDD and ($^{13}C_{12}$)-2,3,7,8-TCDF. The recoveries observed for the extraction and cleanup procedures were between 50 and 70%.

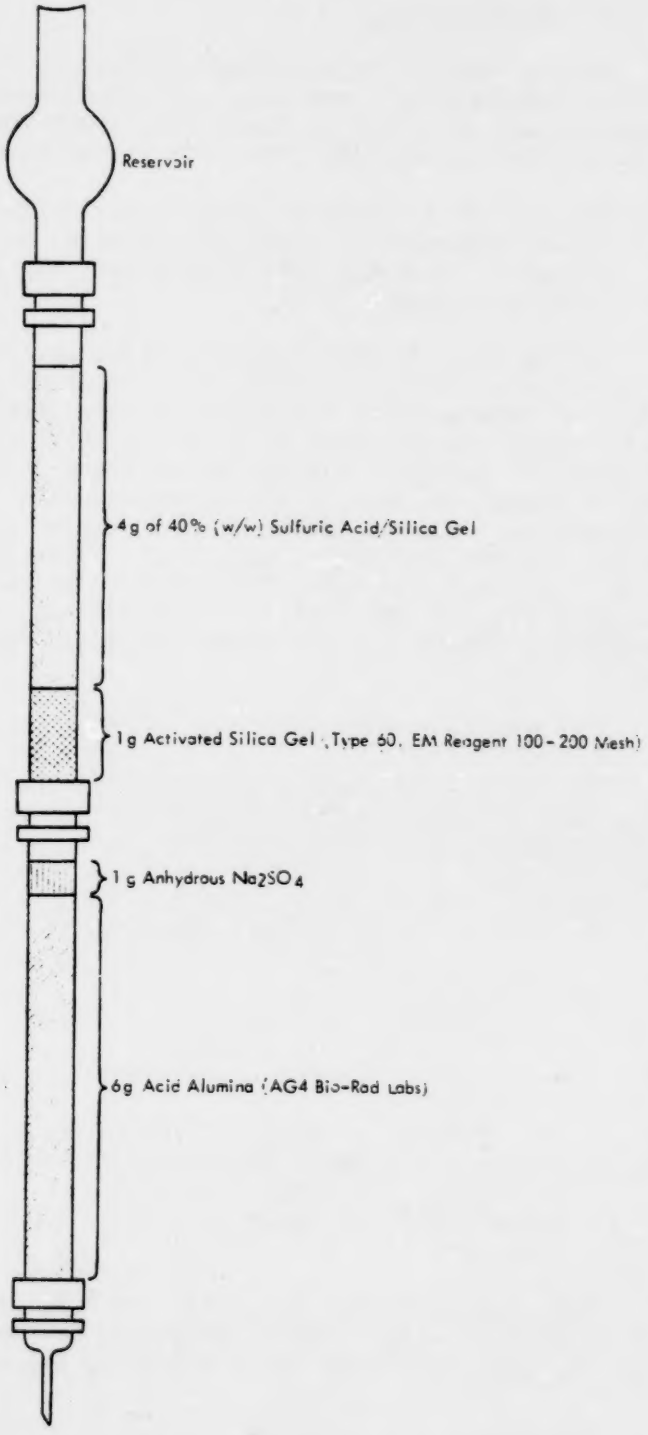
Reservoir
4g of 40% (w/w) Sulfuric Acid/Silica Gel
1g Activated Silica Gel (Type 60, EM Reagent 100-200 Mesh)
1g Anhydrous Na_2SO_4
6g Acid Alumina (AG4 Bio-Rad Labs)

Figure 4. Two-part cleanup column.

3. GC/MS Analysis

During Phase 2, each cleaned extract was analyzed for trichloro-, tetrachloro-, pentachloro-, and hexachlorodibenzofurans, using high resolution gas chromatography and electron impact mass spectrometry detection with selected ion monitoring (HRGC/MS-SIM). Analytical conditions were as follows:

Column: 30 m x 0.25 mm fused silica column, wall-coated with DB-5
Column temperature: 100°C (2 min hold) to 320°C at 10°C/min
Injector: Grob-type, 45 s splitless, 280°C
Electron energy: 70 eV

During Phase 3, each cleaned extract was analyzed for polychlorinated dibenzodioxins (PCDDs), and polychlorinated dibenzofurans (PCDFs). The second half of each extract, which had not been cleaned, was analyzed for PCBs and some of these extracts were screened for other chlorinated organics. Table 5 lists the samples collected during Phase 3, the analyses which were performed on these samples, and the instrument which was used. Among the types of analyses performed on the Phase 3 samples were full scan HRGC/MS, HRGC/MS-SIM, and HRGC/MS-limited mass scan. Three different instruments were used to perform these analyses. The operating parameters for the instruments, Finnigan 4023, Finnigan MAT 311A, and Kratos MS-50, are listed in Table 6. The specific ion masses and mass ranges monitored for each analyte are shown in Table 7.

4. Analyte Quantitation

The PCDFs in the sample extracts from Phase 2 were quantitated by comparing the responses for the sample extract to the response of 2,3,7,8-tetrachlorodibenzofuran (2,3,7,8-TCDF) for an authentic standard solution. These concentrations were calculated using the internal standard method. The internal standard used was ($^{13}C_{12}$)-2,3,7,8-TCDF. First, a response factor (RF) for the standard (2,3,7,8-TCDF) was calculated according to the equation:

$$RF = \frac{(A_s)(C_{is})}{(A_{is})(Cs)}$$

where A_s = Area of the primary characteristic ion of the 2,3,7,8-TCDF (m/z 306)
C_{is} = Concentration or amount of the internal standard
A_{is} = Area of the primary characteristic ion of the internal standard ($^{13}C_{12}$)-2,3,7,8-TCDF (m/z 318)
C_s = Concentration or amount of 2,3,7,8-TCDF in the calibration standard

The response factor calculated for 2,3,7,8-TCDF was used to quantitate all chlorinated dibenzofurans identified in the effluent samples in Phase 2. The quantitation was performed using the equation:

$$\text{Concentration} = \frac{(A_s)(C_{is})}{(A_{is})(RF)}$$

where A_s, A_{is}, C_{is}, and RF are described above.

Table 5. Types of Analyses Used for Samples From Phase 3

Sample no. \ Type of analysis	Full scan analysis[a]	Limited mass scan analysis for PCBs[a]	Analysis of chlorinated dioxins, furans and biphenyls			
			$Cl_1 + Cl_2$	$Cl_3 + Cl_4$	$Cl_5 + Cl_6$	$Cl_7 + Cl_8$
8-07-39-M500	x	x		x[b]	x[c]	x[b]
8-13-40-M500	x	x	x[b]	x[b]	x[c]	x[b]
8-14-41-M500	x	x		x[b]	x[c]	x[b]
8-14-42-BLK	x	x		x[c]	x[c]	x[b]
8-15-43-M5		x		x[c]	x[b]	
8-15-44-M5				x[c]	x[c]	
8-16-45-M50				x[c]	x[c]	
8-16-46-M50				x[c]	x[b]	
8-17-47-S5	x	x		x[c]	x[b]	
8-20-48-S5		x		x[b]	x[c]	x[b]
8-21-49-S50		x		x[b]	x[c]	x[b]
8-21-50-S50		x		x[b]	x[c]	
8-22-51-S500		x	x[b]	x[b]	x[c]	x[b]
8-22-52-S500	x	x	x[b]	x[c]	x[b]	x[b]
8-22-53-BLK	x	x				
8-23-54-CLBZ				x[c]	x[c]	
8-23-55-CLBZ				x[c]	x[c]	x[b]
8-23-56-BLK	x	x	x[b]	x[c]	x[b]	
8-28-57-CLBZ	x	x		x[c]	x[b]	x[b]
8-28-58-CLBZ	x	x		x[c]	x[c]	
8-28-59-BLK	x	x		x[c]	x[b]	
8-29-60-ASKL	x		x[b]	x[c]	x[b]	x[b]
8-30-61-ASKL	x		x[b]	x[c]	x[b]	
8-30-62-ASKL	x		x[b]	x[c]	x[b]	
8-30-63-BLK	x					

[a] Analyzed using Finnigan 4023.
[b] Analyzed using Finnigan MAT 311A.
[c] Analyzed using Kratos MS-50.

Table 6. Operating Parameters for Gas Chromatograph/Mass Spectrometers Used to Analyze Phase 3 Samples

Instrument model	Finnigan 4023		Finnigan MAT 311A	Kratos MS-50
Mass spectrometer type	Quadropole		Magnetic sector;	Magnetic sector;
Mode of operation	Full scan	Limited mass scan	Selected ion monitoring	Selected ion monitoring
Operating parameters (GC)				
Column	30 m x 0.25 mm DB-5	30 m x 0.25 mm DB-5	30 m x 0.25 mm DB-5	15 m x 0.25 mm DB-5
Column temperature	30° (1 min hold) to 325° at 10°/min	80° (1 min hold) to 325° at 6°/min	100° (2 min hold) to 320° at 10°/min	100° (2 min hold) to 320° at 10°/min
Injector	Grob 45 s splitless	Grob 45 s splitless	Grob 45 s splitless	Grob 45 s splitless
Injector temperature (mass spectrometer)	280°	280°	280°	280°
Scan range (m/z)	95-550	Variable, relative to analyte[a]	Variable, relative to analyte[a]	Variable, relative to analyte[a]
Scan time	1 s	1 s	0.9-1 s	0.9-1 s
Resolution	Unit	Unit	800	1200
Ion source temperature	270°	270°	250-270°C	250-270°C
Electron energy	70 eV	70 eV	70 eV	70 eV
Data system	Incos 2300	Incos 2300	Incos 2400	Incos 2400

[a]Scan ranges and selected ion listed for individual analytes in Table 7.

Table 7. Scan Ranges and Selected Ions Monitored for Individual Analytes

Analyte	Polychlorinated biphenyls	Chlorinated biphenylenes		Chlorinated dibenzofurans		Chlorinated dibenzodioxins	
Homolog	Limited mass scan range (m/z)	Primary ion (m/z)	Secondary ion (m/z)	Primary ion (m/z)	Secondary ion (m/z)	Primary ion (m/z)	Secondary ion (m/z)
Cl_1	186-196 (±0.5)	186.04[a]	190.04[a]	202.02[a]	204.02[a]	218.01[a]	220.01[a]
Cl_2	222-226 (±0.5)	220.00	221.99	235.98	237.98	251.97	253.97
Cl_3	256-262 (±0.5)	253.96	255.96	269.14	271.94	285.94	287.93
Cl_4	290-308 (±0.5)	289.92	287.92	305.90	303.90	321.88	319.88
Cl_5	324-330 (±0.5)	323.88	321.88	339.86	337.86	355.85	353.86
Cl_6	358-365 (±0.5)	357.84	359.84	373.82	375.82	389.82	391.81
Cl_7	392-399 (±0.5)	391.80	393.80	407.78	409.78	423.78	425.77
Cl_8	426-447 (±0.5)	427.76	427.76	443.74	441.74	459.74	457.74
Cl_9	460-467 (±0.5)	-	-	-	-	-	-
Cl_{10}	493-511 (±0.5)	-	-	-	-	-	-

[a]Scan range for selected ion monitoring was that of the reported m/z ±0.18.

During Phase 3, a mixed PCDD/PCDF standard was used. This standard contained a number of PCDD isomers and three PCDF isomers. The composition of the PCDD/PCDF standard used during Phase 3 is shown in Table 8. The response factors for this standard were calculated using the equation shown above. As listed in Table 9, any mono- or diCDFs were quantified using the response factor for 2,8-diCDF. Any tri-, tetra-, penta-, or hexaCDFs were quantitated using the response factor for 2,3,7,8-tetraCDF. Any hepta- or octaCDF was quantitated using the response factor for octaCDF. Any PCDDs were quantitated using the corresponding response factors. Two internal standards were used for these calculations. All PCDDs were quantitated using ($^{13}C_{12}$)-2,3,7,8-TCDD as the internal standard, and all PCDFs were quantitated using ($^{13}C_{12}$)-2,3,7,8-TCDF as the internal standard.

D. Statistical Analysis

1. Phase 2

Intermediate statistical analyses were performed as each set of data became available. Each set of data consisted of a half-replicate of a 2^3 factorial design. These were analyzed separately to estimate the main effects. The data then were combined with previous data and the entire available data set analyzed. The purpose of these interim statistical analyses was to indicate the levels that should be tested at the next set of runs. Analysis of variance was used to analyze the half-replicate data. These half-replicates are saturated designs. That is, there is one parameter to be estimated for each data point. Consequently, the analysis could only estimate the main effects and partition the total sum of squares into components for each main effect. No estimate of error or interactions is available.

When the data were pooled with other data, more detailed analysis became possible. This analysis varied with the amount of data and the structure. At one point the usual analysis of variance for a complete 2^3 factorial design was used, but generally the data available were an unbalanced, incomplete design. The analysis for these data sets was that of a general linear model (GLM). Computations were performed using the GLM program in the SAS package. The results and the data structure that finally resulted are discussed in Section VII, where the analysis and conclusions are presented.

2. Phase 3

The data for the PCDFs (in nanograms) were statistically analyzed using regression and ANOVA programs in the SAS package.

Table 8. PCDD/PCDF Standard Used in Phase 3

Compound	Concentration (ng/mL)
2-Chlorodibenzodioxin	4
2,7-Dichlorodibenzodioxin	4
2,8-Dichlorodibenzofuran	4
1,2,4-Trichlorodibenzodioxin	4
2,3,7,8-Tetrachlorodibenzodioxin	20
2,3,7,8-Tetrachlorodibenzofuran	20
1,2,3,7,8-Pentachlorodibenzodioxin	20
1,2,3,4,7,8-Hexachlorodibenzodioxin	10
1,2,3,4,6,7,8-Heptachlorodibenzodioxin	10
Octachlorodibenzodioxin	200
Octachlorodibenzofuran	200
($^{13}C_{12}$)2,3,7,8-Tetrachlorodibenzofuran	200
($^{13}C_{12}$)2,3,7,8-Tetrachlorodibenzodioxin	200
($^{37}Cl_4$)1,2,3,4,6,7,8-Heptachlorodibenzodioxin	2,000
($^{13}C_{12}$)Octachlorodibenzodioxin	2,000

Table 9. Type of Quantitation Used During Phase 3 HRGC/EIMS Analysis

No. of chlorines	Chlorinated dibenzofurans			Chlorinated dibenzodioxins		
	Type of quantitation[a]	Internal std used	Quantitation standard	Type of quantitation[a]	Internal standard	Quantitation standard
1	ES	-	2,8-diCDF	ES	-	2-monoCDD
2	ES	-	2,8-diCDF	ES	-	2,7-diCDD
3	IS	^{13}C-2,3,7,8-TCDF	2,3,7,8-tetraCDF	IS	^{13}C-2,3 7,8-TCDD	1,2,4-tri-CDD
4	IS	^{13}C-2,3,7,8-TCDF	2,3,7,8-tetraCDF	IS	^{13}C-2,3 7,8-TCDD	2,3,7,8-tetraCDD
5	ES	-	1,2,3,7,8-pentaCDD	ES	-	1,2,3,7,8-pentaCDD
6	ES	-	1,2,3,4,7,8-hexaCDD	ES	-	1,2,3,4,7,8-hexaCDD
7	IS	^{13}C-octaCDD	OCDF	IS	^{13}C-octaCDD	1,2,3,4,6,7,8-heptaCDD
8	IS	^{13}C-octaCDD	OCDF	IS	^{13}C-octaCDD	OCDD

[a]ES - external standard; IS = internal standard.

VII. RESULTS AND DISCUSSION

A. Phase 1

The thermal destruction system was operated at two temperatures and two gas flow rates to determine the effects on effluent levels of O_2, CO_2, CO, and on combustion efficiency (CE). Test conditions included two different flow rates and two different types of mineral oil, as noted in Table 10. System blank runs were performed at 600° and 700°C at high O_2 levels (Runs 5-22-01 and 6-05-03, respectively), and at 700°C at low O_2 levels (Run 6-06-04). The rinse samples from the lower temperature run and the low O_2 run were a light yellow color, indicating a high level of organics due to incomplete combustion of the mineral oil. Also, a soot-like material appeared at the entrance to the XAD-2 trap during the low O_2 run. In the 700°C, high O_2 run, both the rinse sample and the XAD-2 sample appeared clean.

The Phase 1 samples were extracted and analyzed for PCBs by full scan HRGC/EIMS. No PCBs were detected. The extracts were analyzed by HRGC/EIMS in the selected ion monitoring mode for the tri- through hexaCDFs. Initially, the samples contained too much background to detect low levels of PCDFs; however, after column chromatographic cleanup, no PCDFs were detected. Based on this information, all Phase 2 samples were cleaned prior to the analysis.

It is apparent from the test results summarized in Table 10 that the CE was affected by incineration temperature, generally increasing with increasing temperature. The data suggested that near ideal stoichiometry results at 700°C or higher temperatures. When the gas flow rate was maintained at a nominal 1 L/min, CO_2 increased with increasing temperature and CO remained fairly constant. However, for tests conducted at a nominal flow rate of 0.5 L/min, the CO_2 still increased with temperature, while CO maximized at an intermediate temperature (600°C). CE was lowest at the 600°C test.

B. Phase 2

1. Test Conditions

Thirty-four test runs were completed during Phase 2. Two of these were considered invalid for reasons noted below. A run was defined as the test period in which an XAD-2 sample was collected. Each run was assigned a unique number, consisting of three fields: first, the date of the run (including the month, a dash, and the date); second, a two-digit sequential run number, beginning with "01" for the first run; and last, a three-letter code for the operating conditions. Low is designated by "L," medium is designated by "M," high is designated by "H," and intermediate between medium and high is designated by "M+." The first letter of this code represents combustion temperature, the second letter represents effluent oxygen concentration, and the final letter represents residence time. System blanks, indicated by the suffix "(B)," were conducted under the same operating conditions as the preceding run, except without feed oil flow.

Table 10. Phase 1 Non-PCB Combustion Test Conditions

Run no.	Combustion temperature (°C)	Vaporization/ pyrolysis temperature (°C)	Effluent gas flow rate (L/min)	Residence time (s)	"Waste" feed rate (μL/min)	Effluent O_2 concentration (%)	Effluent CO_2 concentration (%)	Effluent CO concentration (ppm)	Combustion efficiency (%)	Comments
NA[a]	450[b]	300[b]	~ 0.5	~ 2.3	~ 5[c]	16.2	0.63	2,060	75	
NA	600[b]	300[b]	~ 0.5	~ 1.9	~ 5[c]	16.3	0.81	5,050	62	
NA	700[b]	300[b]	~ 0.5	~ 1.7	~ 5[c]	16.0	1.24	1,250	90.9	
NA	450[b]	300[b]	~ 1.0	~ 1.2	~ 10[c]	19.1	0.27	1,630	62	
NA	700[b]	300[b]	~ 1.0	~ 0.9	~ 10[c]	17.5	1.28	2,050	86	
NA	~ 730	300[b]	~ 1.0	~ 0.9	~ 10[c]	16.6	1.82	270	98.5	
5-22-01 5-31-02[e]	610[d]	362[d]	1.51	0.7	~ 10[c]	16.5	~ 0.37	1,380	73	Rinse was light yellow.
6-05-03	728[d]	416[d]	0.86	1.0	~ 10[f]	15.1	1.6	1,880	89	XAD and rinse appeared clean and colorless. Incineration temperature varied over ~ 50°C range.[g]
6-06-04	705[d]	425[d]	1.02	0.9	~ 10[f]	0.51	0.33	3,210	51	Soot-like material at entrance to XAD. Both XAD and rinse were light yellow.

[a]Not assigned. Testing performed for combustion efficiency determination. XAD-2 sample not taken.
[b]Nominal furnace (refractory) temperature.
[c]"Waste" was pharmaceutical grade mineral oil.
[d]Average of gas temperatures read at 10-min intervals.
[e]Operating conditions were unstable due to inadequate temperature control in vaporization/pyrolysis furnace. XAD-2 sample held but not analyzed.
[f]"Waste" was technical grade mineral oil.
[g]Gas temperature variations apparently due to fluctuations in flow rate.

The actual operating conditions for each run are provided in Table 11. The runs are listed in a hierarchical order: first, by temperature; second, by oxygen level; and third, by residence time. The average CO_2 and CO continuous monitor readings taken during each run and combustion efficiencies calculated from those readings are also presented. Combustion efficiency is calculated from the equation:

$$CE = \frac{[CO_2]}{[CO_2] + [CO]} \times 100$$

where both CO_2 and CO are in the same concentration units.

The selection of operating conditions used for Phase 2 tests was based upon an interactive combination of a statistical experimental design and the results of the chemical analyses of effluent samples. That is, the experimental design was updated when analytical results became available with the objective of maximizing the formation of PCDFs. The evolution of the experimental design is discussed in Section V.C.2. The influence of the various operating conditions upon PCDF formation is also discussed at length in Section VII. Table 12 summarizes the nominal values, means, standard deviations, and ranges of the actual values for the various operating conditions. In general, actual combustion temperatures are within 15° of the nominal values. [Effluent oxygen levels are more difficult to set to prespecified values since the oxygen consumption by the waste itself is a variable.] Actual residence time values are generally within 10-20% of the nominal values.

2. Continuous Monitor Results and Combustion Efficiency

As discussed in Section VI.B above, the desired effluent oxygen concentration was obtained by varying the nitrogen:air ratio in the makeup gas furnace, and thus was an independent variable. However, both carbon dioxide and carbon monoxide concentrations were dependent variables, since they are affected by feed oil flow rate, residence time and total gas flow rate, combustion temperature, and possibly adjusted oxygen concentration. Aside from system blanks, which had very low CO_2 and CO levels, the effluent CO_2 concentrations ranged from 0.08% (in both Run 6-14-06-LLL and Run 7-05-17-LML) to 3.23% (in Run 6-18-09-HHH), and the effluent CO concentration ranged from 0.0015% or 15 ppm (in Run 6-18-09-HHH) to 0.587%, or 5,870 ppm (in Run 7-13-21-HMH).

Table 11. Operating Conditions for Phase 2 Tests

Run no.	Temp. (°C)	Oxygen (%)	Res. time (s)	CO_2 (%)	CO (%)	CE (%)
6-14-06-LLL	459	0.79	0.31	0.08	0.015	85
7-10-18-LLM	464	0.48	0.78	0.10	0.020	84
7-10-19-LLM(B)[a]	464	0.86	0.79	0.05	0.0005	98.9
7-05-17-LML	454	3.66	0.29	0.08	0.011	88
6-14-07-LMM	458	3.93	0.74	0.13	0.030	81
6-22-14-LMM	452	3.67	0.76	0.11	0.031	78
7-03-16-MLL	597	1.18	0.30	0.10	0.033	75
6-13-05-MLM	605	0.61	0.81	0.30	0.098	75
6-15-08-MML	581	3.49	0.29	0.15	0.041	79
7-03-15-MMM	629	3.65	0.74	0.26	0.111	70
7-12-20-MMM	605	3.33	0.80	0.29	0.078	79
7-20-27-MMM	606	3.93	0.80	0.29	0.111	72
7-26-32-MMM	612	3.07	1.21	1.07	0.233	82
6-20-12-MMH[b]	614	3.72	1.62	1.46	0.531	73
6-20-13-MMH	615	3.64	1.65	0.53	0.149	78
7-26-31-MMH	615	3.45	1.55	1.79	0.347	84
7-31-37-MMH	611	3.45	1.66	1.72	0.336	84
7-31-38-MMH(B)[a]	607	3.79	1.59	0.07	0.0017	98
7-24-28-MMH[c]	invalid	invalid	invalid	invalid	invalid	invalid
7-25-29-MMH[c]	invalid	invalid	invalid	invalid	invalid	invalid
7-19-25-MM+M	608	8.15	0.86	0.37	0.1394	73
6-19-11-MHM	604	18.45	0.79	0.36	0.161	69
7-16-23-MHH	616	10.49	1.68	1.50	0.572	72
7-30-35-MHH	610	12.61	1.49	1.56	0.536	74
7-30-36-MHH	611	12.65	1.52	1.62	0.502	76
7-17-24-M+MM	680	2.67	0.79	0.35	0.1670	67
7-25-30-M+MM+	689	3.22	1.22	1.49	0.362	80
7-27-33-M+MH	677	3.04	1.60	2.22	0.393	85
7-27-34-M+MH(B)[a]	677	3.52	1.56	0.05	0.0000	100
7-19-26-M+M+M	683	7.71	0.80	0.37	0.298	55
6-19-10-HMM	759	3.27	0.82	1.39	0.133	91
7-13-21-HMH	754	3.32	1.67	1.07	0.588	65
7-16-22-HHM	771	11.55	0.82	1.55	0.0077	99.5
6-18-09-HHH	750	12.93	1.52	3.23	0.0015	99.95

[a] No waste flow (system blank).
[b] Only XAD-2 sample analyzed, not rinse.
[c] Operational problems with the reaction system prevented completion of this test run.

Table 12. Nominal and Actual Values for Operating Conditions During Phase 2 Tests

Operation condition	Test codes for various levels of operating conditions			
	L	M	M+	H
Combustion temperature (°C)				
Nominal	450	600	675	750
Mean ± std. dev.	458 ± 5	609 ± 10	681 ± 5	758 ± 9
Range (no. tests)	451 - 464(6)	581 - 629(17)	677 - 689(5)	750 - 771(4)
Effluent oxygen concentration (%)				
Nominal	< 1	3 - 4	8	≥ 12
Mean ± std. dev.	0.78 ± 0.27	3.56 ± 0.25	7.93 ± 0.31	13.11 ± 2.77
Range (no. tests)	0.48 - 1.18(5)	3.07 - 3.93(15)	7.71 - 8.15(2)	10.49 ± 18.45(6)
Residence time (sec)				
Nominal	0.3	0.8	1.15	1.5
Mean ± std. dev.	0.30 ± 0.01	0.79 ± 0.03	1.22 ± 0.01	1.59 ± 0.06
Range (no. tests)	0.29 - 0.31(4)	0.74 - 0.86(14)	1.21 - 1.22(2)	1.52 - 1.68(12)

The observed values for O_2, CO_2, and CO are averages of readings taken during each test. Strip chart recordings of effluent levels of O_2, CO_2, and CO are shown in Figures 5 and 6 and for two representative tests (Run 6-19-11-MHM and Run 6-20-13-MMH, respectively). In each figure, background levels are shown prior to turning on the waste flow, followed by a stabilization period prior to beginning a test. The start and end times for sampling are also shown. Some perturbation of concentration of the monitored gases occurs following switchover of sampling systems. This causes the spikes at the beginning and end of each run. Under some test conditions, wide variations (swings) occur in some or all of the monitored gases, as shown in Figure 6. Other test conditions produce relatively stable patterns, as shown in Figure 5. There is no clear explanation for these differences in apparent stability. The average of readings taken at 1-min intervals was reported to dampen out the fluctuations. Absolute values for CO_2 and CO should not be directly compared between runs, since the gaseous flow rates varied while the feed oil flow rate remained constant (13.5 µL/min). That is, the source of the CO and CO_2 remained constant, but different dilution factors resulted from varying the total gas flow rate to establish the desired residence time. The calculated combustion efficiencies compensate for variations in flow rate and can be compared between runs.

In Phase 2 tests, the CE ranged from 55 to 99.95%, i.e., less than one "nine" to greater than three "nines." It is not certain whether CE is related to PCDF formation, but it may be a useful parameter in relating the conditions in the combustion unit to those occurring in a transformer fire. Figure 7 shows a plot of CE as a function of combustion temperature for the Phase 2 tests, excluding system blanks.

The target sampling period for each run was 60 min. Since the spiked mineral oil was fed at a constant rate of 0.0135 mL/min, each run had a nominal feed oil volume of 0.81 mL. For the Phase 2 tests, a solution of three specified PCB congeners in Exxon mineral oil comprised the feed oil solution, at the following nominal concentrations: 0.5 mg/mL 2,3,5,6-tetrachlorobiphenyl, 0.5 mg/mL 3,3',4,4',5,5'-hexachlorobiphenyl, and 1.0 mg/mL 2,2',4,4',6,6'-hexachlorobiphenyl, or a total of 2.0 mg/mL PCBs. The amounts of each PCB congener and the total input during each run are given in Table 13.

3. PCBs Input During Tests

The actual sampling periods for the Phase 2 tests ranged from 34 min (during Run 6-14-07-LMM) to 65 min (during Run 6-20-12-MMH). The short run (6-14-07-LMM) was terminated early because the syringe pump was nearly emptied of feed oil. It was repeated as Run 6-22-14-LMM, with fairly consistent results between runs. The total input feed oil volume varied from 0.46 mL to 0.88 mL, depending on the length of the sampling period. In addition, the concentrations of the three PCB congeners also varied slightly from one batch of feed oil to the next (as shown in Table 2).

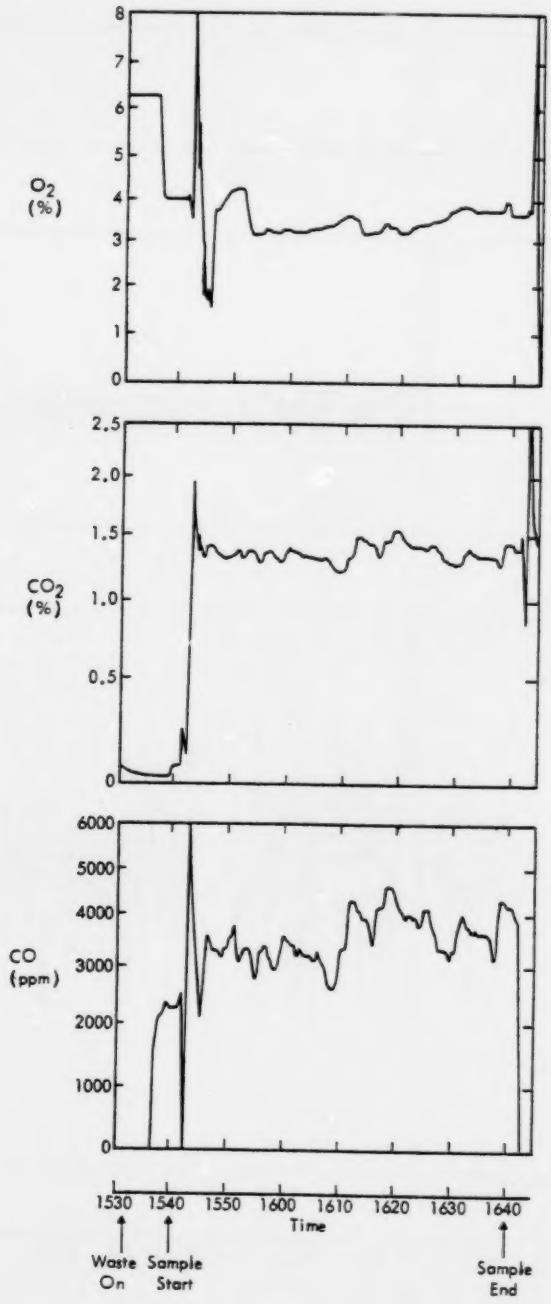

Figure 5. Continuous gas monitoring results for Run 6-20-13-MMH.

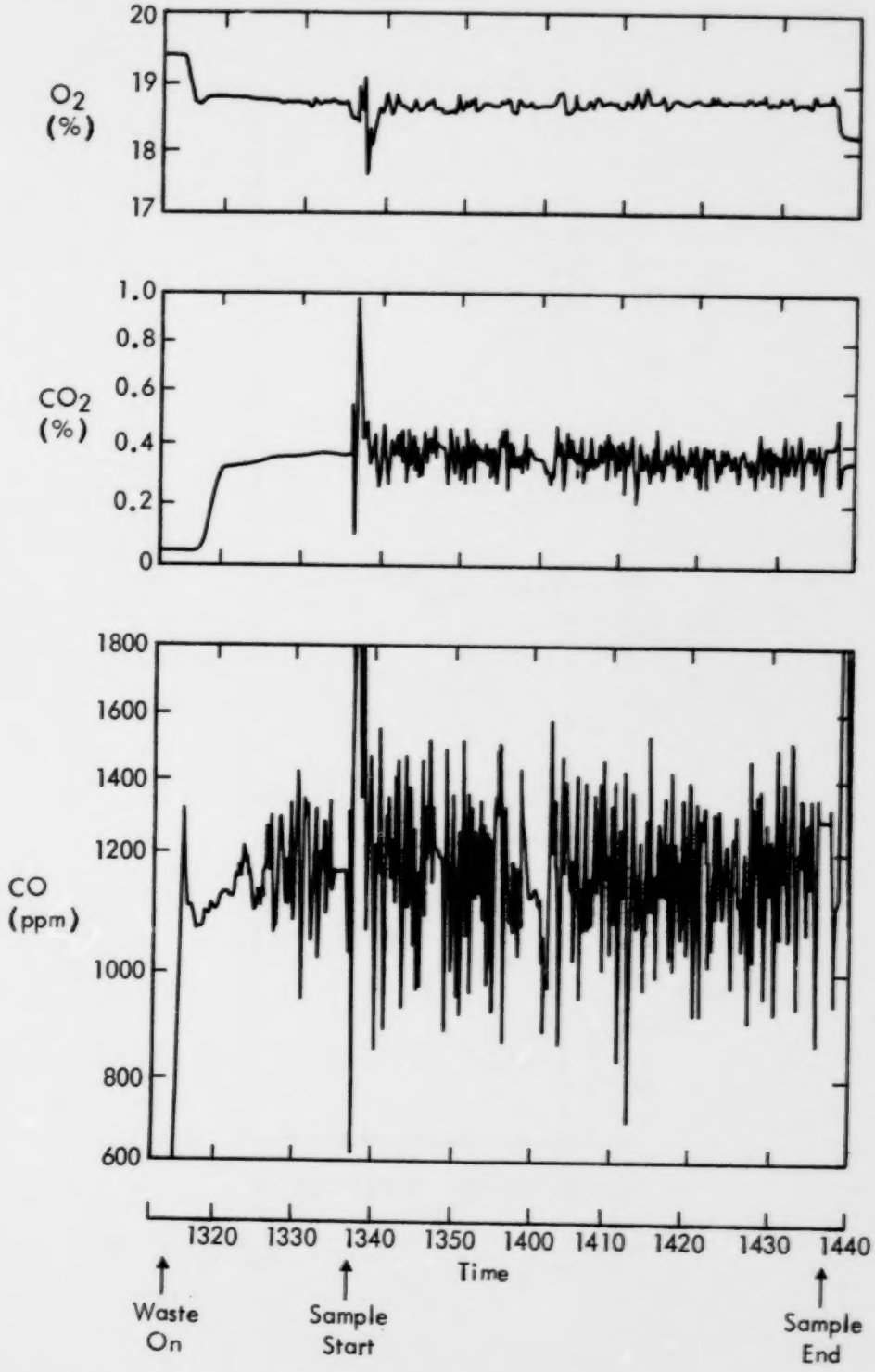

Figure 6. Continuous gas monitoring results for Run 6-19-11-MHM.

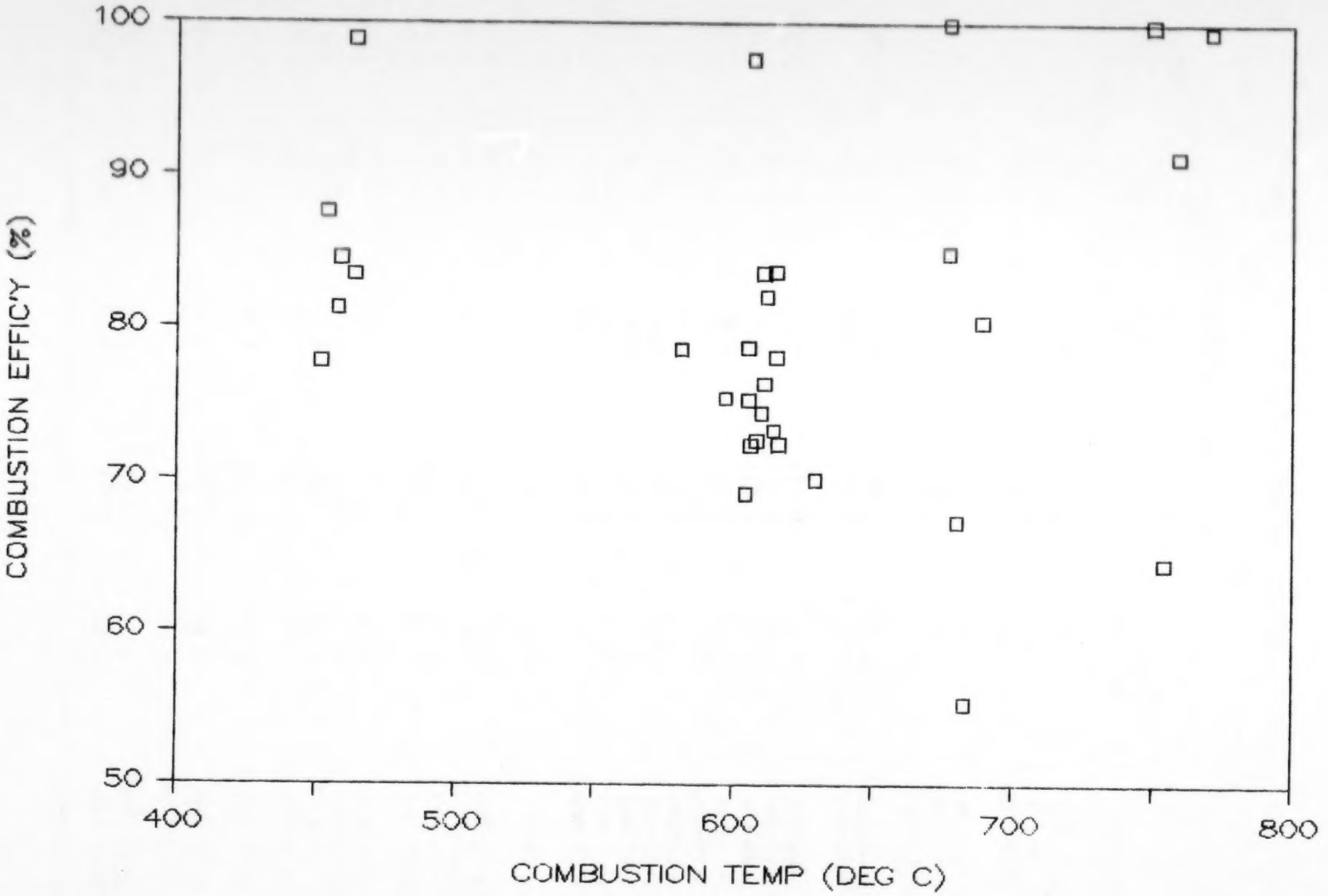

Figure 7. Combustion efficiency versus temperature.

Table 13. Weights of PCBs Used During Phase 2 Tests

Run no.	Feed oil vol. (mL)	Chlorobiphenyl congener: 2,3,5,6-Tetra (mg)	2,2',4,4',6,6'-Hexa (mg)	3,3',4,4',5,5'-Hexa (mg)	Total PCB (mg)
6-14-06-LLL	0.78	0.42	0.84	0.29	1.55
7-10-18-LLM	0.81	0.41	0.83	0.38	1.61
7-10-19-LLM(B)	0.82	0.41	0.84	0.38	1.64
7-05-17-LML	0.81	0.41	0.83	0.38	1.61
6-14-07-LMM	0.46	0.25	0.49	0.17	0.91
6-22-14-LMM	0.81	0.41	0.81	0.39	1.61
7-03-16-MLL	0.76	0.38	0.77	0.35	1.50
6-13-05-MLM	0.81	0.44	0.87	0.30	1.61
6-15-08-MML	0.81	0.41	0.81	0.39	1.61
7-03-15-MMM	0.81	0.41	0.83	0.38	1.61
7-12-20-MMM	0.81	0.41	0.83	0.38	1.61
7-20-27-MMM	0.81	0.41	0.83	0.38	1.61
7-26-32-MMM+	0.81	0.41	0.81	0.41	1.62
6-20-12-MMH	0.88	0.44	0.88	0.42	1.75
6-20-13-MMH	0.81	0.41	0.81	0.39	1.61
7-26-31-MMH	0.81	0.41	0.81	0.41	1.62
7-31-37-MMH	0.81	0.41	0.81	0.41	1.62
7-31-38-MMH(B)	0.80	0.40	0.80	0.40	1.59
7-19-25-MM+M	0.84	0.42	0.85	0.39	1.66
6-19-11-MHM	0.81	0.41	0.81	0.39	1.61
7-16-23-MHH	0.82	0.41	0.84	0.38	1.64
7-30-35-MHH	0.81	0.41	0.81	0.41	1.62
7-30-36-MHH	0.81	0.41	0.81	0.41	1.62
7-17-24-M+MM	0.84	0.42	0.85	0.39	1.66
7-25-30-M+MM+	0.81	0.41	0.81	0.41	1.62
7-27-33-M+MH	0.81	0.41	0.81	0.41	1.62
7-27-34-M+MH(B)	0.81	0.41	0.81	0.41	1.62
7-19-26-M+M+M	0.81	0.41	0.83	0.38	1.61
6-19-10-HMM	0.68	0.34	0.68	0.32	1.34
7-13-21-HMH	0.86	0.43	0.88	0.40	1.72
7-16-22-HHM	0.84	0.42	0.85	0.39	1.66
6-18-09-HHH	0.81	0.41	0.81	0.39	1.61

4. PCDF Results

The results of analysis of the Phase 2 samples for trichlorodibenzofuran (triCDF), tetrachlorodibenzofuran (tetraCDF), pentachlorodibenzofuran (pentaCDF), and hexachlorodibenzofuran (hexaCDF) are shown in Table 14. When the PCDF homolog was not detected, "< 5 ng" is noted. The total PCDFs resulting from the four homologs of interest are given in the final column. In the final column, the summation of four "< 5 ng" values yields a total PCDF value of "< 20" where no PCDFs were detected. As footnoted in the table, only the XAD-2 sample from Run 6-20-12-MMH was analyzed, as the rinse portion of the total sample was lost and not analyzed. Run 6-20-13-MMH was a replicate of that run, and the XAD-2 extract and rinse were analyzed individually to determine the relative abundance of the PCDFs in the two fractions. The amounts were summed for the reported value. Only a minor amount of triCDF was detected in the rinse sample, with none of the tetra-, penta-, or hexachlorodibenzofurans detected. Therefore, the PCDF values for Run 6-20-12-MMH were judged valid.

The conversion efficiencies of the specific PCB congeners to the anticipated PCDF, i.e., percent yield, are shown in Table 15. According to results previously reported in the literature, it was presumed during this study that triCDF is formed from 2,3,5,6-tetrachlorobiphenyl, that both tetra- and pentaCDFs are formed from 2,2',4,4',6,6'-hexachlorobiphenyl and that hexaCDF is formed from 3,3',4,4',5,5'-hexachlorobiphenyl, as noted previously in Section IV. A total conversion efficiency for each run is also given in Table 15. In this case, the total nanograms of the four PCDF homologs are divided by the total of the three PCB congeners fed in the feed oil. This is not an average of the four individual conversion efficiencies.

The primary PCDFs formed from the three individual PCB congeners were triCDF and tetraCDF. Maximum values detected were 8,870 ng and 3,520 ng, respectively. In contrast, relatively low levels of the pentaCDF and hexaCDF were found. Maximum values detected were 244 ng and 125 ng, respectively. Apparently, the reactions for producing these PCDFs are not as efficient as those for producing tri- and tetrachlorodibenzofuran. The maximum conversion efficiency observed for producing triCDF was 2.2%; for producing tetraCDF it was 0.43%; for producing pentaCDF it was 0.03%; and for producing hexaCDF it was 0.03%. The maximum total conversion efficiency of PCBs to PCDFs during Phase 2 tests was 0.78% (Run 7-19-26-M+M+M). Conversion efficiency is used to evaluate the PCDF formation, rather than the absolute amount of PCDFs formed, because the conversion efficiency normalizes the results with respect to the different amounts of PCBs fed during the runs.

In most Phase 2 samples a single isomer triCDF and a single tetraCDF were observed. In those samples which had the highest concentration of these isomers (7-27-33, 7-30-35, 7-30-36, 7-19-26), six to ten additional isomers were also observed at lower concentrations for each homolog. These isomers were not included in the results listed in Tables 14 and 15. The presence of these other isomers suggests that reactions in addition to those described in Section IV.B are occurring during the combustion process. These reactions may involve dechlorination of penta- or hexaCDFs or may involve rearrangements of the tri- or tetraCDFs.

Table 14. Weights of PCDFs in Combined XAD-2/Rinse Samples from Phase 2 Tests

Run no.	TriCDF (ng)	TetraCDF (ng)	PentaCDF (ng)	HexaCDF (ng)	PCDFs (ng)
6-14-06-LLL	< 5	303	5	< 5	308
7-10-18-LLM	< 5	< 5	< 5	< 5	< 20
7-10-19-LLM(B)[a]	< 5	< 5	< 5	< 5	< 20
7-05-17-LML	< 5	946	< 5	< 5	946
6-14-07-LMM	< 5	95	21	< 5	116
6-22-14-LMM	< 5	256	< 5	< 5	256
7-03-16-MLL	< 5	324	< 5	< 5	324
6-13-05-MLM	< 5	169	15	< 5	184
6-15-08-MML	690	240	31	2	963
7-03-15-MMM	< 5	985	< 5	< 5	985
7-12-20-MMM	< 5	174	< 5	< 5	174
7-20-27-MMM	1,800	740	6	< 5	2,546
7-26-32-MMM+	605	446	125	21	1,197
6-20-12-MMH[b]	990	517	49	4	1,560
6-20-13-MMH	1,316	966	100	< 5	2,382
7-26-31-MMH	599	263	54	7	923
7-31-37-MMH	508	498	170	36	1,212
7-31-38-MMH(B)[a]	< 5	< 5	< 5	< 5	< 20
7-19-25-MM+M	2,280	800	19	< 5	3,099
6-19-11-MHM	905	629	19	< 5	1,553
7-16-23-MHH	1,160	240	45	< 5	1,445
7-30-35-MHH	1,788	1,159	213	125	3,285
7-30-36-MHH	2,111	1,241	208	115	3,675
7-17-24-M+MM	1,190	337	38	trace	1,565
7-25-30-M+MM+	2,066	942	194	93	3,295
7-27-33-M+MH	1,992	1,186	244	81	3,503
7-27-34-M+MH(B)[a]	< 5	< 5	< 5	< 5	< 20
7-19-26-M+M+M	8,870	3,520	96	< 5	12,486
6-19-10-HMM	178	224	19	< 5	421
7-13-21-HMH	92	59	5	< 5	156
7-16-22-HHM	35	12	< 5	< 5	47
6-18-09-HHH	192	23	0.4	< 5	215

[a] System blank; no feed oil flow.
[b] Only XAD-2 sample analyzed; rinse sample was not analyzed.

Table 15. Conversion Efficiencies (PCBs to PCDFs) for Phase 2 Tests

Run no.	Conversion efficiency (%)[a]				
	TriCDF	TetraCDF	PentaCDF	HexaCDF	PCDFs[b]
6-14-06-LLL	0[c]	0.036	0.0006	0	0.020
7-10-18-LLM	0	0	0	0	0
7-10-19-LLM(B)[d]	0	0	0	0	0
7-05-17-LML	0	0.11	0	0	0.059
6-14-07-LMM	0	0.020	0.0042	0	0.013
6-22-14-LMM	0	0.032	0	0	0.016
7-03-16-MLL	0	0.042	0	0	0.022
6-13-05-MLM	0	0.019	0.0017	0	0.012
6-15-08-MML	0.17	0.03	0.0038	0.0005	0.060
7-03-15-MMM	0	0.12	0	0	0.061
7-12-20-MMM	0	0.02	0	0	0.011
7-20-27-MMM	0.44	0.090	0.0007	0	0.16
7-26-32-MMM+	0.15	0.055	0.015	0.052	0.074
6-20-12-MMH[e]	0.22	0.059	0.0056	0.0009	0.089
6-20-13-MMH	0.32	0.12	0.012	0	0.15
7-26-31-MMH	0.15	0.033	0.0067	0.0017	0.057
7-31-37-MMH	0.13	0.061	0.0210	0.0089	0.075
7-31-38-MMH(B)[d]	0	0	0	0	0
7-19-25-MM+M	0.54	0.094	0.0022	0	0.19
6-19-11-MHM	0.22	0.077	0.0023	0	0.096
7-16-23-MHH	0.28	0.029	0.0054	0	0.088
7-30-35-MHH	0.44	0.14	0.026	0.0309	0.20
7-30-36-MHH	0.52	0.15	0.026	0.0284	0.23
7-17-24-M+MM	0.28	0.040	0.0045	0	0.094
7-25-30-M+MM+	0.51	0.12	0.024	0.0230	0.20
7-27-33-M+MH	0.50	0.15	0.030	0.0200	0.22
7-27-34-M+MH(B)[d]	0	0	0	0	0
7-19-26-M+M+M	2.2	0.43	0.012	0	0.78
6-19-10-HMM	0.052	0.033	0.0028	0	0.031
7-13-21-HMH	0.021	0.0067	0.0006	0	0.0091
7-16-22-HHM	0.0084	0.0014	0	0	0.0028
6-18-09-HHH	0.047	0.0028	0	0	0.013

[a] Conversion efficiency = ng PCDF formed/ng PCB fed x 100%.
[b] The total nanograms of the four PCDF homologs are divided by the total of the three PCB congeners fed in the feed oil. This is not an average of the four individual conversion efficiencies.
[c] All "not detected" values from Table 10 are expressed as "0" is this table for statistical calculation purposes.
[d] System blank; no feed oil flow.
[e] Only XAD-2 sample analyzed, not rinse.

The total conversion efficiencies for PCDF and tetraCDF formation are plotted versus the effluent oxygen concentration in Figures 8 and 9. It can be seen that the highest conversion efficiencies occurred at the medium and medium-high temperatures. Extreme variability occurred in the medium (3-4%) oxygen range, but conversion efficiencies were more consistently high for oxygen levels of ≧ 8%. The Y-scale is shown broken in both figures, since the highest values for conversion efficiency, from one test, are significantly higher than all other values. It is possible that this test was an anomaly. Differences in residence time are ignored in these figures, since statistical analysis indicated residence time to be the least significant operating condition.

5. Statistical Evaluation

Statistical analysis of the measured efficiencies of conversion from PCBs to PCDFs relative to temperature, oxygen, and residence time conditions was employed to identify optimum conversion conditions for Phase 3 runs. The total PCB to PCDF conversion efficiencies were given highest priority. However, conversion efficiencies to tetraCDFs were also evaluated in view of their typically higher toxicity and general environmental concern.

Data from 29 runs, excluding blanks and invalid runs, were obtained under various combinations of the levels of temperature, residence time, and oxygen concentration, as shown in Table 15. The table also includes a number of blank runs that were done for quality control to ensure that no contamination was present from one run to a subsequent run. All of the blank determinations gave zero on all components of the PCDFs and were not included in the statistical analysis.

The data were analyzed using the general linear model approach to the analysis of variance from an unbalanced and incomplete design. The total conversion efficiency was used as the dependent variable for analysis. Table 16 gives the analysis of variance for the full model that includes main effects and all two-way and three-way interactions. As can be seen from the low values in the "P" column, the main effects of temperature (T) and oxygen (O) are statistically significant ($P < .05$), as is the two-way interaction of these two variables (T*O). The interpretation of these results is that the mean conversion efficiency differed among the levels of temperature and oxygen, but not by residence time. The interaction was that mean conversion efficiency at the optimum level for temperature and oxygen was higher than would be expected from the addition of the temperature and oxygen effects. This is indicative of a synergistic relationship between temperature and oxygen. None of the other effects was significant.

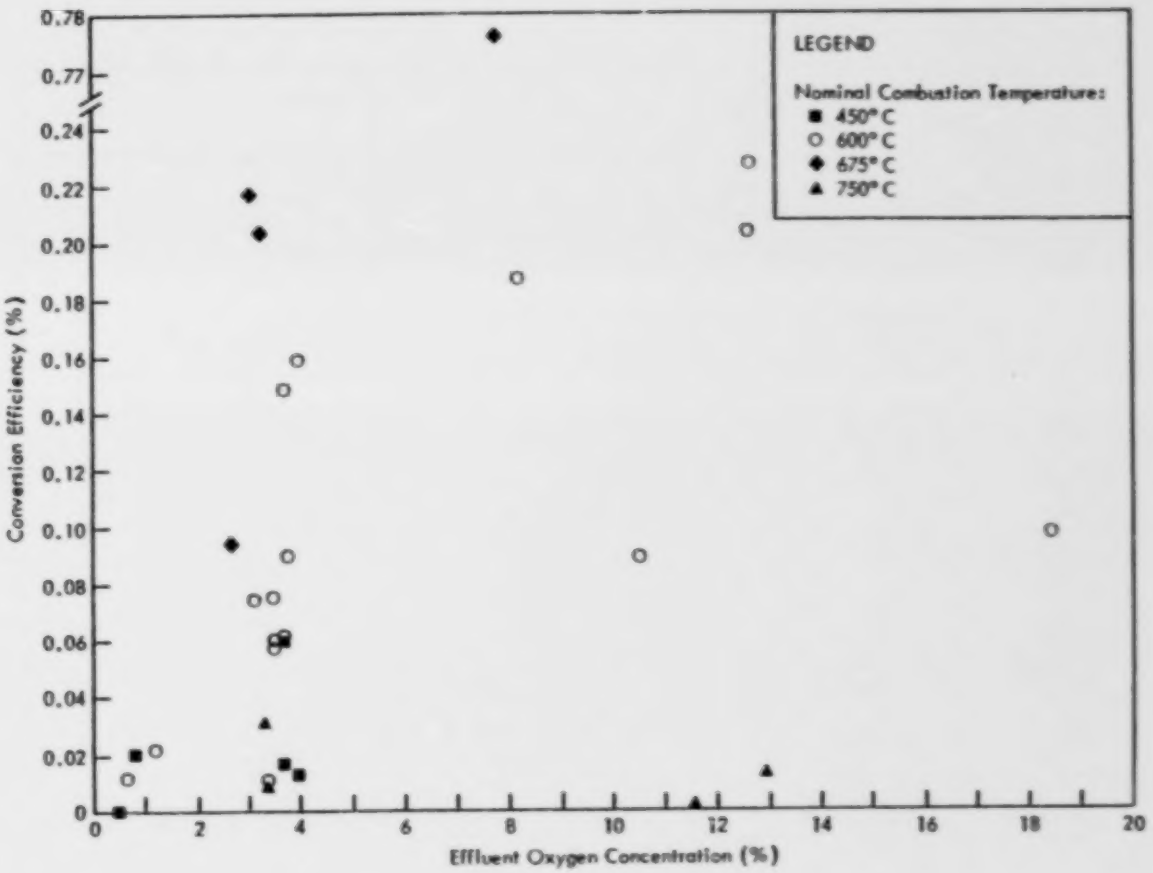

Figure 8. Total PCDFs formed as a function of oxygen.

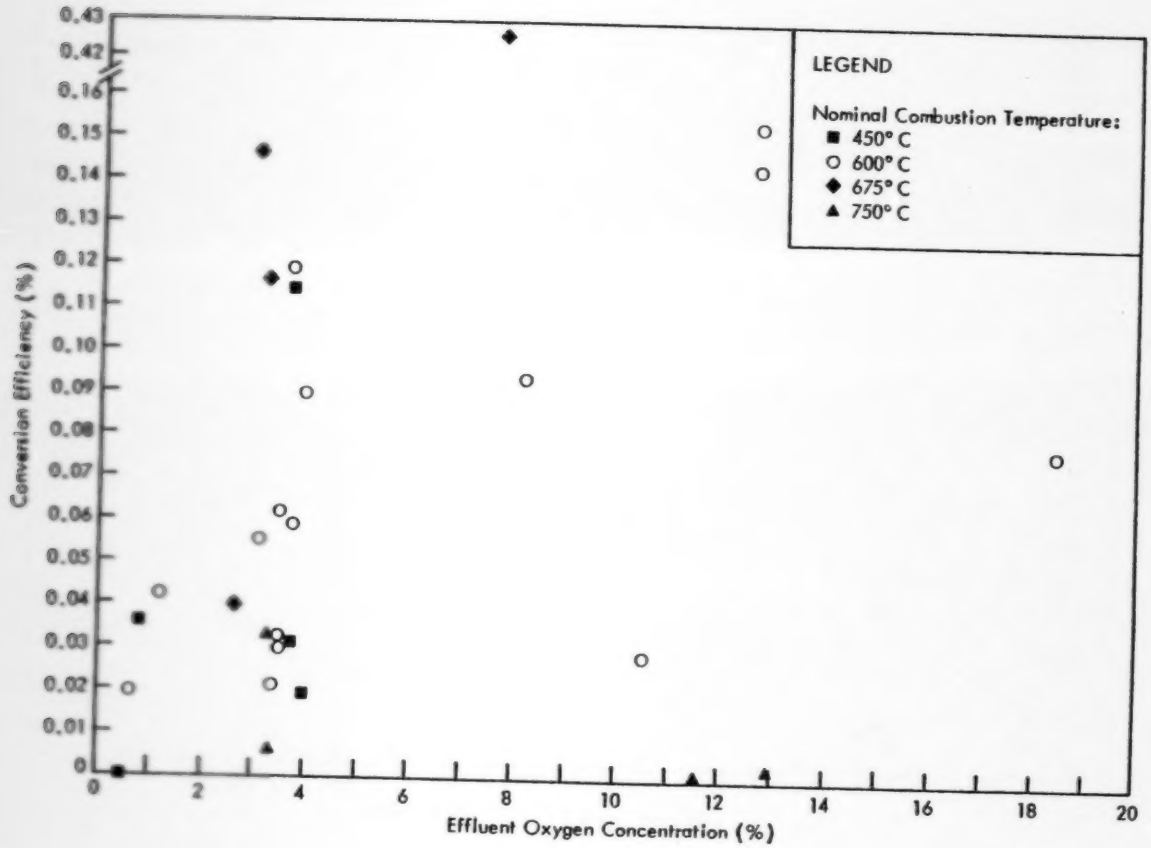

Figure 9. Tetra CDFs formed as a function of oxygen concentration.

Table 16. Full Model Analysis of Variance

Dependent variable: Total

Source	DF	Sum of squares	Mean square	F value	P	R-square	C.V.
Model	20	0.5852	0.0293	8.72	0.0019	0.9561	55.6118
Error	8	0.0268	0.0034		Root MSE		Total mean
Corrected total	28	0.6120			0.0579		0.1042

Source	DF	Type III SS	F value	P
T[a]	3	0.1617	16.06	0.0010
O[b]	3	0.1652	16.42	0.0009
R[c]	3	0.0084	0.84	0.5110
T*R	4	0.0084	0.62	0.6594
T*O	3	0.1000	9.94	0.0045
O*R	2	0.0013	0.20	0.8254
T*O*R	2	0.0005	0.08	0.9282

[a]Temperature.
[b]Oxygen.
[c]Residence time.

The analysis of variance model was refit using only the main effects and the oxygen by temperature interaction. The resulting analysis of variance is shown in Table 17. Again, the main effects of temperature and oxygen and their interaction are significant. The analysis of variance was also run on each PCDF separately. The tri and tetra components gave the same results as the total PCDF. The pattern for the pentaCDF was slightly different. For pentaCDF, the main effects of temperature and residence time were significant ($P = 0.04$ and $P = 0.02$, respectively), while the effect of oxygen was nonsignificant. None of the effects was significant when hexaCDF was used as the dependent variable in the analysis, probably due to the high number of "not detected" values.

The mean total PCDF conversion efficiencies, grouped by variable, are presented in Table 18. These are the mean values of all of the conversion efficiencies in Table 15 which have the same level of a given variable. For example, five runs at 450°C (T = L) have a mean conversion efficiency of 0.0214%. Table 18 also shows that conversion was highest at a temperature of 675°C (M+). Likewise, conversion was highest at 8% oxygen (M+). Conversion was about the same for all levels of residence time. Although the mean was lower at the lowest residence time, this effect did not reach significance. The final part of the table gives the mean by each combination of temperature and oxygen, together with the number of observations in that combination.

Because of the particular toxicological importance of the tetra component, the analysis of variance and associated table of means are presented in Tables 19 and 20. The conclusions are the same as for the variable total percent conversion.

The results of the Phase 2 statistical analysis indicate that, within the ranges studied, the variables of temperature, oxygen, and residence time appear to have maximum conversion near a temperature of 675°C, oxygen concentration of 8%, and for a residence of about 0.8 s. Conversion is significantly higher near the middle of the ranges for temperature and oxygen, but does not vary significantly by residence time. Nevertheless, the suggestive lower value at the short residence time of 0.3 s indicates that such a short residence time should be avoided in the next phase. Consequently, the recommended conditions for the next phase would be temperature 675°C, oxygen 8%, and residence time between 0.8 and 1.6 s. A convenient residence time could be chosen within that range as it does not appear to affect conversion.

C. Phase 3

1. Test Conditions

A total of 24 tests were performed in Phase 3, employing four types of dielectric fluids and spanning a range of PCB concentrations from 0 to 70%. All runs used the same nominal operating conditions obtained from statistical evaluation of Phase 2 results. These nominal conditions are a 675°C combustion temperature, an 8% effluent oxygen concentration, and a 0.8-s. residence time in the combustion zone. The gas temperature in the pyrolysis furnace was about 395°C in all tests except the askarel tests, in which a 461°C temperature was used, for reasons discussed below.

Table 17. Reduced Analysis of Variance Model Using Only Temperature and Oxygen

Dependent variable: Total

Source	DF	Sum of squares	Mean square	F value	P	R-square	C.V.
Model	12	0.5754	0.0480	20.96	0.0001	0.9402	45.92
Error	16	0.0366	0.0023		Root MSE		Total mean
Corrected total	28	0.6120			0.0478		0.1042

Source	DF	Type II SS	F value	P
T[a]	3	0.1175	17.13	0.0001
R[b]	3	0.0066	0.96	0.4377
O[c]	3	0.1939	28.26	0.0001
T*O	3	0.1088	15.85	0.0001

[a]Temperature.
[b]Oxygen.
[c]Residence time.

Table 18. Means for Total PCDF Conversion Efficiency (%) Grouped by Variable

Variable		Sample size (N)	Mean
T			
L		5	0.0214
M_+		16	0.0979
M		4	0.3225
H		4	0.0142
O			
L		4	0.0132
M_+		17	0.0808
M		2	0.4813
H		6	0.1051
R			
L		4	0.0400
M_+		13	0.1121
M		2	0.1387
H		10	0.1126
T	O		
L	L	2	0.0099
L	M	3	0.0291
M	L	2	0.0166
M	M_+	9	0.0814
M	H	1	0.1864
M_+	M_+	4	0.1536
M	M	3	0.1712
H	M	1	0.7762
H	H	2	0.0202
		2	0.0081

Table 19. Analysis of Variance for TetraCDF

Dependent variable: Tetra

Source	DF	Sum of squares	Mean square	F value	P	R-square	C.V.
Model	12	0.1600	0.0133	6.85	0.0003	0.8371	60.42
Error	16	0.0311	0.0019		Root MSE		Tetra mean
Corrected total	28	0.1911			0.0441		0.0730

Source	DF	Type II SS	F value	P
T	3	0.0356	6.10	0.0057
R	3	0.0027	0.46	0.7108
O	3	0.0494	8.46	0.0013
T*O	3	0.0382	6.54	0.0043

Table 20. Means for TetraCDF Conversion Efficiency (%) Grouped by Variable

Variable		Sample size (N)	Mean
T			
L		5	0.0402
M_+		16	0.0714
M^+		4	0.1820
H		4	0.0110
O			
L		4	0.0243
M_+		17	0.0643
M^+		2	0.2598
H		6	0.0677
R			
L		4	0.0555
M_+		13	0.0747
M^+		2	0.0857
H		10	0.0752
T	O		
L	L	2	0.0180
L	M	3	0.0551
M	L	2	0.0307
M	M_+	9	0.0651
M	M^+	1	0.0937
M_+	H	4	0.1006
M^+	M_+	3	0.1007
M^+	M^+	1	0.4260
H	M	2	0.0199
H	H	2	0.0021

The list of runs, operating conditions, gas concentrations and calculated combustion efficiencies is provided in Table 21. The run numbering system is similar to that used for Phase 2. The first three segments are the month, date, and sequential run number, all separated by dashes. In the suffixes "M" represents mineral oil, "S" represents silicone oil, "CLBZ" represents chlorobenzene, and "ASKL" represents askarel. The 5, 50, and 500 represent total PCB concentrations in ppm (w/w, i.e., µg/g). System blank runs are noted by a "(B)."

The combustion efficiencies (CEs) are generally low, as would be expected for the combustion temperature selected for maximum PCDF generation. However, CE for blank runs should be near 100%, as CO levels should be near zero. This was not the case in Runs 8-22-53-S500(B) and 8-23-56-CLBZ(B) as unexpectedly high CO levels were observed. This is presumably due to slow decomposition of carbonaceous material remaining in the pyrolysis furnace, as discussed below.

For the tests involving mineral oil and silicone oil, three concentrations of PCBs (Aroclor 1254) were used. The chlorobenzene dielectric fluid was analyzed by GC/ECD and contained mostly trichlorobenzene isomers, some tetrachlorobenzene, and no detectable PCBs, PCDFs or PCDDs. The askarel-type dielectric fluid contained a high level of PCBs, 70% (w/v) Aroclor 1260 by GC/ECD analysis, and no PCDFs or PCDDs. For each fluid except askarel, the density was determined to allow conversion of the concentrations units from weight/weight to weight/volume. This step was necessary because the syringe pump used for injecting the feed oil solution operates at a constant volume rate. The sample period for each test and resulting dielectric fluid volume pumped are shown in Table 22. Also shown are the fluid densities and PCB concentrations (in both µg/g and µg/mL). Finally, the total milligrams of PCBs subjected to thermal degradation are indicated for each test.

2. Operational Problems

No serious difficulties were encountered during the Phase 3 mineral oil tests. As noted in Table 21, a longer residence time was used (1.23 s) for the first run (8-07-39-M500). This was a preliminary test performed before final test conditions had been identified.

Two major problems developed during the silicone oil tests. The first problem became readily apparent when the first run (8-17-47-S5) commenced. Large quantitites of a fine, white silicate powder were generated. Although the bulk of this material was deposited on the condensation tube walls and on the glass wool plug of the XAD-2 trap, significant quantities of the particulate passed through the resin trap and into the tubing leading to the continuous gas monitors. This particulate condensed on the inlet filter in the CO_2 monitor and stopped the gas flow to both the CO_2 and the CO monitors. CO_2 and CO data were not obtained from this run. In addition, the deposition of large quantities of particulate clogged the glass wool at the front of the XAD-2 trap, which presented flow control problems. Although the placement of in-line filters at different locations helped to control this problem, frequent flow rate corrections and shutdowns were necessary during the silicone oil tests.

Table 21. Operating Conditions for Phase 3 Tests

Run no.	Combustion temperature (°C)	Oxygen (%)	Residence time (s)	CO_2 (%)	CO (%)	Combustion efficiency (%)	Pyrolysis temperature (°C)
8-15-43-M5	679	8.0	0.84	0.56	0.28	67	396
8-15-44-M5	679	8.1	0.83	0.58	0.29	67	395
8-17-47-S5	677	8.5	0.85	ND	ND	ND	395
8-20-48-S5	675	7.6	0.78	0.06	0.13	32	394
8-16-45-M50	679	8.0	0.83	0.55	0.29	65	395
8-16-46-M50	679	7.8	0.81	0.54	0.28	66	395
8-21-49-S50	678	8.2	0.83	0.08	0.32	20	395
8-21-50-S50	679	7.8	0.82	0.06	0.32	16	394
8-07-39-M500	685	8.3	1.23	1.53	0.55	73	396
8-13-40-M500	678	7.7	0.81	0.53	0.24	69	395
8-14-41-M500	678	7.9	0.82	0.55	0.24	70	395
8-14-42-M500(B)	675	8.2	0.81	0.06	0.001	99	395
8-22-51-S500	680	8.2	0.79	0.05	0.35	12	394
8-22-52-S500	680	8.3	0.82	0.06	0.36	14	394
8-22-53-S500(B)	679	8.2	0.82	0.05	0.14	26	395
8-29-60-ASKL[b]	680	ND	ND	ND	ND	ND	461
8-30-61-ASKL	680	8.8	0.87	0.07	0.23	23	462
8-30-62-ASKL	679	8.5	0.81	0.06	0.18	25	461
8-30-63-ASKL(B)	679	7.9	0.75	0.05	0.001	99	461
8-23-54-CLBZ	680	8.3	0.81	0.07	0.41	15	395
8-23-55-CLBZ	680	8.3	0.81	0.07	0.33	17	395
8-23-56-CLBZ(B)	679	8.2	0.82	0.06	0.12	33	395
8-28-57-CLBZ	679	8.1	0.82	0.07	0.05	56	394
8-28-58-CLBZ	679	7.7	0.83	0.07	0.10	41	395
8-28-59-CLBZ(B)	680	8.2	0.80	0.07	0.002	98	395

[a]ND = no data.
[b]Conditions unstable; continuous monitoring data was unreliable.

Table 22. PCB Feed Characteristics in Phase 3

Run no.	Sample period (min)	Feed volume (mL)	PCB conc. (µg/g)	PCB conc. (µg/mL)	PCBs in feed (mg)
8-15-43-M5	67	0.90	5	4.28	0.004
8-15-44-M5	73	0.99	5	4.28	0.004
8-17-47-S5	58	0.78	5	4.66	0.004
8-20-48-S5	67	0.90	5	4.66	0.004
8-16-45-M50	61	0.82	50	42.8	0.035
8-16-46-M50	63	0.85	50	42.8	0.036
8-21-49-S50	59	0.80	50	46.6	0.037
8-21-50-S50	53	0.72	50	46.6	0.033
8-07-39-M500	60	0.81	500	428	0.35
8-13-40-M500	61	0.82	500	428	0.35
8-14-41-M500	61	0.82	500	428	0.35
8-14-42-M500(B)	60	0	NA[a]	NA	0
8-22-51-S500	56	0.76	500	466	0.35
8-22-52-S500	61	0.82	500	466	0.38
8-22-53-S500(B)	58	0	NA	NA	0
8-29-60-ASKL	120	1.62	UNK[b]	700,000	1,130
8-30-61-ASKL	35	0.47	UNK	700,000	330
8-30-62-ASKL	35	0.47	UNK	700,000	330
8-30-63-ASKL(B)	35	0	NA	NA	0
8-23-54-CLBZ	64	0.86	0	0	0
8-23-55-CLBZ	58	0.78	0	0	0
8-23-56-CLBZ(B)	52	0	NA	NA	0
8-28-57-CLBZ	60	0.81	0	0	0
8-28-58-CLBZ	59	0.80	0	0	0
8-28-59-CLBZ(B)	60	0	NA	NA	0

[a]NA = not applicable.
[b]UNK = unknown.

The second problem that developed during the silicone oil tests was less obvious initially. High CO levels in the effluent gases remained even when the waste feed was shut off. This situation continued even during the first three chlorobenzene runs (Runs 54, 55, and 56). Also, both the system blanks run during this period showed very high CO levels. At this point, the pyrolysis furnace tube was opened and several milliliters of an oily liquid were visible in the tube. It was apparent that the operating temperature for the pyrolysis furnace was too low to completely vaporize the silicone oil. Slow decomposition of this residue was likely caused by the high CO levels observed up to several hours after the flow of silicone oil was stopped. This residual pool of oil was rinsed out before repeating the now suspect chlorobenzene tests. Fortunately, subsequent analysis of the rinse sample did not detect any PCBs. This indicated that either (1) all PCBs passed through the system, or (2) if any PCBs remained, they were eventually decomposed in the pyrolysis furnace. As discussed below, thermal analysis was later performed on the silicone oil, verifying that the pyrolysis furnace temperature was too low for complete vaporization. The second group of three chlorobenzene runs was conducted without incident.

Thermal degradation of the askarel fluid resulted in the formation of black, sooty materials that passed through the XAD-2 trap and resulted in minor clogging and flow control problems. The pyrolysis furnace temperature was elevated during these runs to enhance vaporization, although later thermal analysis of the askarel fluid indicated that this measure was probably unnecessary.

3. Thermal Analysis of Dielectric Fluids

Because of operational problems encountered during the Phase 3 degradation tests, as described above, attempts were made to better characterize the various dielectric fluids. Two types of thermal analysis, differential scanning calorimetry (DSC) and thermogravimetric analysis (TGA), were conducted. DSC indicates chemical or physical changes (either exothermic or endothermic) occurring in a substance as it is heated. TGA indicates weight loss (or gain, if appropriate) of a substance as a function of temperature. Both DSC and TGA were performed using a heating rate of 20°C/min and an atmosphere of prepurified nitrogen, flowing at 20 or 30 mL/min. Sample sizes for the analyses ranged from 3 to 6 mg. All four dielectric fluids used in the Phase 3 thermal degradation tests were studied by DSC. Only the silicone oil and askarel were analyzed by TGA.

Several interesting results were obtained from the thermal analyses. Mineral oil undergoes an exothermic reaction at 232°C (probably a decomposition or rearrangement) and boils at less than 348°C at atmospheric pressure. This value was obtained from a closed-pan DSC analysis, which may have had an elevated pressure and thus represents an upper limit. A weight loss of 97% resulted from heating to 400°C. The chlorobenzene dielectric fluid had a measured boiling point at or below 264°C. Heating to 300°C resulted in a 97% weight loss. The askarel fluid exhibited a boiling point of approximately 230°C. Essentially complete weight loss occurred from heating to 300°C.

The polydimethylsiloxane (silicone oil) exhibited a strongly exothermic reaction at approximately 285°C. This is probably a polymerization reaction. Heating to 350°C caused very little weight loss, leaving a sticky, viscous liquid. The TGA indicated a boiling point of approximately 450°C with about 90% weight loss occurring between 300 and 500°C. Thus, only about 30% of the silicone fluid shou'd have vaporized at the pyrolysis furnace operating temperature (395°C) used during the Phase 3 tests. This coincided with the visual observation of residual oil remaining in the pyrolysis furnace following the silicone oil tests.

4. PCDF and PCDD Analysis Results

The results of the analysis of the Phase 3 samples are presented in Tables 23 through 28. PCDFs were found in all samples, except two laboratory blanks. PCDDs were found in the effluent from the chlorobenzene runs, and occasionally at low levels in other samples (Tables 26 through 28). PCBPs are not reported, since they were not distinguishable from PCBs under the analysis conditions.

As described in Section VII.C.2, runs 39, 54, 55, and 56 were conducted under different conditions than the other runs. Also the first askarel run (No. 60) produced CO, CO_2, and O_2 levels which varied from those for the other runs. Since these five runs could not be compared with the other runs, these runs were not included in Tables 23 through 28.

Since the sampling periods varied from 35 to 120 min and the amount of feed oil fed varied commensurately, the amount of PCDFs (Tables 23 and 26) found is also expressed in nanograms (ng) PCDF per milliliter (mL) feed oil in Tables 24 and 27. This permits direct comparison between runs. The conversion efficiencies shown in Tables 25 and 28 were calculated in a different manner than for the Phase 2 samples. The conversion efficiencies shown in Table 15 (Phase 2) for individual PCDF homologs were calculated by dividing the concentration of the PCDF by the concentration of the corresponding individual PCB isomer in the feed. In Tables 25 and 28 (Phase 3), the conversion efficiencies for the individual PCDF and PCDD homologs were calculated by dividing the concentration of the PCDF or PCDD homolog by the total PCB concentration in the feed. Consequently, a direct comparison of Tables 15 and 25 cannot be made for the individual PCDF homologs. The total (PCDF) conversion efficiencies in these two tables are, however, comparable, since each was calculated by dividing the total amount of PCDF formed by the total amount of PCB feed and then multiplying by 100.

Although a single value is reported for each homolog, characteristic clusters of isomers were generally observed. The responses for all identified peaks were simply summed to give the reported values. Representative isomeric distributions are shown in Figures 10 through 20.

Table 23. Amounts of PCDFs Formed in Phase 3

Run no.	MonoCDF (ng)	DiCDF (ng)	TriCDF (ng)	TetraCDF (ng)	PentaCDF (ng)	HexaCDF (ng)	HeptaCDF (ng)	OctaCDF (ng)	PCDFs (ng)
8-15-43-M5	-[a]	-	130	49	NQ[b]	0[c]	-	-	180
8-15-44-M5	-	-	43	23	0	0	-	-	66
8-17-47-S5	-	-	26	0	90	0	-	-	116
8-20-48-S5	-	-	31	9	150	0	-	-	190
8-16-45-M50	-	-	200	110	39	8.5	-	-	350
8-16-46-M50	-	-	140	82	21	2.2	-	-	250
8-21-49-S50	-	-	290	73	62	0	0	0	420
8-21-50-S50	-	-	530	640	83	0	0	0	1,300
8-13-40-M500	1,700	0	2,200	690	43	7	0	0	4,700
8-14-41-M500	-	-	1,300	620	170	13	0	0	2,100
8-14-42-M500(B)	-	-	0	13	0	0	0	0	13
8-22-51-S500	-	-	2,000	740	340	45	-	-	3,100
8-22-52-S500	50	1,300	5,000	2,100	170	12	0	0	8,600
8-22-53-S500(B)	0.4	0	0	0	0	0	0	0	0.4
8-30-61-ASKL	810	5,100	440,000	1,400,000	6,400,000	910,000	29,000	3,400	9,200,000
8-30-62-ASKL	1,900	7,000	220,000	1,100,000	4,700,000	660,000	19,000	1,300	6,700,000
8-30-63-ASKL(B)	28	190	310	1,200	17,000	3,000	-	-	22,000
8-28-57-CLBZ	-	-	2,400	2,600	5,000	0	-	-	9,900
8-28-58-CLBZ	2,000	29,000	>13,000	>19,000	>22,000	5,200	0	0	>90,000
8-28-59-CLBZ(B)	-	-	81	25	5	0	-	-	110
Lab Blank	0	0	0	0	0	0	-	-	0

[a] - = not analyzed.
[b] NQ = not quantitated.
[c] 0 = not detected.

Table 24. PCDF Formation in Phase 3

Run no.	MonoCDF formation (ng/mL)	DiCDF formation (ng/mL)	TriCDF formation (ng/mL)	TetraCDF formation (ng/mL)	PentaCDF formation (ng/mL)	HexaCDF formation (ng/mL)	HeptaCDF formation (ng/mL)	OctaCDF formation (ng/mL)	PCDFs formation (ng/mL)
8-15-43-M5	-[a]	-	150	54	NQ[b]	0[c]	-	-	200
8-15-44-M5	-	-	44	23	0	0	-	-	67
8-17-47-S5	-	-	33	0	120	0	-	-	150
8-20-48-S5	-	-	34	10	170	0	-	-	210
8-16-45-M50	-	-	240	130	48	10	-	-	430
8-16-46-M50	-	-	170	96	25	3	0	0	290
8-21-49-S50	-	-	360	92	78	0	0	0	530
8-21-50-S50	-	-	740	900	120	0	0	0	1,800
8-13-40-M500	2,100	0	2,700	830	52	9	0	0	5,700
8-14-41-M500	-	-	1,600	760	210	16	0	0	2,600
8-14-42-M500(B)	NA[d]	NA	NA	NA	NA	NA	NA	NA	NA
8-22-51-S500	-	-	2,600	980	450	60	0	0	4,100
8-22-52-S500	61	1,600	6,100	2,500	210	15	0	0	11,000
8-22-53-S500(B)	NA	NA	NA	NA	NA	NA	NA	NA	NA
8-30-61-ASKL	1,700	11,000	940,000	3,000,000	14,000,000	1,900,000	61,000	7,200	19,000,000
8-30-62-ASKL	4,000	15,000	470,000	2,400,000	9,900,000	1,400,000	39,000	2,700	14,000,000
8-30-63-ASKL(B)	NA	NA	NA	NA	NA	NA	NA	NA	NA
8-28-57-CLBZ	-	-	2,900	3,200	6,100	0	-	-	12,000
8-28-58-CLBZ	2,500	36,000	> 16,000	> 24,000	> 28,000	6,500	0	0	> 110,000
8-28-59-CLBZ(B)	NA	NA	NA	NA	NA	NA	NA	NA	NA

[a] - = not analyzed.
[b] NQ = not quantified.
[c] 0 = not detected.
[d] NA = not applicable.

Table 25. Conversion Efficiencies (PCBs to PCDFs) for Phase 3

Run no.	MonoCDF conversion efficiency (%)	DiCDF conversion efficiency (%)	TriCDF conversion efficiency (%)	TetraCDF conversion efficiency (%)	PentaCDF conversion efficiency (%)	HexaCDF conversion efficiency (%)	HeptaCDF conversion efficiency (%)	OctaCDF conversion efficiency (%)	PCDFs conversion efficiency (%)
8-15-43-M5	-[a]	-	3.4	1.3	NQ[b]	0[c]	-	-	4.7
8-15-44-M5	-	-	1.0	0.55	0	0	-	-	1.6
8-17-47-S5	-	-	0.71	0	2.5	0	-	-	3.2
8-20-48-S5	-	-	0.74	0.21	3.6	0	-	-	4.5
8-16-45-M50	-	-	0.55	0.31	0.11	0.024	-	-	1.0
8-16-46-M50	-	-	0.40	0.22	0.058	0.0060	-	-	0.67
8-21-49-S50	-	-	0.78	0.20	0.17	0	0	0	1.1
8-21-50-S50	-	-	1.6	1.9	0.25	0	0	0	3.8
8-13-40-M500	0.49	0	0.64	0.19	0.012	0.0020	0	0	1.3
8-14-41-M500	-	-	0.38	0.18	0.048	0.0037	0	0	0.61
8-14-42-M500(B)	NA[d]	NA	NA	NA	NA	NA	NA	NA	NA
8-22-51-S500	-	-	0.56	0.21	0.096	0.013	-	-	0.88
8-22-52-S500	0.013	0.35	1.3	0.54	0.044	0.0031	0	0	2.3
8-22-53-S500(B)	NA	NA	NA	NA	NA	NA	NA	NA	NA
8-30-61-ASKL	0.0002	0.0015	0.13	0.43	1.9	0.28	0.0087	0.0010	2.8
8-30-62-ASKL	0.006	0.0021	0.067	0.34	1.4	0.20	0.0056	0.0004	2.0
8-30-63-ASKL(B)	NA	NA	NA	NA	NA	NA	NA	NA	NA
8-28-57-CLBZ	NA	NA	NA	NA	NA	NA	NA	NA	NA
8-28-58-CLBZ	NA	NA	NA	NA	NA	NA	NA	NA	NA
8-28-59-CLBZ(B)	NA	NA	NA	NA	NA	NA	NA	NA	NA

[a] - = not analyzed.
[b] NQ = not quantitated.
[c] 0 = not detected.
[d] NA = not applicable.
[e] High levels saturated the detector signal.

Table 26. Amounts of PCDDs Formed in Phase 3

Run no.	MonoCDD (ng)	DiCDD (ng)	TriCDD (ng)	TetraCDD (ng)	PentaCDD (ng)	HexaCDD (ng)	HeptaCDD (ng)	OctaCDD (ng)	PCDDs (ng)
8-15-43-M5	-[a]	-	0[b]	0	0	0	-	-	0
8-15-44-M5	-	-	0	0	0	0	-	-	0
8-17-47-S5	-	-	0	0	0	0	-	-	0
8-20-48-S5	-	-	0	0	0	0	-	-	0
8-16-45-M50	-	-	0	0	0	0	-	-	0
8-16-46-M50	-	-	0	0	0	0	-	-	0
8-21-49-S50	-	-	0	0	0	0	0	0	0
8-21-50-S50	-	-	0	0	0	0	0	0	0
8-13-40-M500	0	0	0	0	0	0	0	0	0
8-14-41-M500	-	-	0	0	0	0	0	0	0
8-14-42-M500(B)	-	-	0	0	0	0	0	0	0
8-22-51-S500	-	-	0	0	7.7	0	-	-	7.7
8-22-52-S500	0	0	0	0	1.7	0	0	0	1.7
8-22-53-S500(B)	0	0	0	0	0	0	0	0	0
8-30-61-ASKL	0	0	0	0	0	0	330	37	360
8-30-62-ASKL	0	0	0	0	0	0	230	51	280
8-30-63-ASKL(B)	0	0	0	0	0	0	-	-	0
8-28-57-CLBZ	-	-	1,100	440	0	0	-	-	1,500
8-28-58-CLBZ	0	0	630	520	0	72	0	0	1,200
8-28-59-CLBZ(B)	-	-	0	0	0	0	-	-	0
Lab Blank	0	0	0	0	0	0	-	-	0

[a] - = not analyzed.
[b] 0 = not detected.

Table 27. PCDD Formation in Phase 3

Run no.	MonoCDD formation (ng/mL)	DiCDD formation (ng/mL)	TriCDD formation (ng/mL)	TetraCDD formation (ng/mL)	PentaCDD formation (ng/mL)	HexaCDD formation (ng/mL)	HeptaCDD formation (ng/mL)	OctaCDD formation (ng/mL)	PCDDs formation (ng/mL)
8-15-43-M5	-[a]	-	0[b]	0	0	0	-	-	0
8-15-44-M5	-	-	0	0	0	0	-	-	0
8-17-47-S5	-	-	0	0	0	0	-	-	0
8-20-48-S5	-	-	0	0	0	0	-	-	0
8-16-45-M50	-	-	0	0	0	0	-	-	0
8-16-46-M50	-	-	0	0	0	0	-	-	0
8-21-49-S50	-	-	0	0	0	0	-	-	0
8-21-50-S50	-	-	0	0	0	0	-	-	0
8-13-40-M500	0	0	0	0	0	0	0	0	0
8-14-41-M500	-	-	0	0	0	0	0	0	0
8-14-42-M500(B)	NA[c]	NA	0	0	0	0	0	0	0
8-22-51-S500	-	-	NA	NA	NA	NA	NA	NA	NA
8-22-52-S500	-	-	0	0	10	0	-	-	10
8-22-53-S500(B)	NA	NA	0	0	2	0	-	-	2
8-30-61-ASKL	0	0	NA	NA	NA	NA	NA	NA	NA
8-30-62-ASKL	0	0	0	0	0	0	690	78	770
8-30-63-ASKL(B)	NA	NA	0	0	0	0	490	110	600
8-28-57-CLBZ	-	-	NA	NA	NA	NA	NA	NA	NA
8-28-58-CLBZ	0	0	1,300	540	0	0	-	-	1,900
8-28-59-CLBZ(B)	NA	NA	790	650	0	90	0	0	1,500
			NA	NA	NA	NA	NA	NA	NA

[a] - = not analyzed.
[b] 0 = not detected.
[c] NA = not applicable.

Table 28. Conversion Efficiencies (PCBs to PCDDs) for Phase 3

Run no.	MonoCDD conversion efficiency (%)	DiCDD conversion efficiency (%)	TriCDD conversion efficiency (%)	TetraCDD conversion efficiency (%)	PentaCDD conversion efficiency (%)	HexaCDD conversion efficiency (%)	HeptaCDD conversion efficiency (%)	OctaCDD conversion efficiency (%)	PCDDs conversion efficiency (%)
8-15-43-M5	-[a]	-	0[b]	0	0	0	-	-	0
8-15-44-M5	-	-	0	0	0	0	-	-	0
8-17-47-S5	-	-	0	0	0	0	-	-	0
8-20-48-S5	-	-	0	0	0	0	-	-	0
8-16-45-M50	-	-	0	0	0	0	-	-	0
8-16-46-M50	-	-	0	0	0	0	-	-	0
8-21-49-S50	-	-	0	0	0	0	-	-	0
8-21-50-S50	-	-	0	0	0	0	0	0	0
8-13-40-M500	0	0	0	0	0	0	0	0	0
8-14-41-M500	-	-	0	0	0	0	0	0	0
8-14-42-M500(B)	NA[c]	NA	NA	NA	NA	NA	NA	NA	NA
8-22-51-S500	-	-	0	0	0.0022	0	-	-	0.0022
8-22-52-S500	0	0	0	0	0.0004	0	0	0	0.0004
8-22-53-S500(B)	NA	NA	NA	NA	NA	NA	NA	NA	NA
8-30-61-ASKL	0	0	0	0	0	0	0.000099	0.000011	0.00011
8-30-62-ASKL	0	0	0	0	0	0	0.000070	0.000015	0.00009
8-30-63-ASKL(B)	NA	NA	NA	NA	NA	NA	NA	NA	NA
8-28-57-CLBZ	NA	NA	NA	NA	NA	NA	NA	NA	NA
8-28-58-CLBZ	NA	NA	NA	NA	NA	NA	NA	NA	NA
8-28-59-CLBZ(B)	NA	NA	NA	NA	NA	NA	NA	NA	NA

[a] - = not analyzed.
[b] 0 = not detected.
[c] NA = not applicable.
[d] High levels saturated the detector signal.

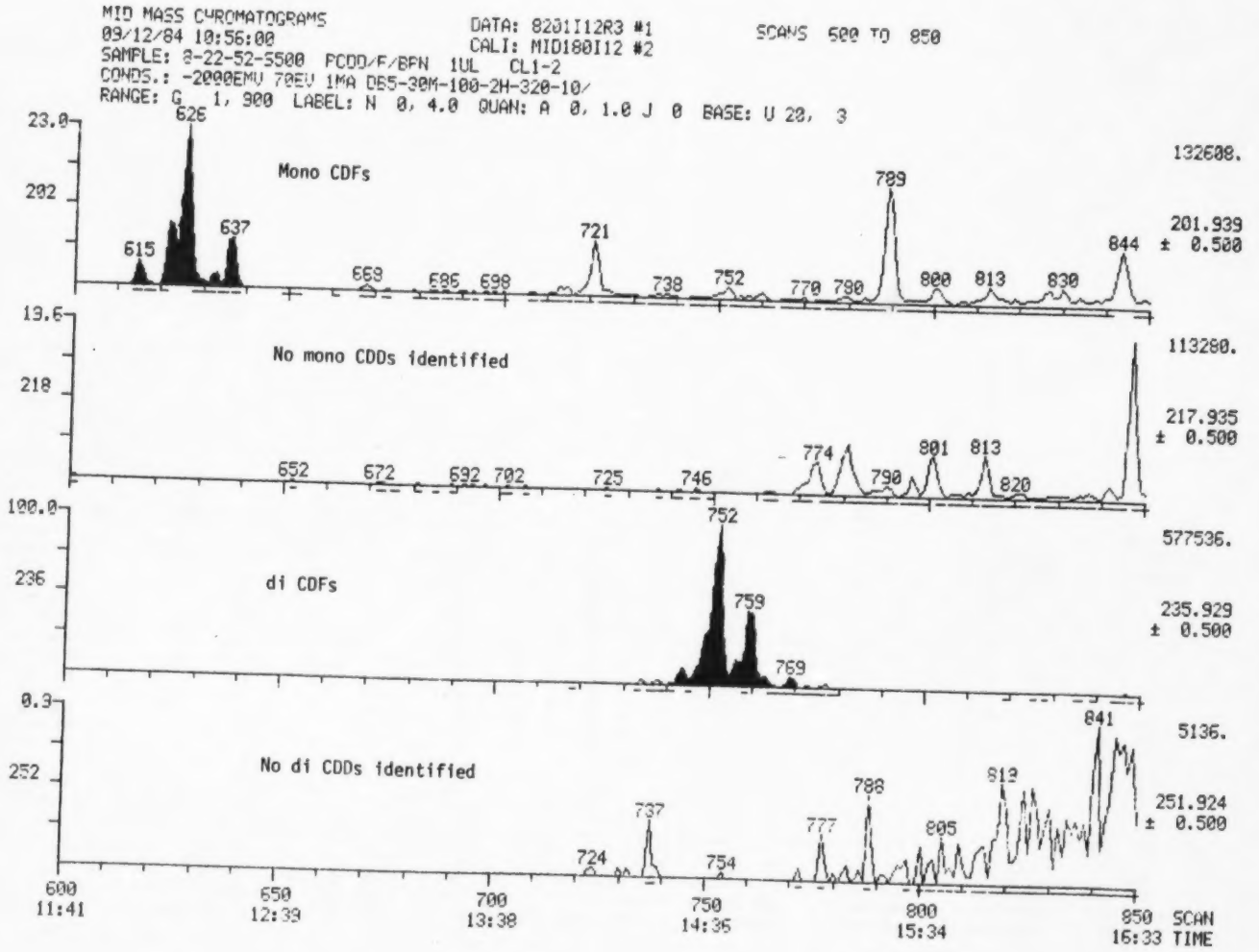

Figure 10. Mono and di CDFs and CDDs in sample 8-22-52-S500.

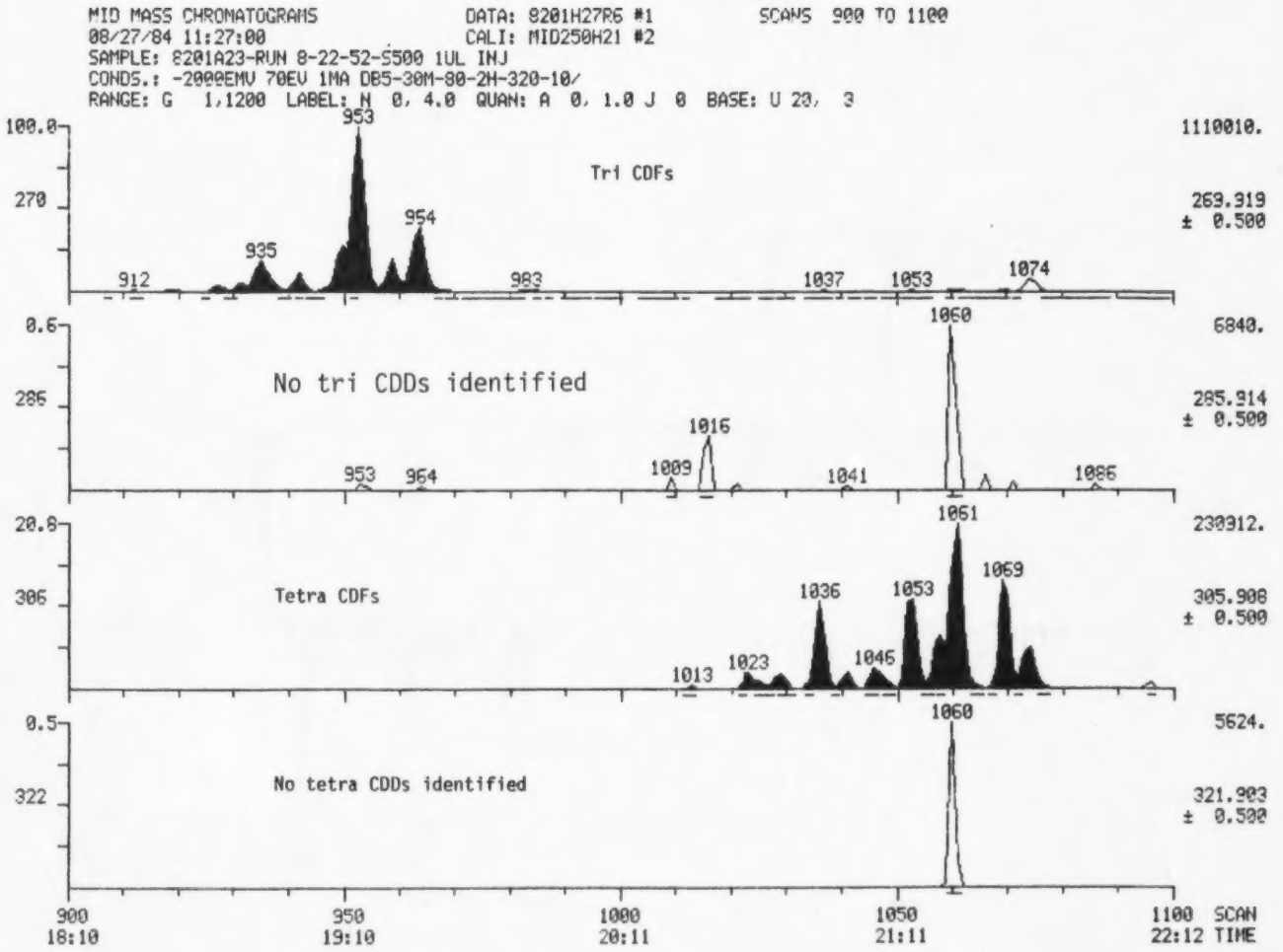

Figure 11. Tri and tetra CDFs and CDDs in sample 8-22-52-S500.

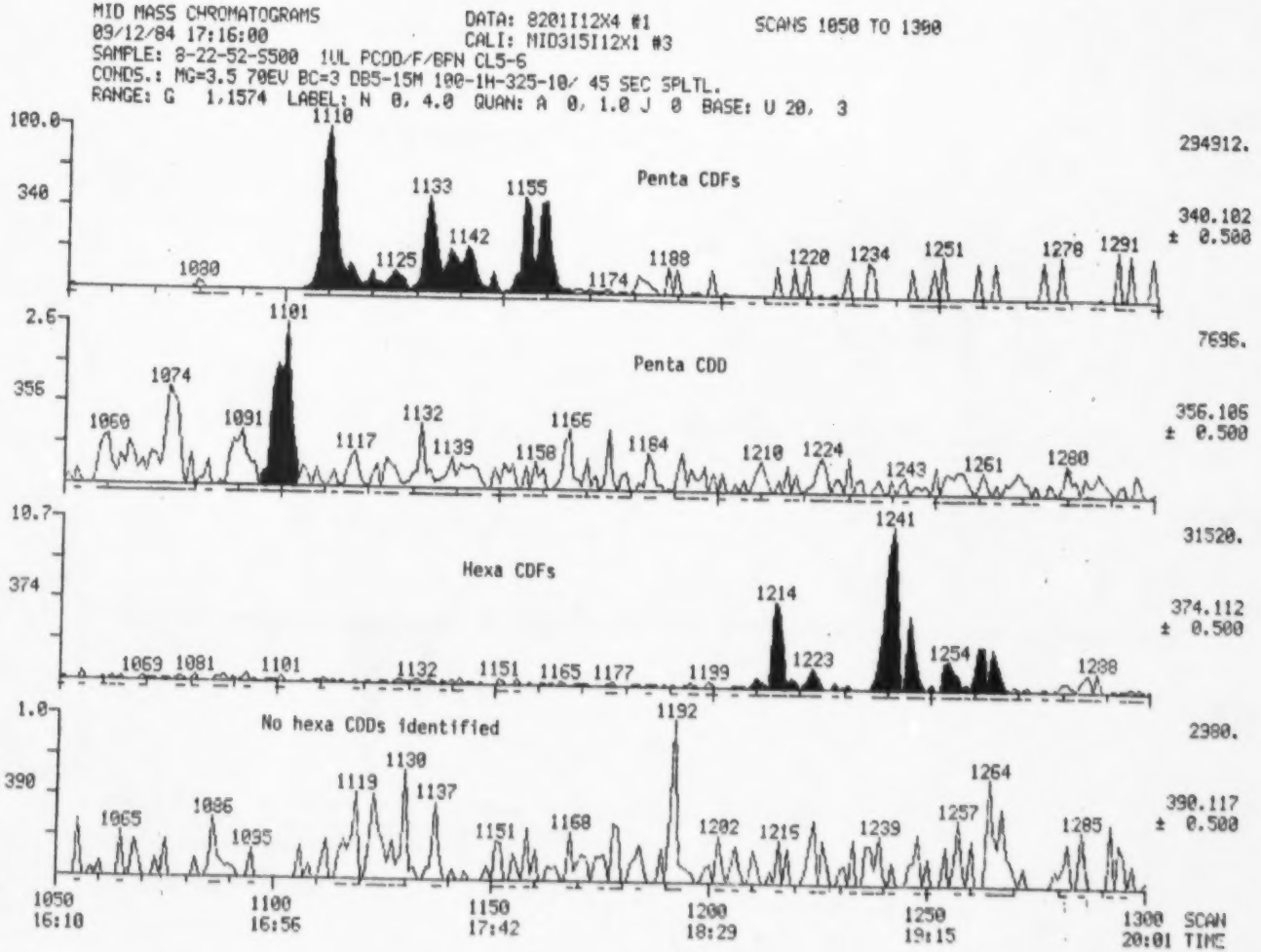

Figure 12. Penta and hexa CDFs and CDDs in sample 8-22-52-S500.

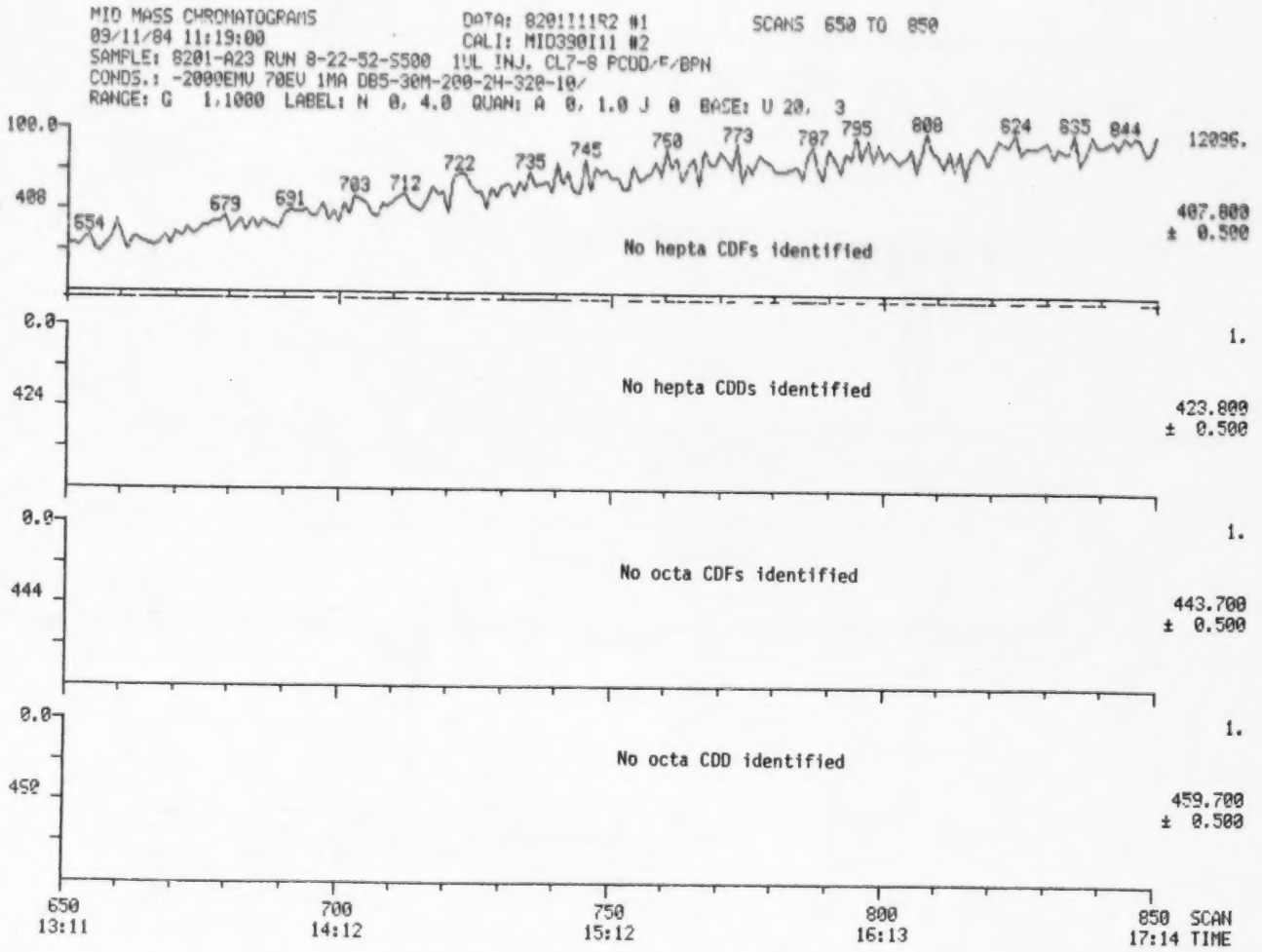

Figure 13. Hepta and octa CDFs and CDDs in sample 8-22-52-S500.

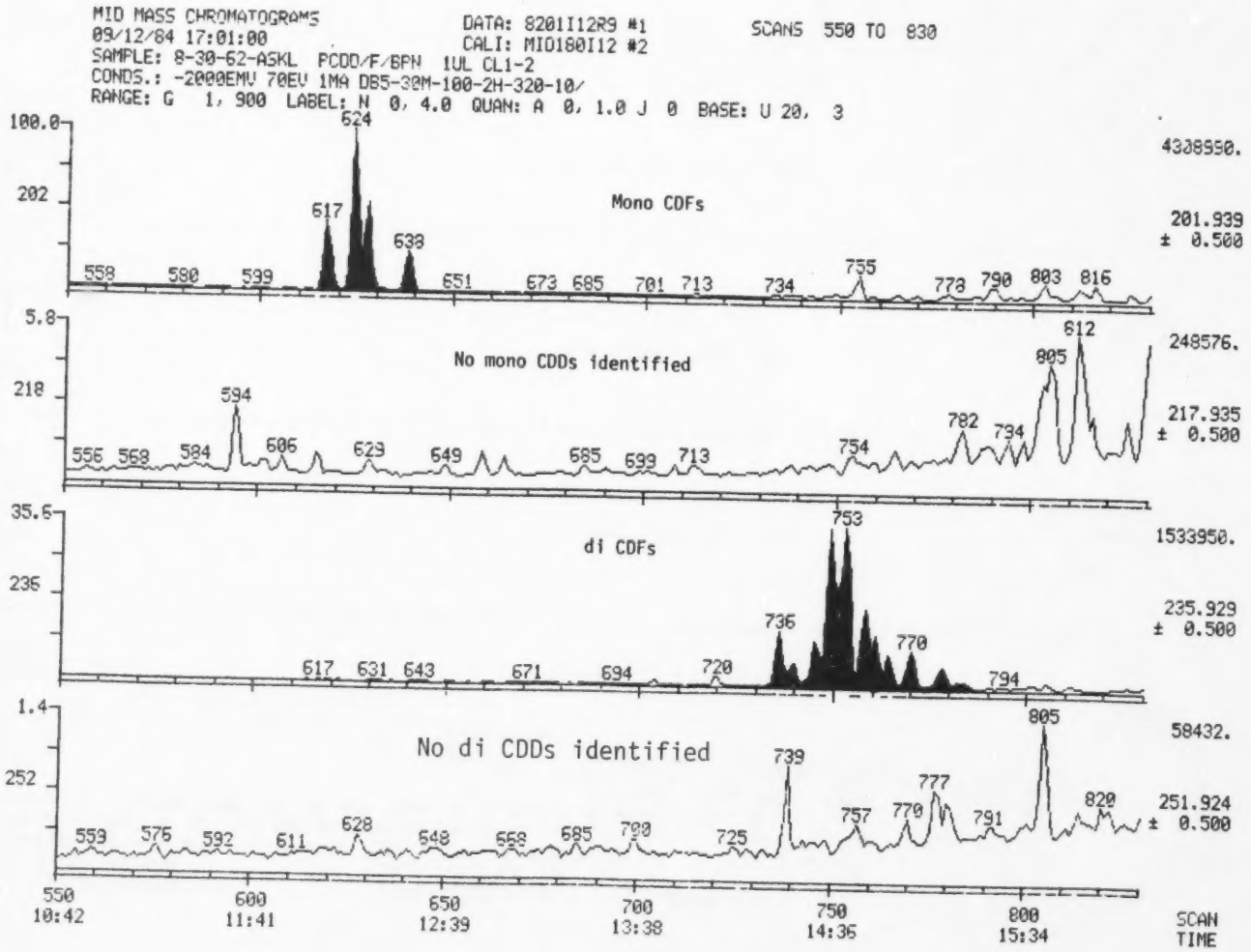

Figure 14. Mono and di CDFs and CDDs in sample 8-30-62-ASKL.

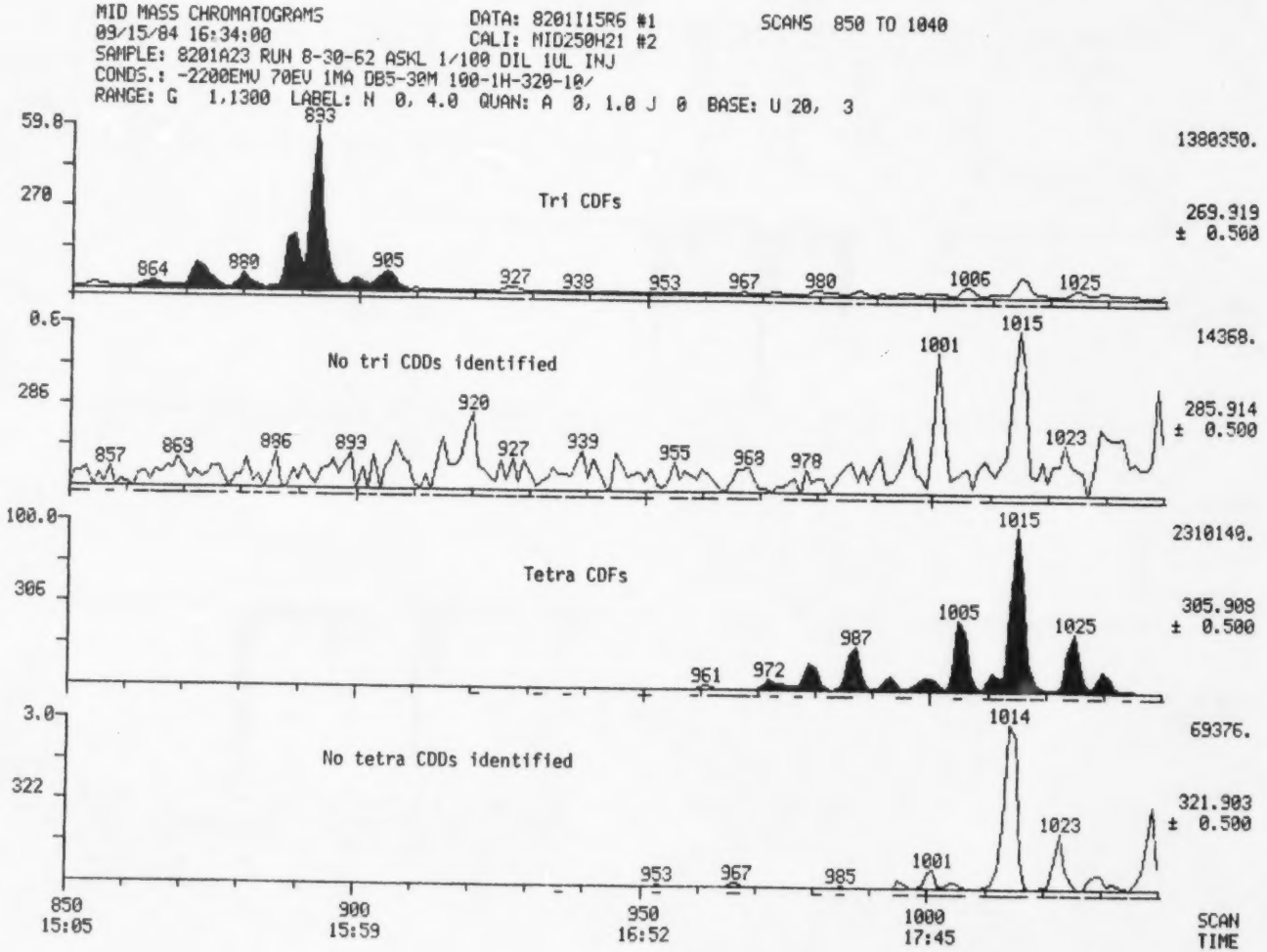

Figure 15. Tri and tetra CDFs and CDDs in sample 8-30-62-ASKL.

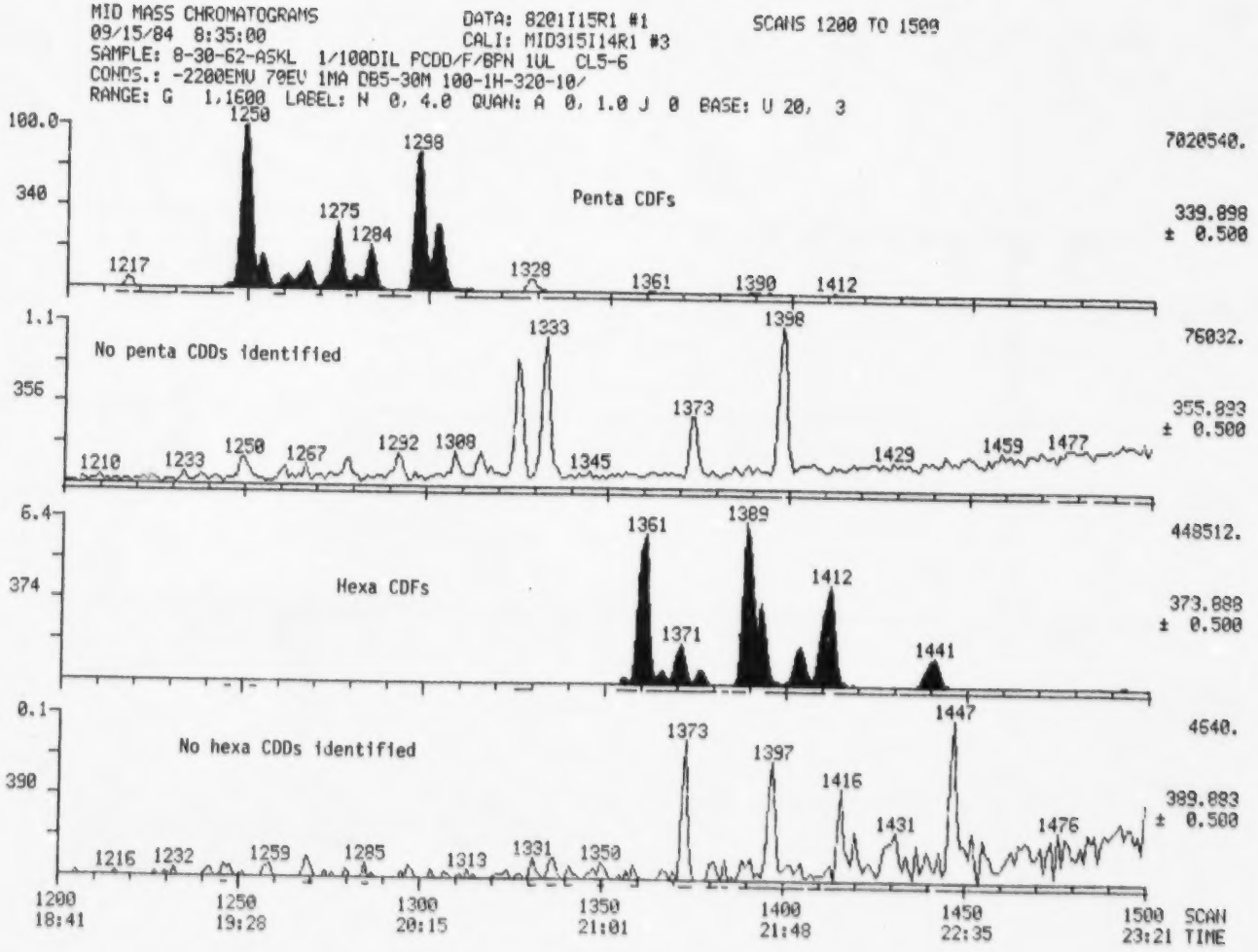

Figure 16. Penta and hexa CDDFs and CDDs in sample 8-30-62-ASKL.

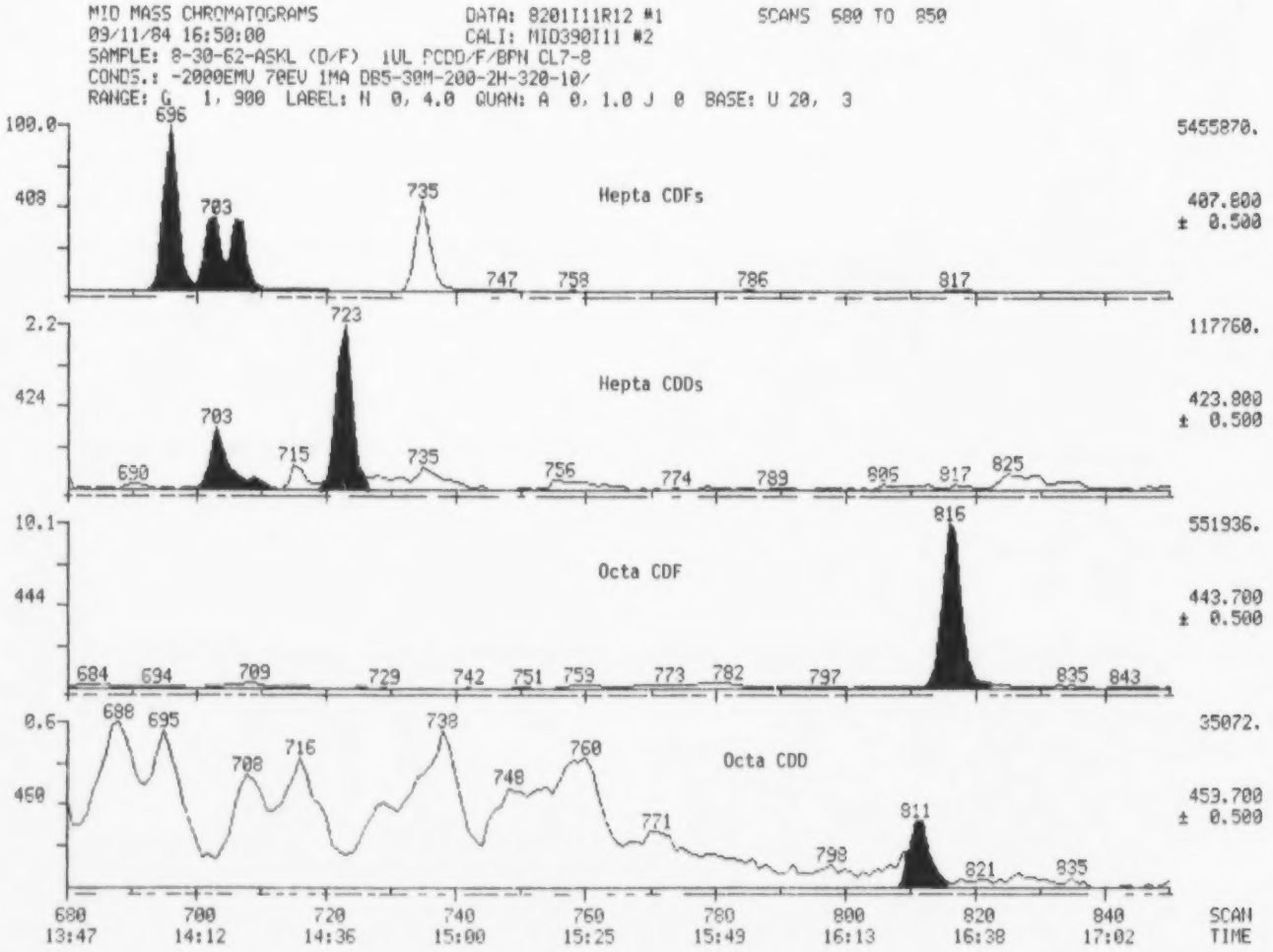

Figure 17. Hepta and octa CDFs and CDDs in sample 8-30-62-ASKL.

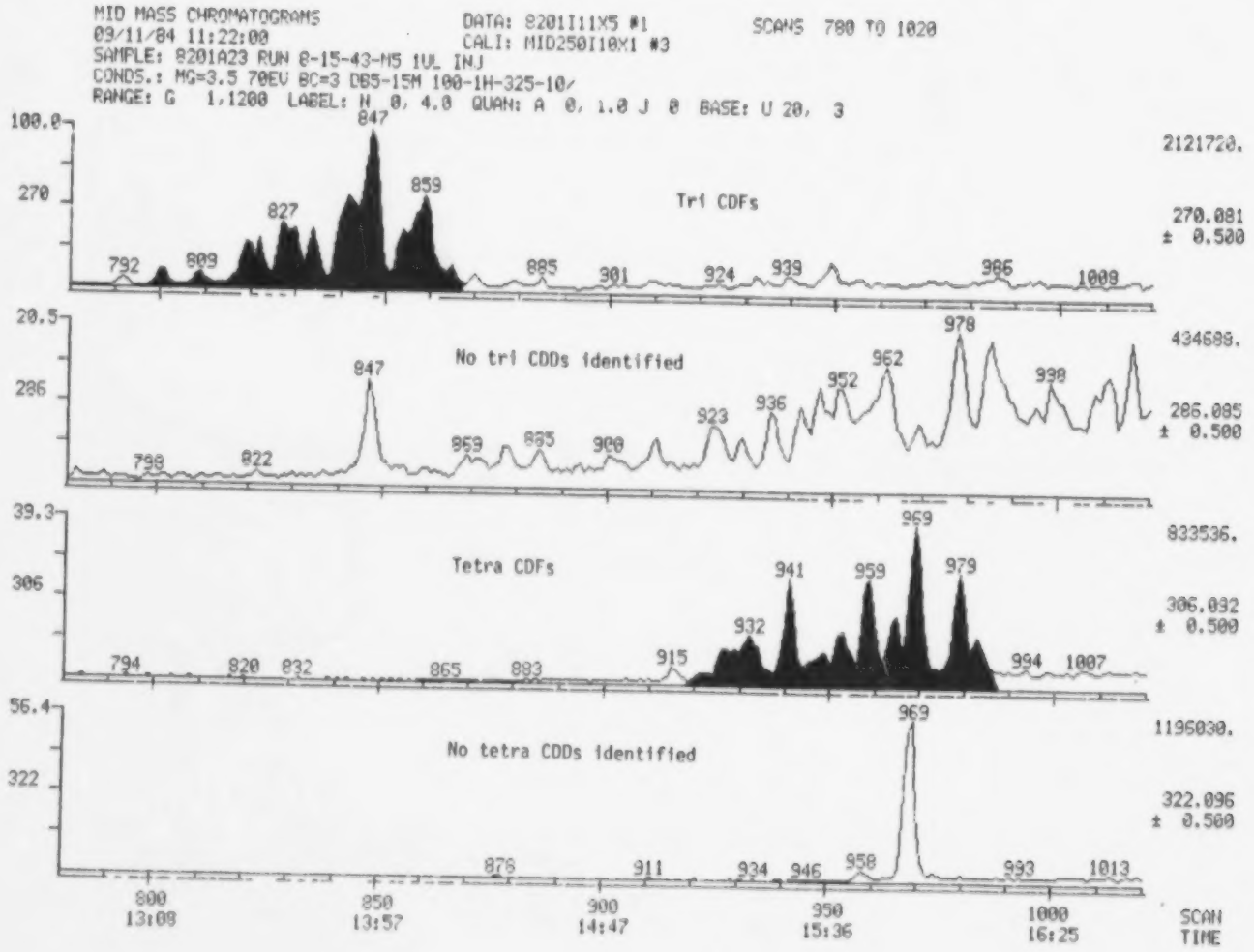

Figure 18. Tri and tetra CDFs and CDDs in sample 8-15-43-M5.

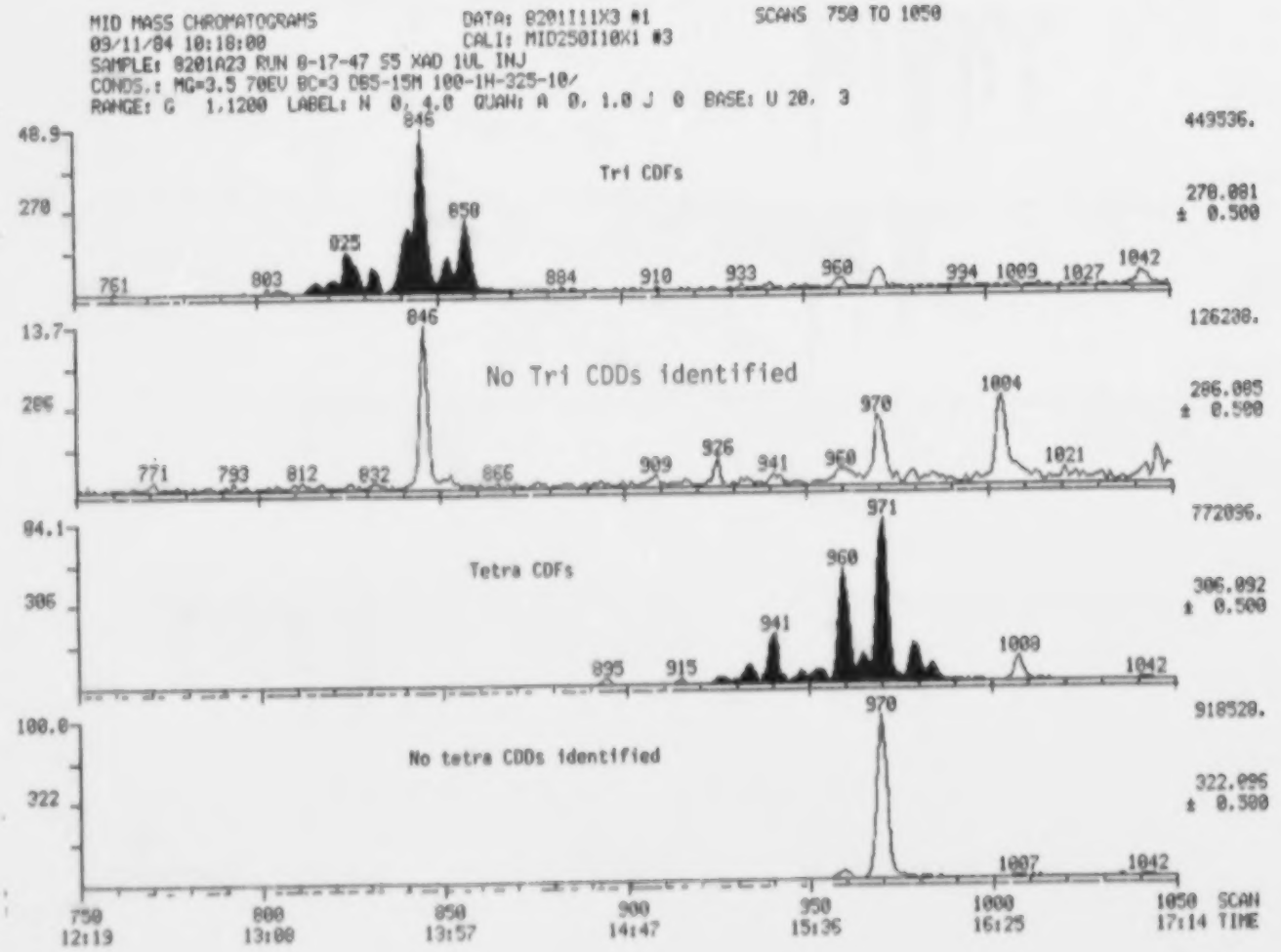

Figure 19. Tri and tetra CDFs and CDDs in sample 8-17-47-S5.

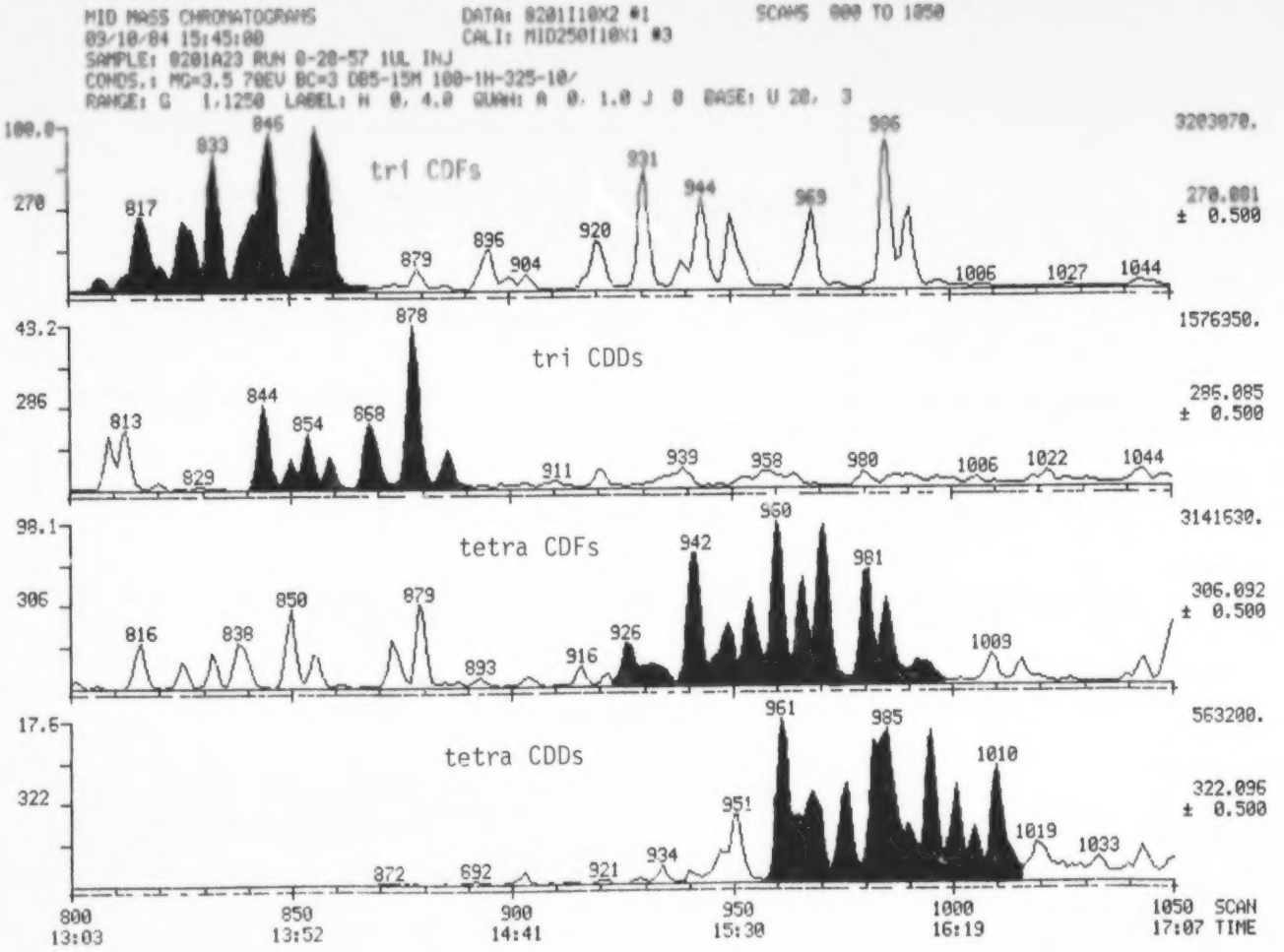

Figure 20. Tri and tetra CDFs and CDDs in sample 8-28-57-CLBZ.

As shown in Tables 23 and 24 and Figure 21, the amount of PCDF formed generally increased with amount of PCBs fed. It should also be noted in Table 23 that two blank runs [8-28-59-CLBZ(B) and 8-30-63-ASKL(B)] contained measurable amounts of PCDFs. Each of these blank runs was made immediately after runs which produced PCDFs in the microgram to milligram range. This possibility had been anticipated, and the run order was designed to minimize the influence of analyte carryover on consecutive runs.

In addition to investigating the effects of PCB concentration on the rate of PCDF formation, it is also instructive to compare the relative distribution by homolog. This is presented in Figures 22 through 24. The askarel tests yielded a normal distribution, peaking at pentaCDF. The M500 and S500 tests yielded somewhat less regular patterns, although the maximum formation was in the tri-, tetra-, and pentaCDF homologs. This irregular pattern is particularly apparent in Figure 22, where a large amount of monoCDF was found in one M500 sample, but no diCDF was found in that sample.

PCDFs and, to a lesser extent, PCDDs are formed from chlorobenzene dielectric fluid under the optimum PCB-to-PCDF conversion conditions. The conversion efficiency of the trichlorobenzene feed was > 0.004% to PCDFs and 0.0001% to PCDDs. The homolog distribution of PCDFs is similar to that found from feeding PCBs as shown in Figure 25. The rate of formation is one to two orders of magnitude lower than for askarel, but substantially higher than that for dielectric fluid containing 500 ppm or less PCBs.

5. PCB Analysis Results

The Phase 3 samples from the spiked mineral oil and spiked silicone oil runs (Runs 40 through 53) were analyzed for PCBs. Table 29 lists the results of these analyses. No PCBs were detected in the blank samples above the limit of detection. However, these results were not included in this table. The results of analysis of the 5-ppm and 50-ppm spiked mineral oil samples are not included because the high hydrocarbon background in these samples prevented the quantitation of PCBs. Table 29 also lists the percent composition of Aroclor 1254 by homolog as presented by Brinkman and De Kok (1980).

From these PCB concentrations, the PCB destructon efficiency (D.E.) was calculated for each run using the following equation:

$$D.E. = \frac{(W_{in} - X_{out})}{W_{in}} \times 100$$

where W_{in} = PCB feed (Table 22)
W_{out} = PCBs in combustion effluent (Table 29)

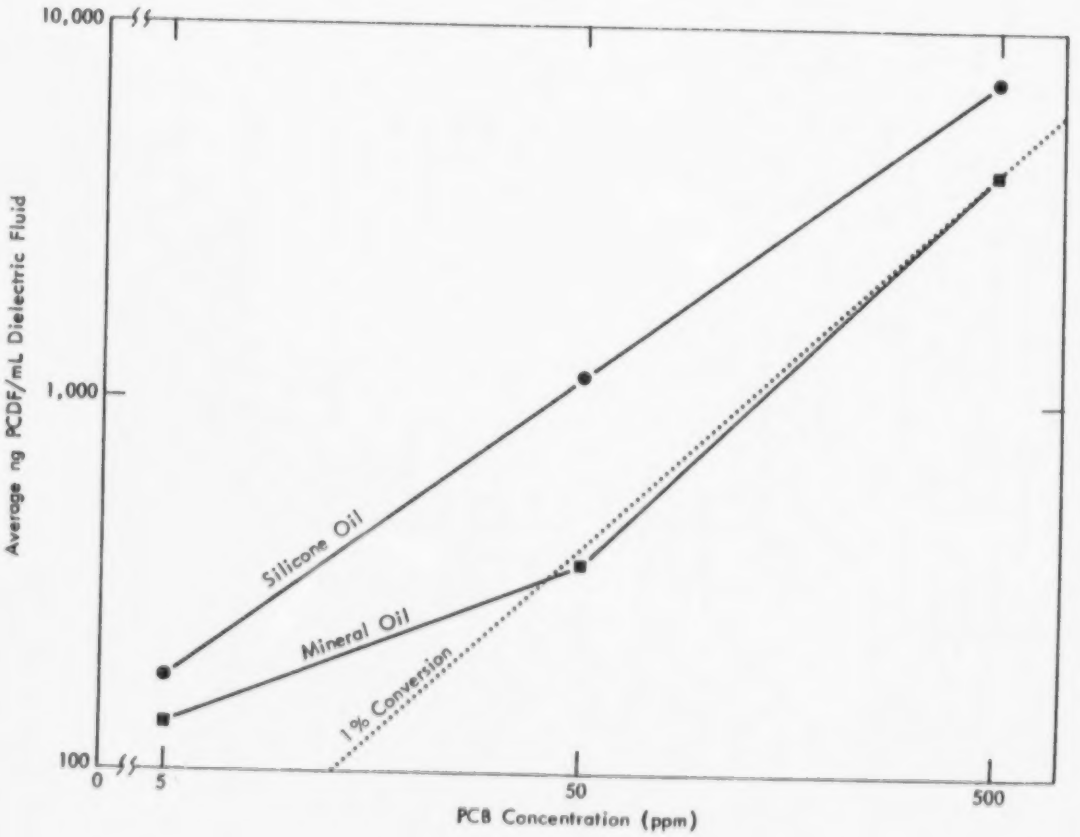

Figure 21. Average PCDF formation versus PCB concentration for Phase 3.

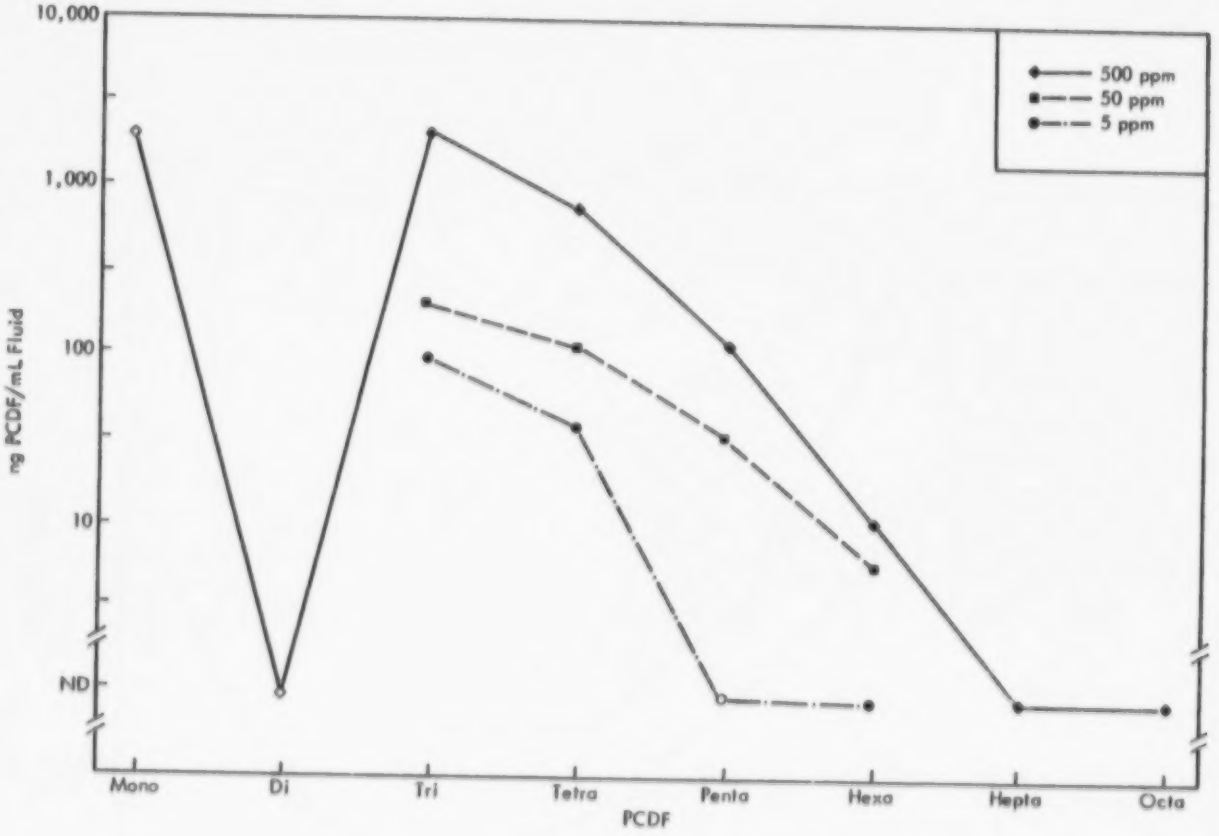

Figure 22. PCDF formation in PCB-spiked mineral oil by homolog. Closed symbols are averages of two values; open symbols are single determinations; missing points are no data.

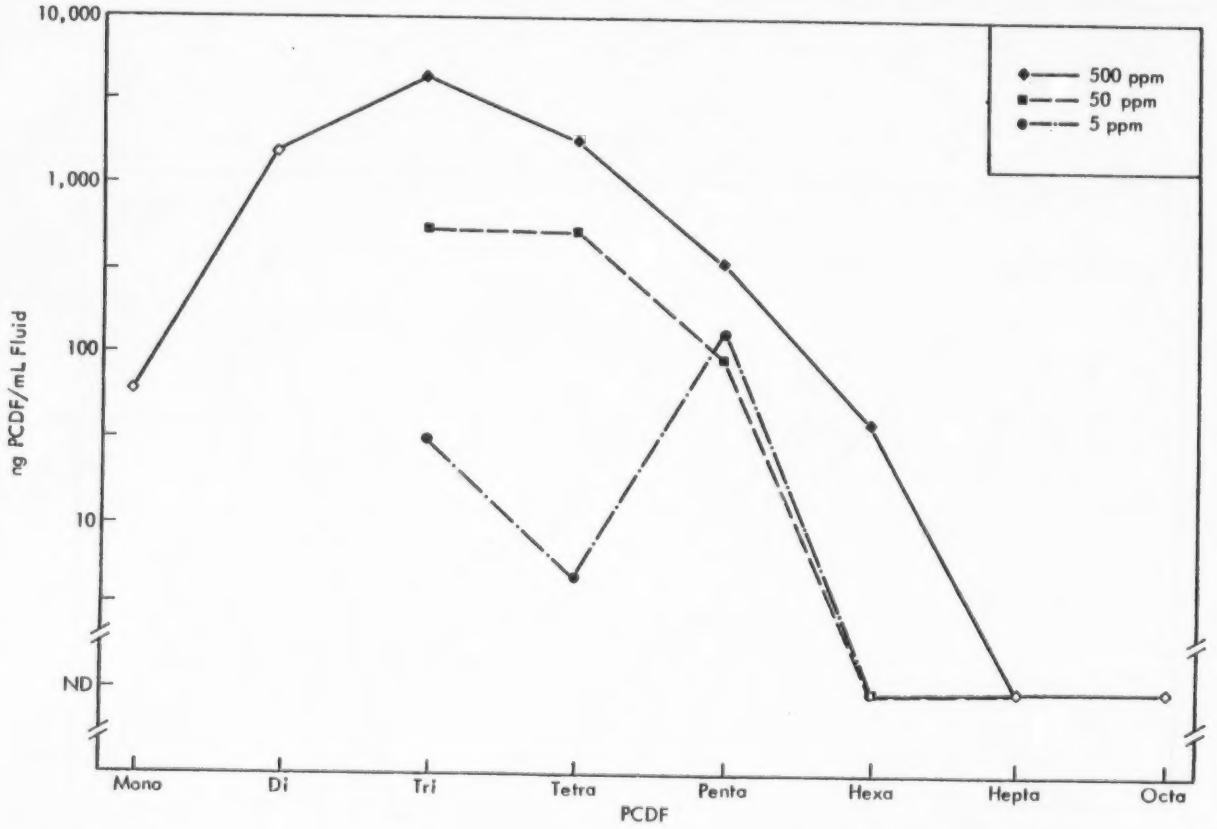

Figure 23. PCDF formation in PCB-spiked silicone oil by homolog. Closed symbols are averages of two values; open symbols are single determinations; missing points are no data.

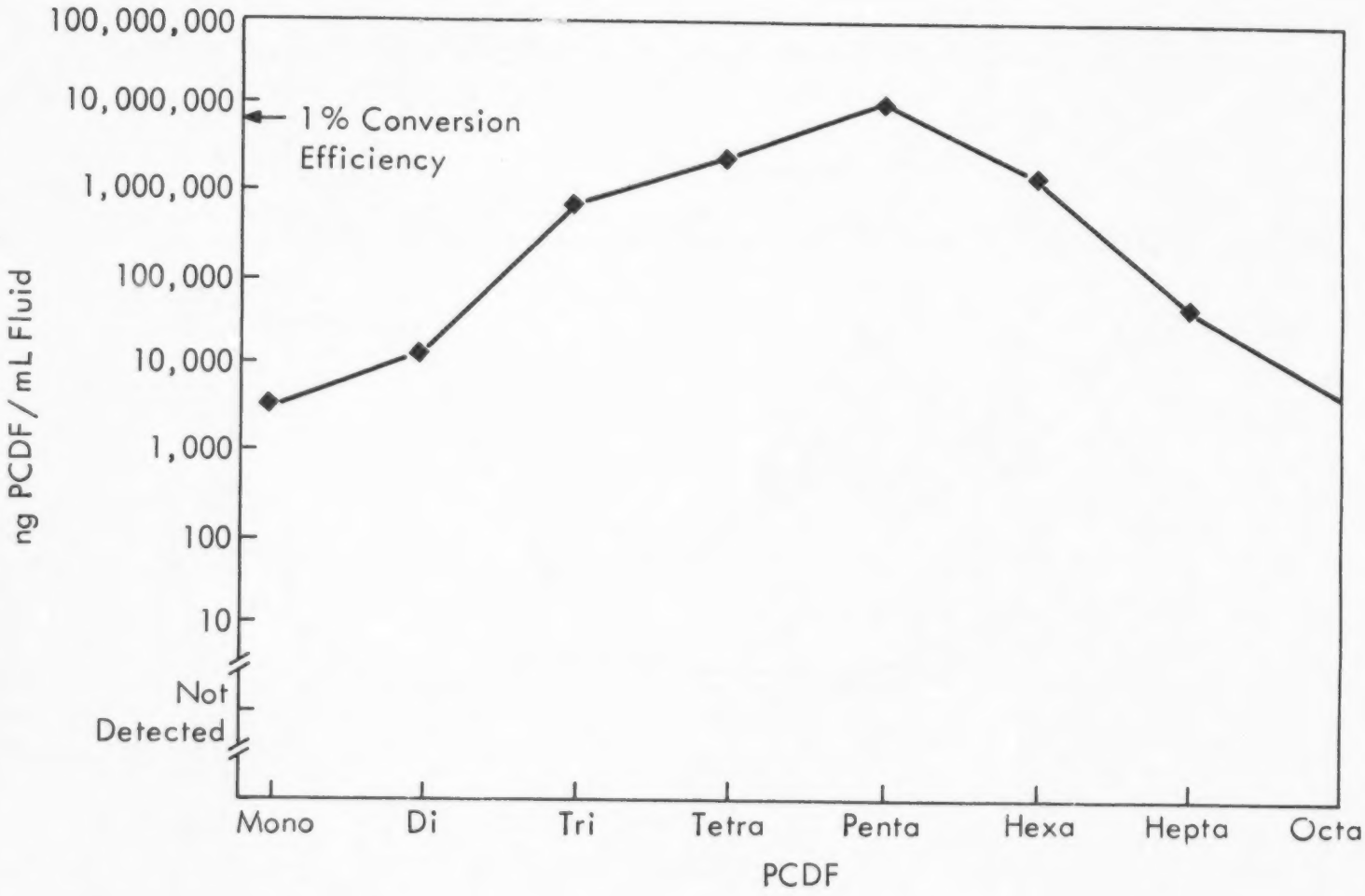

Figure 24. PCDF formation from PCB askarel fluid. Points are averages of two values.

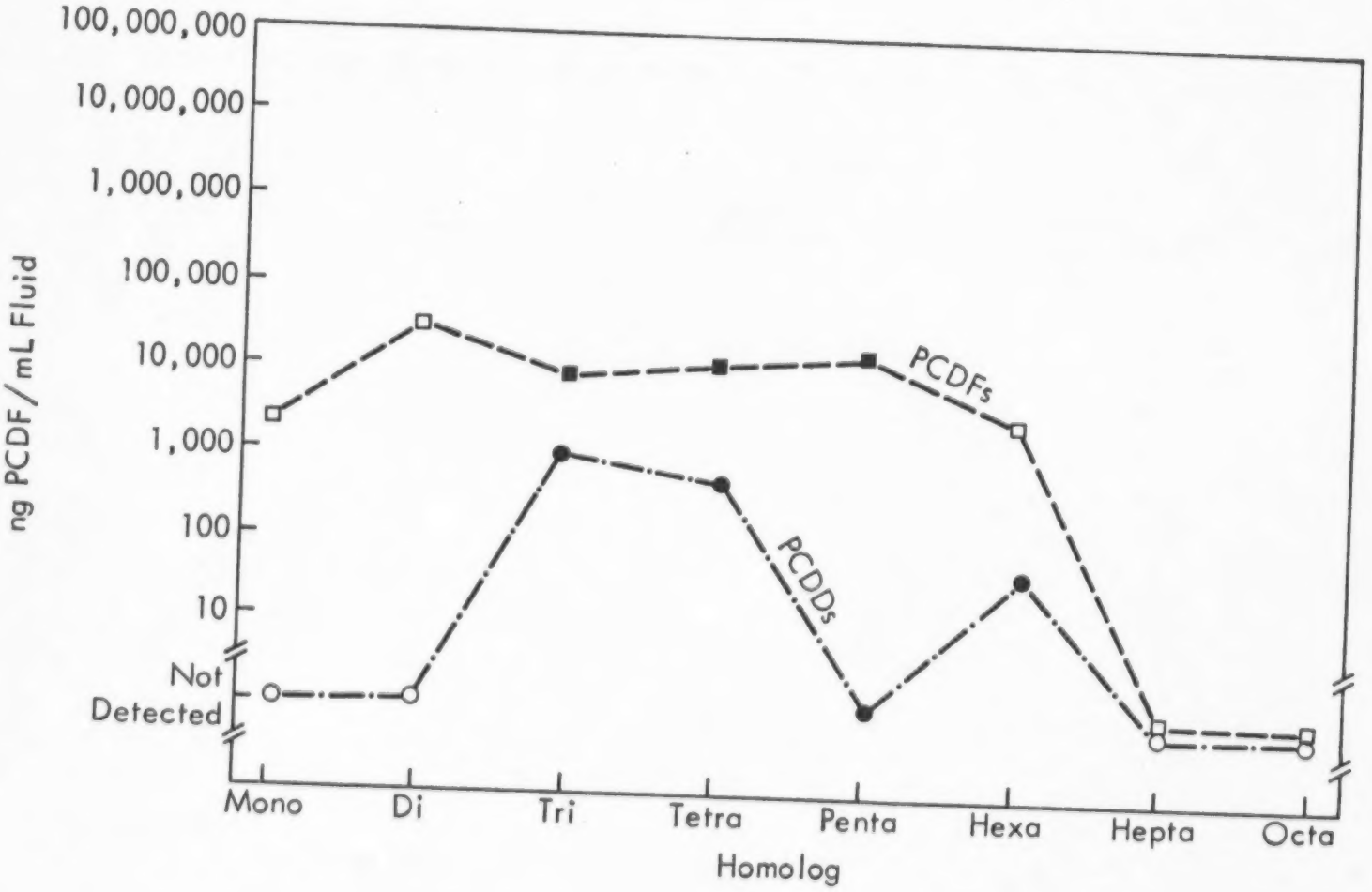

Figure 25. PCDF and PCDD formation from trichlorobenzene transformer fluid. Closed symbols are averages of two values; open symbols are single determinations.

Table 29. Results of Analysis of PCBs in Phase 3 Samples (ng/sample)

Analyte \ Sample no.	8-17-47-S5	8-22-48-S5	8-21-49-S50	8-21-50-S50	8-22-51-S500	8-22-52-S500	8-13-40-M500	8-14-41-M500	Aroclor 1254 (% composition)[a]
Monochlorobiphenyl	< 20	< 20	< 20	< 20	< 50	< 50	< 50	< 50	0
Dichlorobiphenyl	< 20	< 20	< 20	< 20	< 50	< 50	< 50	< 50	0
Trichlorobiphenyl	< 20	< 20	< 20	150	96	640	< 50	< 50	1
Tetrachlorobiphenyl	< 50	360	600	1,800	5,600	17,000	20,000	13,000	15
Pentachlorobiphenyl	< 75	160	6,000	2,600	7,400	19,000	11,000	16,000	53
Hexachlorobiphenyl	< 75	< 75	1,100	1,100	2,800	10,000	3,000	5,800	26
Heptachlorobiphenyl	< 75	< 75	< 75	< 75	< 150	540	< 150	< 150	4
Octachlorobiphenyl	< 100	< 100	< 100	< 100	< 200	< 200	< 200	< 200	0
Nonachlorobiphenyl	< 100	< 100	< 100	< 100	< 200	< 200	< 200	< 200	0
Decachlorobiphenyl	< 100	< 100	< 100	< 100	< 200	< 200	< 200	< 200	0
Total PCBs[b]		520	7,700	5,600	13,000	47,000	34,000	35,000	

[a] Literature value, taken from Brinkman and De Kok (1980).
[b] In calculating total PCB concentration, less than values were considered zero.

The calculated destruction efficiencies are shown in Table 30.

Table 30. PCB Destruction Efficiencies in Phase 3 Runs

Run no.	Destruction efficiency
8-13-40-M500	90
8-14-41-M500	90
8-17-47-S5	> 99
8-20-48-S5	87
8-21-49-S50	79
8-21-50-S50	83
8-22-51-S500	96
8-22-52-S500	86

As described above, destruction efficiency calculation for the 5-ppm and 50-ppm spiked mineral oil runs was not possible. Destruction efficiencies were not measured for the askarel runs (Runs 61 and 62).

6. Statistical Analysis

The data for the PCDFs from the three concentrations, 5, 50, and 500 ppm, in both mineral oil and silicone oil were statistically analyzed. Separate analyses were performed on the total PCDFs and the four homologs, tri-, tetra-, penta-, and hexaCDF, which exhibited sufficient response for analysis.

Because of slightly different burn times, the amounts of PCDFs from different runs would not be directly comparable. Consequently, a multiple regression approach to the analysis was preferred over the two-way analysis of variance. This allowed for consideration of the amount of PCBs in the feed oil rather than just the three nominal levels. The results of both methods of analysis (regression and ANOVA) agreed closely.

All five of the variables analyzed were consistent with a zero intercept. That is, the test of the intercept equal to zero was nonsignificant at the 5% level in all cases. A quadratic in the concentrations was also considered. This was also nonsignificant at the 5% level, so the linear component in the means is sufficient.

The mean PCDF values in the silicone oil were higher than in mineral oil. However, the differences were not statistically significant for the total nor for any homolog except pentaCDF. This is interpreted to mean that production of PCDFs under these conditions may be higher for silicone oil. The differences were substantial, but were not statistically significant, probably because of large variability and relatively small sample size. No significant interaction between concentration and oil type was found.

The levels of triCDF, tetraCDF, pentaCDF, hexaCDF, and total PCDF all showed a significant relationship to the levels of PCB in the feed oil. In each case, the mean amount of the isomer of furans produced in the thermal combustion system increased monotonically with the concentration of PCB in the waste. Table 31 presents the means by isomer, by matrix, by concentration, and by matrix-concentration combination.

In conclusion, the Phase 3 results indicate that PCDFs are readily formed from PCBs and trichlorobenzenes under the conditions used in this study (675°C for 0.8 s, with 8% excess oxygen). The statistical analysis indicates that the PCDF formation is approximately linear with the amount of PCBs in the feed, with a zero intercept. The amount of PCDF produced may be about a factor of two higher for a silicone oil matrix than for a mineral oil matrix.

7. Comparison of Feed and Product Compositions

As can be seen from the results (Tables 23 through 25 and Figures 22 through 24), the PCDFs formed from the feed oils containing PCBs have a homolog distribution which maximizes at triCDF for the Aroclor 1254 feeds and at pentaCDF for the Aroclor 1260 feeds. Figures 26 through 28 present the data in Figures 22 through 24 with an overlay of the Aroclor feed. In both cases, the PCDF curve is about two orders of magnitude lower, reflecting about 1% conversion efficiency (as noted in Table 25). In addition, the PCDF profiles peak at a lower chlorination number than for the corresponding PCB feed, indicating a loss of chlorine in the thermochemical reactions. The PCDFs formed from the M500 and S500 oils contained 2.7 and 3.0 chlorines per molecule, respectively. The Aroclor 1254 has an average of 5 chlorines, indicating that the average reaction has a loss of about 2 chlorines. This would be consistent with Mechanism 1 in Section IV.B. For Runs 61 and 62, Aroclor 1260 with an average of 6.25 chlorines per molecule was fed. The PCDF composition of the products had an average of 4.8 chlorines per molecule. Thus, for these runs, the average reaction involved a loss of 1.5 chlorines, indicating that other mechanisms, in addition to Mechanism 1, must be involved.

Table 31. Means of PCDF Formed in Phase 3, Grouped by Matrix and Concentration

Matrix	Concentration	N	TriCDF	TetraCDF	PentaCDF	HexaCDF	PCDFs
M		6	682	262	46	5	995
S		6	1,310	591	149	10	2,060
	5	4	58	20	60	0	139
	50	4	290	227	51	3	570
	500	4	2,641	1,033	181	19	3,874
M	5	2	88	36	0	0	124
M	50	2	170	95	30	5	301
M	500	2	1,789	656	107	10	2,561
S	5	2	29	5	120	0	153
S	50	2	409	359	73	0	840
S	500	2	3,494	1,410	255	29	5,187

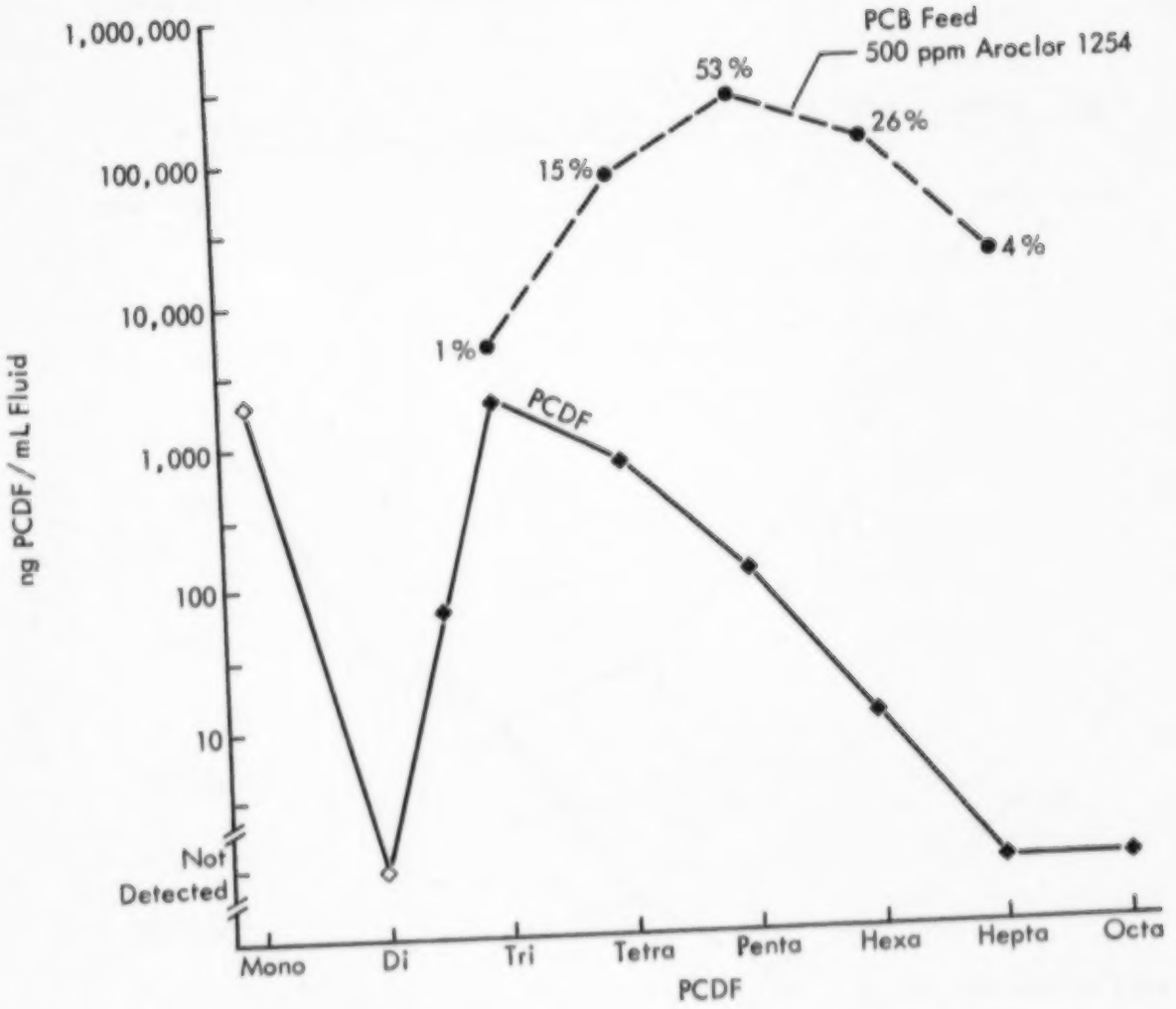

Figure 26. Comparison of PCDFs formed with PCB feed composition (mineral oil)

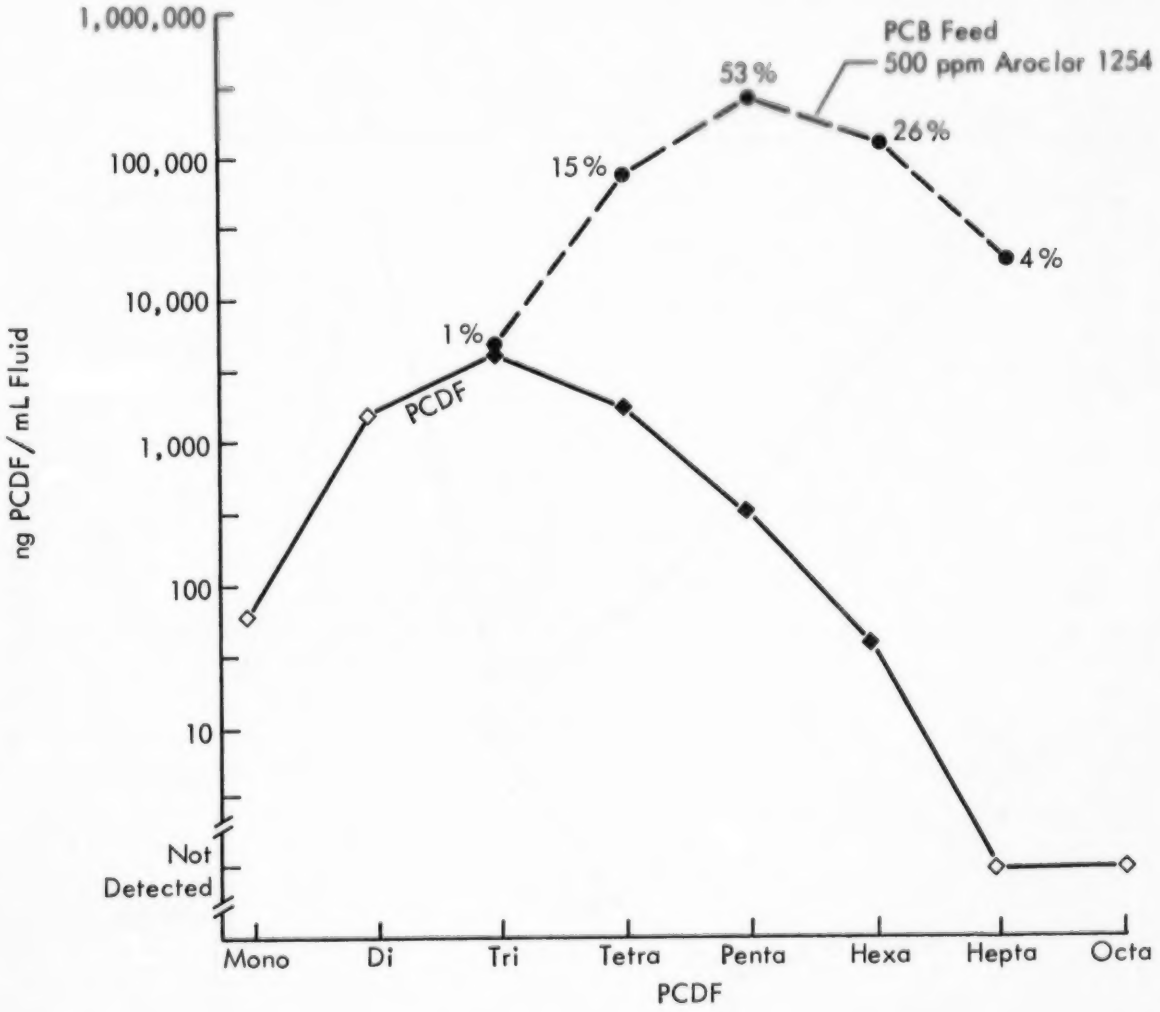

Figure 27. Comparison of PCDFs formed with PCB feed composition (silicone oil).

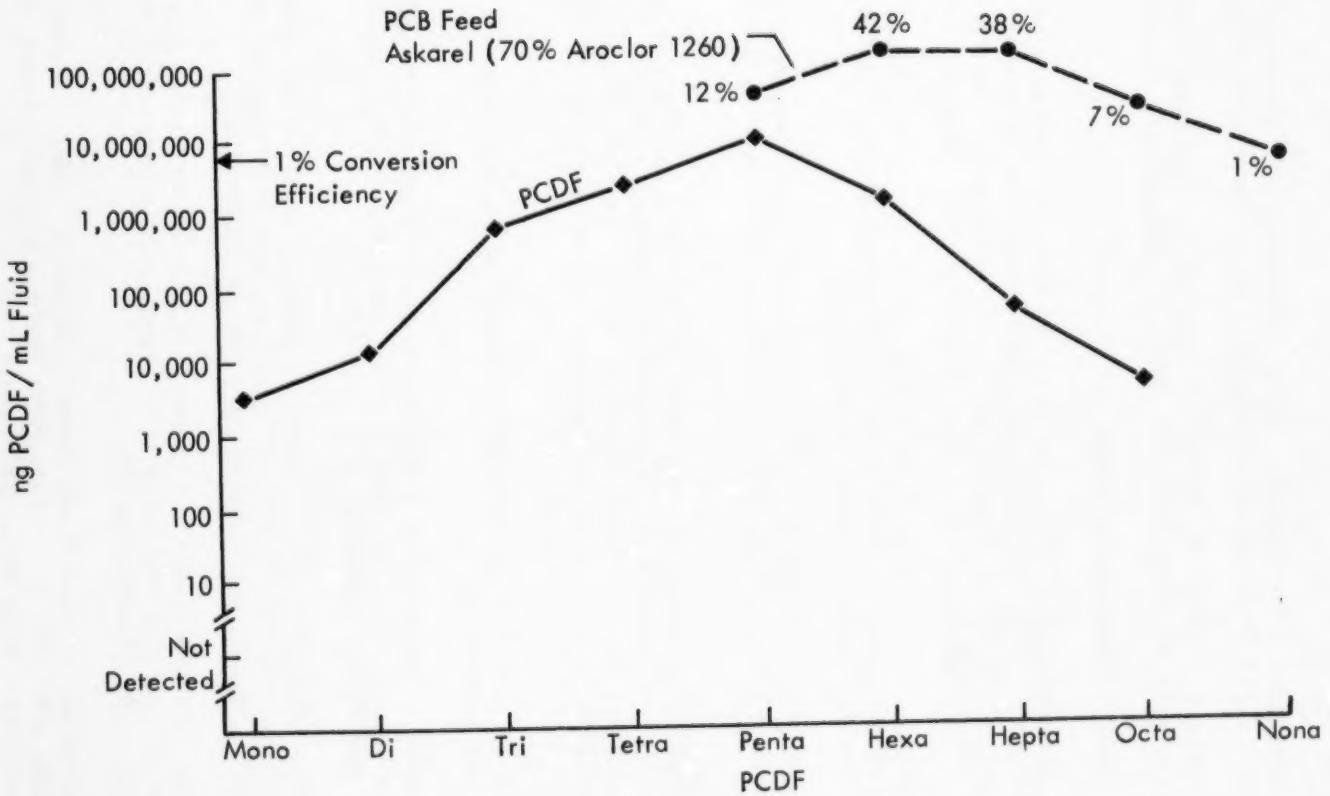

Figure 28. Comparison of PCDFs formed with PCB feed composition (askarel).

VIII. REFERENCES

Brinkman UATh, De Kok A. 1980. In: Halogenated biphenyls, terphenyls, naphthalenes, dibenzodioxins and related products. Production, properties and usage. Kimbrough RD, ed. New York: Elsevier/North-Holland Biomedical Press, pp. 1-40.

Buser HR, Bosshardt H-P, Rappe C. 1978. Formation of polychlorinated dibenzofurans (PCDFs) from the pyrolysis of PCBs. Chemosphere 7(1):109-119.

Buser HR, Rappe C. 1979. Formation of polychlorinated dibenzofurns (PCDFs) from the pyrolysis of individual PCB isomers. Chemosphere 8(3):157-174.

Buser HR. 1979. Chemosphere 8:415.

Jansson B, Sundstrom G. 1982. Formation of polychlorinated dibenzofurans (PCDF) during a fire accident in capacitors containing polychlorinated biphenyls. In: Chlorinated dioxins and related compounds, impact on the environment. Hutzinger O, et al., eds. Elmsford, NY: Pergamon Press.

Morita M, Nakagawa J, Akiyama N, Minura S, Isono N. 1977. Detailed examination of polychlorinated dibenzofurans in PCB preparations and Kanemi Yusho Oil. Bull Environ Contam Toxicol 18(1):67-73.

Morita M, Nakagawa J, Rappe C. 1978. Polychlorinated dibenzofuran (PCDF) formation from PCB mixture by heat and oxygen. Bull Environ Contam Toxicol 19:665-670.

Rappe C, Marklund S, Bergquist P-A, Hansson M. 1983. Polychlorinated dibenzo-p-dioxins, dibenzofurans, and other polynuclear aromatics formed during incineration and polychlorinated biphenyl fires. In: Chlorinated dioxins and dibenzofurans in the total environment. Choudhary G, Keith LH, Rappe C, eds. Butterworth Publishers, pp. 99-124.

Rappe C. 1984. Analysis of polychlorinated dioxins and furans. Environmental Sci and Tech 18:78A.

Smith RM. 1982. Analysis for 2,3,7,8-tetrachlorodibenzofuran and 2,3,7,8-tetrachlorodibenzodioxin in a soot sample from a transformer explosion in Binghamton, New York. Chemosphere 11:715-720.

USEPA. 1984a. Polychlorinated biphenyls (PCBs); manufacture, processing, distribution in commerce and use prohibitions; use in electrical transformers. Advanced notice of proposed rulemaking. (49 FR 11070-11083).

USEPA. 1984b. Polychlorinated biphenyls (PCBs); manufacture, processing, distribution in commerce and use prohibitions; use in electrical transformers. Proposed rule. (49 FR 39966-39989).

Vuceta J, Marsh JR, Kennedy S, Heldeman L, Wiley S. 1983. State-of-the-art review: PCDDs and PCDFs in utility PCBF fluid. CS-3308. Electrical Power Research Institute. Palo Alto, California.

United States
Environmental Protection
Agency

Office of
Toxic Substances
Washington DC 20460

b
1h29
8241